DM

Spheroid Development
for *in vitro* Chondrogenesis
Preliminary studies
MASTER DISSERTATION

Filipa Raquel Nunes Jardim
MASTER IN APPLIED BIOCHEMISTRY

UNIVERSIDADE da MADEIRA
A Nossa Universidade
www.uma.pt

September | 2022

Spheroid Development
for *in vitro* Chondrogenesis
Preliminary studies

Filipa Raquel Nunes Jardim
MASTER IN APPLIED BIOCHEMISTRY

ORIENTATION
Helena Maria Pires Gaspar Tomás

CO-ORIENTATION
Mara Isabel Jesus Gonçalves

UNIVERSIDADE da MADEIRA

Faculdade de Ciências Exatas e da Engenharia

Centro de Química da Madeira

Spheroid Development for *in vitro* Chondrogenesis
Preliminary studies

Dissertation submitted to the University of Madeira in fulfilment of the requirements for the degree of Master in Applied Biochemistry

By Filipa Raquel Nunes Jardim

Work developed under the supervision of Professor Dr. Helena Maria Pires Gaspar Tomás, and co-supervision of Dr. Mara Isabel Jesus Gonçalves

Funchal – Portugal

September, 2022

CQM
CENTRO DE QUÍMICA DA MADEIRA

Molecular Materials
RESEARCH GROUP
MADEIRA ISLAND - PORTUGAL

ORIGINALITY STATEMENT

"Plagiarism consists of the presentation, as your own and even if there has been translation, of ideas, opinions, phrases/texts, results, or conclusions of others. The practice of plagiarism is a serious violation of academic ethics and may lead to failure or withdrawal of the withdrawal of the degree, as well as civil, criminal, and disciplinary liability."

I hereby declare on my honour that this dissertation is of my own exclusive authorship, it is original, and that I have referenced and quoted all sources used in it.

September | 2022

Filipa Raquel Nunes Jardim

Filipa Raquel Nunes Jardim

neighbour (also known as *"vizinha de cubículo"*), thank you for all your motivational words, little treats and trips to the stationery shop. All your encouragement and advice throughout this year was essential, thank you for making my work-breaks fun and interesting! It was a huge pleasure working with you all.

A very special thanks, from the bottom of my heart, goes to *Marta Diana Fernandes.* Thank you for all the assistance, dedication, and reassurance. Thank you so very much for always believing I could do this challenging work.

I would also like to thank all my friends. To my long-standing besties, *Aline Lima, Carina Spranger and Madalena Anjo*, thank you for your unstinting support, I am so grateful to have been able to grow up with you. Apart from my old school besties, I couldn't fail to thank all the friendships I had the pleasure of making and keeping throughout my academic journey. Especially to those who have accompanied me, whether near or far, throughout this dissertation challenge. To my dearest "Island Girls", *Ana Basílio* and *Maria Gouveia*, for always motivating me and making me put my workaholic side out of action for a few moments. To my loving Master's partners, *Carolina Andrade and Cristina Berenguer*, my "Violet Wonders", the biggest thank you for all the shared gossip, advice and support, without you the days of "sofrência" would be much much darker. To the rest of my "Lunch Pack", *Matilde Loja, Onofre Figueira* and *Verónica Pereira*, thank you for always making me laugh, for giving me motivation when I thought I wouldn't make it, and, of course, for always understanding my craziest schedules. Our coffees, snacks and lunches made this whole process lighter. Each one of your friendships is a crucial feature in my life.

There will never be enough thanks to my family, without them I could never have gotten this far, they are the ones who brought me up and made me who I am today. I thank all my family members, those who are here and those who have left, but I wanted to show special appreciation to those who have always supported me, motivated me and always made me feel able to try harder and reach further. I am particularly grateful to my parents and my brother. You three were the first role models I had in my life; you always taught me not to give up on my dreams and to always give my best. Thank you for giving me the opportunity to get so far in my academic journey, and for always encouraging me

to try harder, even when life throws adversity at us. Thank you for your support and affection throughout my life. I love you all.

Last but not least, my biggest thank you goes to my boyfriend *Vítor* – the Chandler to my Monica –; for you it is difficult to find words of thanks that are enough to describe the gratitude I feel for having you in my life. I thank you for all your support, patience, love and care. Thank you for making me stop, take a deep breath and think clearly in the midst of all my anxiety piercing. Thank you for always believing in me, in my potential, and in my ability to fight through adversity. Thank you for taking me out to unwind, and to find balance between rest and work. Thank you for being my greatest support in good times, as well as in bad ones. You're the best in every sense of the word, love you with all my heart and soul.

Moving on now to thank my four-legged *paw*rtners, as I could not end this very important chapter of my life without thanking you. To *Joris*, my oldest boy, and *Tex*, who was taken away from me so early and unfairly, even though I lost you at the beginning of this adventure, thank you for supporting me during so many stages of my life, for being such fundamental advisers that even without words they comfort; thank you for being cute and crazy enough at all times, for filling my days with love without measure. I will never forget you. I also want to thank my new she-dog, *Binny*, the sweetest and most loving girl I have ever met. Thank you for bringing joy back into our home, for looking after us in your own special unique way. Thank you even for simply giving me your paw when you sense I'm down, and for staying by my side and keeping me awake while I write. Love you *furr-iends*.

A deep and sincere THANK YOU, to all those who have contributed, directly or indirectly, in my academic path. Thank You!!

ABSTRACT

This thesis presents the first set of experimental work done at CQM – Centro de Química da Madeira aimed at the implementation of a new research line focused on spheroids for chondrogenesis study.

Three different techniques for spheroid preparation using human mesenchymal stem cells (hMSCs) were tested. The preparation of spheroids by cell self-aggregation in ultra-low adhesion (ULA) cell culture plates was shown to be easy to use, and to lead to stable spheroids. The addition of 50 ng/mL carboxymethyl cellulose (CMC) to the cell culture medium helped to control spheroid's size and spheroidicity, improving cell viability as well. The influence of different culture medium compositions on cell metabolic activity and on cell differentiation towards the chondrogenic lineage was evaluated in 2D cell cultures. The addition of TGF-β1, as well as other supplements, to the chondrogenic medium (CM) increased cell proliferation, and induced chondrogenesis (revealed through histochemical staining).

For the assessment of the chondrogenesis in 3D constructs, spheroids were initially prepared and matured for 14 days (50 ng/mL of CMC was added to the medium at day 5) in ULA plates (poly-HEMA coating) in BM with high glucose content, at a high cell seeding density. Then, a spheroid group was exposed to CM; and another maintained in Basal medium (BM), as a control (CTRL) group for more 28 days (chondrogenesis induction). Spheroid's growth was observed in the CM group, whereas their shrinking was evident in CTRL group. Also, CM led to higher cell viability values in spheroids. Histochemistry staining experiments were only successful using the Fast Green/Safranin O system, revealing the occurrence of chondrogenesis in spheroids exposed to CM. ALP activity measurements showed the absence of the hypertrophic phenotype in the differentiated spheroids (chondrospheres). Finally, ELISA assays allowed the detection of collagen type II and aggrecan in the chondrospheres cultured in CM.

Keywords: Human Mesenchymal Stem Cells (hMSC), Spheroids, Chondrogenic Differentiation, Cartilage Regeneration.

Esta tese apresenta o primeiro conjunto de trabalhos experimentais realizados no CQM – Centro de Química da Madeira com vista à implementação de uma nova linha de investigação centrada nos esferóides para o estudo da condrogénese.

Foram testadas três técnicas diferentes para a preparação de esferóides utilizando células estaminais mesenquimais humanas (hMSCs). A preparação de esferóides por auto-agregação celular em placas de cultura celular de aderência ultra-baixa (ULA) demonstrou ser acessível, conduzindo a esferóides estáveis. A adição de 50 ng/mL de carboximetilcelulose (CMC) ao meio de cultura celular ajudou a controlar parâmetros como o tamanho e a esferoidicidade, melhorando também a viabilidade celular. A influência de diferentes composições do meio de cultura na atividade metabólica celular e na diferenciação condrogénica foi avaliada em culturas celulares 2D. A adição de TGF-β1, bem como de outros suplementos, ao meio condrogénico (CM) aumentou a proliferação celular, e induziu a condrogénese, tendo sido revelada através de coloração histoquímica.

Para a avaliação do processo condrogénico em modelos tridimensionais, os esferóides foram inicialmente preparados e maturados durante 14 dias (tendo-se adicionado 50 ng/mL de CMC ao meio de cultura no quinto dia) em placas ULA (revestidas com poly-HEMA) em BM com elevado teor de glicose (4.5 g/L), e com uma alta densidade celular. Depois, um grupo esferóides foi exposto ao CM; e outro mantido em BM, como grupo de controlo (CTRL) durante mais 28 dias (indução da condrogénese). O crescimento dos esferóides foi observado no grupo CM, enquanto que a sua contração foi evidente no grupo CTRL. Além disso, o CM conduziu a uma viabilidade celular superior. A coloração histoquímica só foi bem sucedida utilizando o sistema Fast Green/Safranin O, revelando a ocorrência de condrogénese nos esferóides expostos ao CM. A atividade ALP revelou a ausência do fenótipo hipertrófico nos esferóides diferenciados (condroesferas). Finalmente, os ensaios ELISA permitiram a deteção de colagénio tipo II e agrecano nas mesmas.

Palavras-chave: Células Estaminais Mesenquimais humanas (hMSC), Esferóides, Diferenciação Condrogénica, Regeneração de cartilagem.

x

EXTENDED ABSTRACT

Problems in articular cartilage constitute a huge healthcare problem needing new and more efficient treatment approaches. In this scope, research on spheroids (3D cell aggregates that can mimic biological tissues) has been very active in recent years, promising interesting outcomes in the future. This thesis presents the first set of experimental work done at CQM – Centro de Química da Madeira aimed at the implementation of a new research line focused on spheroids for chondrogenesis study. Necessarily being of preliminary nature, the obtained results can be organized in three parts.

In a **first step**, different techniques for the preparation of spheroids based on human mesenchymal stem cells (hMSCs) were tested. While pellet cultures resulted in heterogeneous spheroids, and the hanging drop technique was shown to be difficult to execute (spheroids easily lose their integrity during the needed transference to cell culture plates), the preparation of spheroids by cell self-aggregation in ultra-low adhesion/attachment (ULA) cell culture plates (coated with agarose) was shown to be easy to use, leading to stable and reproducible spheroids. Although a natural process of shrinking was observed for the prepared spheroids, the addition of carboxymethyl cellulose (CMC) to the cell culture medium (tested at different concentrations) helped to control the size and spheroidicity of the cell aggregates, improving cell viability as well. Further experiments aimed at the optimization of spheroid formation in ULA plates resorted to poly-2-hydroxyethyl methacrylate (poly-HEMA) coated plates, a higher cell seeding density, an increased glucose content in the medium (to potentiate cell viability) and CMC addition to the cell culture medium only at day 7 of culture time (50ng/mL). These experimental conditions led to uniform and reproducible spheroids that attained stability in diameter, circularity, and solidity (parameters that were assessed by optical microscopy).

In a **second step**, the effects of the composition of the culture medium on cell metabolic activity (which was assayed by the resazurin reduction assay as an indirect measure of cell viability/proliferation) and on cell differentiation towards the chondrogenic lineage were evaluated in 2D cell cultures. The addition of TGF-β1 to the

basal medium (BM) was shown to increase cell proliferation (as expected), but the chondrogenic medium (CM) contained other components that also contributed for cell proliferation. When used as supplements, glutamine, glucose, and insulin, did not had a mitotic effect even when combined (glutamine + glucose, or glucose + insulin). Histochemical staining generally revealed that chondrogenesis occurred in all cultures conducted in CM, independently of the presence of glutamine, glucose, and insulin. While cells were already in stationary phase of growth from day 21 to day 28 of culture, an increase in the total protein content was observed in that period, which was mainly attributed to extracellular matrix (ECM) production. Alkaline phosphatase (ALP) activity measurements showed that cells, at day 28 of culture, did not reach the undesirable hypertrophic phenotype.

In a **third step**, experiments were performed to study the chondrogenesis process in spheroids. For this, spheroids were firstly prepared in ULA plates (polyHEMA coating) in BM with high glucose content, at a high cell seeding density, and allowed to mature for 14 days, being 50 ng/mL of the CMC polymer added to the medium from day 5. Then, the medium was changed to CM and the cultures were monitored for 28 more days corresponding to the chondrogenesis induction period. Spheroid's growth was observed when in CM, whereas their shrinking was evident in BM (control). Also, the CM led to superior cell viability within the spheroids compared to the BM, as assessed by fluorescence microscopy through the Live/Dead assay. In accordance with dsDNA measurements, cell viability in spheroids decreased from day 21 to day 28 as more necrotic zones were observed in the cell aggregates. Histochemical staining experiments were only successful using the Fast Green/Safranin O system, which revealed the occurrence of chondrogenesis in spheroids exposed to CM. Like in the 2D experiments, ALP activity showed that the differentiated spheroids did not reach the hypertrophic stage during the differentiation period. Finally, ELISA assays allowed the detection of collagen type II and aggrecan (two well-known markers of chondrogenesis) in the spheroids cultured in CM. Overall, the results showed the feasibility of preparing spheroids in the laboratory and using them as models for chondrogenesis.

CONTENTS

LIST OF FIGURES

LIST OF TABLES

2D	Two-dimensional
3D	Three-dimensional
α-MEM	α-minimal essential medium
a.u.	Arbitrary units
AA	Antibiotic/antimycotic
AC	Articular Cartilage
ACAN	Aggrecan
ACI	Autologous chondrocyte implantation
ALP	Alkaline phosphatase
BCA	Bicinchoninic acid
BM	Basal Medium
BMP	Bone morphogenic protein
BSA	Bovine serum albumin
CM	Chondrogenic Medium
CMC	Carboxymethylcellulose
Col II	Collagen type II
CTRL	Control groups
DNA	Deoxyribonucleic acid
dsDNA	Double-stranded DNA
ECM	Extracellular matrix
ELISA	Enzyme-Linked Immunosorbent Assay
FBS	Fetal bovine serum
FDA	Fluorescein diacetate
GAGs	Glycosaminoglycans
GFs	Growth factos
HD	Hanging drop
HMDS	Hexamethyldisilazane

hMSCs	Human mesenchymal stem cells
IGF-I	Insulin-like growth factor I
ITS	Insulin-transferrin-selenium
LOT	Liquid overlay technique
MACI	Matrix-assisted autologous chondrocyte implantation
MC	Methylcellulose
MSCs	Mesenchymal stem/stromal cells
NaCMC	Sodium carboxymethyl cellulose
OA	Osteoarthritis
PBS	Phosphate buffered saline solution
PI	Propidium iodide
p-NPP	p-nitrophenyl phosphate
Poly-HEMA	Poly(2-hydroxyethyl)methacrylate
RA	Rheumatoid arthritis
RER	Rough endoplasmic reticulum
SEM	Scanning electron microscopy
SOX-9	Box transcription factor 9
SRY	Sex-determining region
TE	Tissue engineering
TFs	Transcription factos
TGFs	Transforming growth factors
TGF-β	Transforming growth factor-β
ULA	Ultra-low attachment/adhesion

1. Introduction

1.1. Cartilage

1.1.1. Cartilage formation and composition

Cartilage is a specialized connective tissue composed of cellular elements (chondroblasts and chondrocytes) dispersed in a gel-like highly specialized extracellular matrix (ECM) [1]. Mature human cartilage contains only 1-5% of the total volume of cells, while ECM components account for the remaining 95-99% [1]. Cartilage is present in different areas of the body, forming part of the fetal skeleton, articular surfaces, costal ends, and intervertebral discs [1]. Cartilage presents itself as an avascular lacking innervation tissue, in which cells are nourished by diffusion through the aqueous phase of the matrix, being housed in small cavities known as *lacunae* [1].

1.1.2. Cellular components

The cellular elements are bounded by a layer of irregular dense connective tissue surrounding the cartilage, the perichondrium. Cartilage formation commences with the differentiation of mesenchymal cells into cartilage precursor cells called chondroblasts. These cells are located in the inner cell layer of the perichondrium, and have highly developed organelles for protein synthesis, and abundant rough endoplasmic reticulum (RER), Golgi apparatus, numerous mitochondria, and secretory organelles [1]. In addition to these organelles, they contain lipid droplets and glycogen in the cytoplasm [1].

Chondrocytes are located within the *lacunae*, these specialized cells originated from chondroblasts are responsible for producing and maintaining the ECM [1]. Chondrocytes are relatively large spherical cells (about 40 μm in diameter). These cells have characteristic flat borders, prominent nuclei, also present abundant RER and Golgi apparatus; presenting lipid and glycogen inclusions in their cytoplasm as well [1]. Their arrangement varies according to the depth of the cartilage. Thus, mature chondrocytes are located in the deepest zone [1]. Chondrocytes, being the most differentiated cells of

cartilage, engage in tissue homeostasis, producing and regulating the ECM constitution [2].

1.1.3. *Extracellular matrix (ECM)*

In all tissues, the ECM presents itself as a nutrient-enriched physical support platform, that delivers important molecules for cell adhesion, migration, and proliferation [3]. Even though full complexity of biomolecules present in tissue-specific ECM is not altogether characterized, it is known that every tissue type presents a range of molecular features coupled with a specific set of physical properties that support the specialized cells' phenotype within each tissue [4–6]. Both tissue architecture and the ECM constitution significantly influence cell responses to microenvironmental signals [7].

ECM is usually a fibre-reinforced gel containing tissue-specific proteins, glycoproteins, and glycosaminoglycans (GAGs). This matrix also sequesters growth factors, hyaluronic acid (also known as hyaluronan), collagens, laminins, and fibronectin; all crucial cues for each tissue's homeostasis [8]. ECM stiffness also influences cellular pathways, through various forms of physical interactions with ECM [8].

Cartilage's ECM is an amorphous ground substance, composed of water (70-80%) and collagen fibres [1]. In cartilaginous tissues, the ECM mostly presents structural molecules like collagens, fibronectin, GAGs, hyaluronic acid, and elastin (Figure 1), being relatively pliable, despite being solid and firm [1]. ECM is also essential in guiding each tissue's differentiation pathway, endowing tissue specific molecules, such as growth factors, cytokines, and membrane receptors' precursors [3].
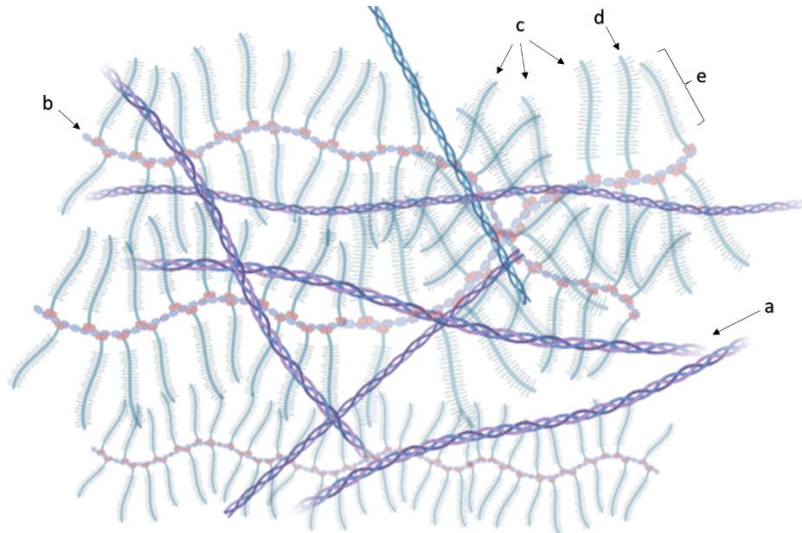
Figure 1 – Main components present in cartilage's ECM: Collagen fibrils (a); Hyaluronic acid molecules (hyaluronan) (b) and proteoglycans (c), composed of a core protein (d) with side glycosaminoglycan chains (e). Illustration constructed using BioRender website (biorender.com).

On account of its avascular nature, the composition of cartilage ECM emerges as a critical aspect in chondrocytes' survival. GAGs' higher proportion in the matrix, compared with the amount of collagen Type II fibres allows diffusion between blood vessels in the surrounding connective tissue and the dispersed chondrocytes [1]. The balance between tension-resisting collagen fibrils and the large amounts of heavily hydrated proteoglycan aggregates maintains the viability of the tissue, being also the reason for cartilage's ability to bear weight, especially at points of movement, as in synovial joints [1].

Collagen molecules

Collagen is one of the most abundant human ECM proteins; in cartilage, it is primarily secreted in a soluble form by chondrocytes. Afterwards, specific amino-terminal and carboxyl-terminal ECM proteinases process the procollagen trimers [1].

Collagen type II is the most abundant form in articular cartilage, constituting one of the most significant components (approximately 40% of ECM's dry weight), accompanied by some collagen fibres of types IX, X, and XI [1]. Collagen fibres are organized in different orientations depending on its location depth, conferring stiffness to the tissue, allowing it to support large loads [1]. Other collagen isoforms, such as types I and X are also present in articular cartilage [1]. Type I collagen is only present on the

surface, forming part of the perichondrium; while type X collagen has a very restricted distribution, limited to the matrix bordering the areas of chondrocyte hypertrophy, as well as in areas of endochondral ossification [9–11].

Four types of collagens participate in the formation of a 3D meshwork of short and thin matrix fibrils. Type II collagen is the main preponderant of the previously mentioned fibrils; type IX collagen facilitates fibril interaction with the proteoglycan molecules; type XI collagen regulates the fibril size, and type X collagen organizes the collagen fibrils into a tree-dimensional hexagonal lattice [1]. This organization is crucial to achieve a successful mechanical function. In addition to that, type VI collagen can also be found in the matrix, mainly at the periphery of the chondrocytes where it helps to attach these cells to the matrix framework [1]. Because types II, VI, IX, X, and XI are found in significant amounts only in the cartilage matrix, they are referred to as cartilage-specific collagen molecules [1].

Proteoglycans

Proteoglycans are a family of glycoconjugates formed by a protein core, from which perpendicularly emerging polysaccharides, mainly GAGs, emerge [10]. GAGs are linear, unbranched polysaccharides whose repeating units are composed of disaccharides linked by glycosidic bonds.

The most representative GAGs are hyaluronic acid, dermatan, keratan and chondroitin 4- or 6-sulfate (Figure 2) [1,12]. An important proteoglycan in cartilage is aggrecan which will be later described.
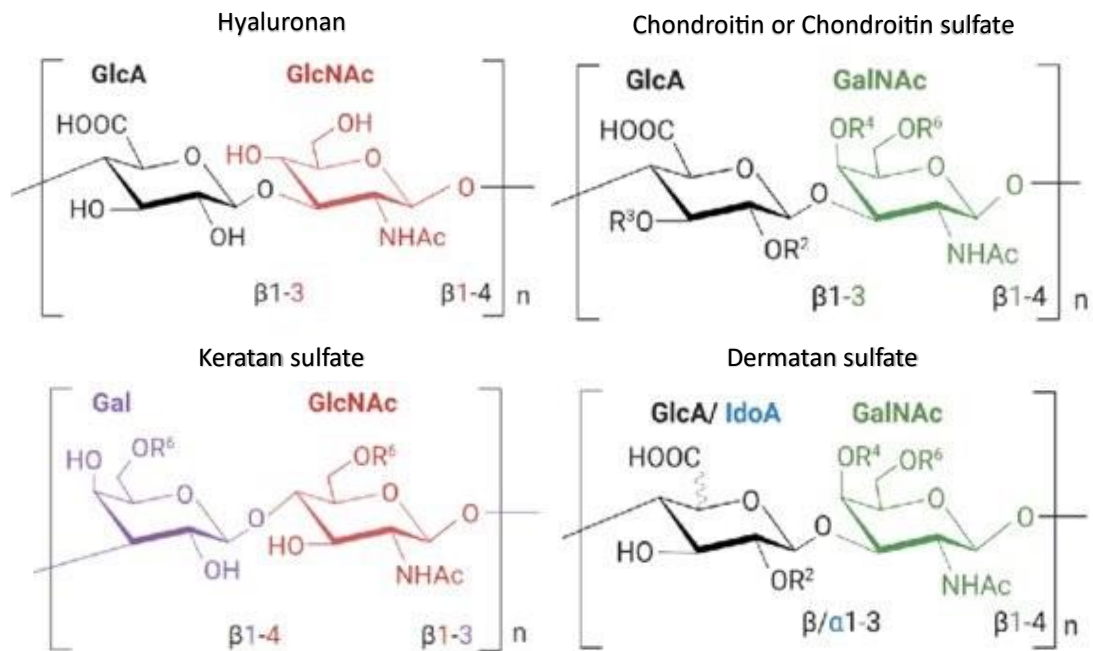
Figure 2 – Structures of the main glycosaminoglycans (GAGs). The disaccharides building block monomers are exemplified in a simplistic way, being represented through abbreviations: GlcA – D-glucoronic acid; GlcNAc – N-acetyl-D-glucosamine; Gal – D-galactose; GalNAc – N-acetyl-D-galactosamine; IdoA – L-iduronic acid; GlcN – D-glucosamine. Hyaluronan suffers no post-polymerization modifications; Keratan sulfate may suffer the action of O-sulphotransferases action, presents either di-, mono- and non-sulfated disaccharide units (R^6= H, or R^6 = SO_3H); Chondroitin is the simplest non-sulfated backbone (all R groups consist of H), being able to suffer modifications through tissue-specific O-sulphotransferases forming Chondroitin sulfate (each R group can become a SO_3H group); Dermatan sulfate results from chondroitin through the epimerization of GlcA into IdoA, followed by the action of O-sulphotransferases [13].

Multiadhesive glycoproteins

In addition to proteoglycans, other glycoproteins and non-glycosylated proteins are present in smaller quantities. Among the adhesive glycoproteins is chondronectin, which has binding sites for chondrocytes, collagen II fibres, and other complex elements [14,15]. An additional molecule critical for cartilage function is the superficial zone protein (SZP). This protein presents itself in the surface zone of articular cartilage and synovial fluid, binding to hyaluronic acid, exerting a crucial role in lubricating the articular surface [14,15].

Multiadhesive glycoproteins, also referred to as noncollagenous and nonproteoglycan-linked glycoproteins, influence interactions between chondrocytes and ECM molecules. Multiadhesive glycoproteins present clinical value as markers of cartilage turnover and degeneration. Examples of such proteins are anchorin CII (cartilage annexin V), functioning as a collagen receptor on chondrocytes, tenascin, and fibronectin, which help anchor chondrocytes to the matrix as well [11,16].

1.1.4. Types of cartilage

Cartilage is classified into three different types, according to the appearance and mechanical properties of its matrix (Figure 3). **Hyaline cartilage** is characterized by a matrix containing type II collagen fibers, GAGs, proteoglycans, and multiadhesive glycoproteins. In turn, **elastic cartilage** is characterized by elastic fibers and elastic lamellae in addition to the matrix material present in hyaline cartilage. Lastly, **fibrocartilage** is characterized by abundant type I collagen fibers as well as the matrix material of hyaline cartilage [1].
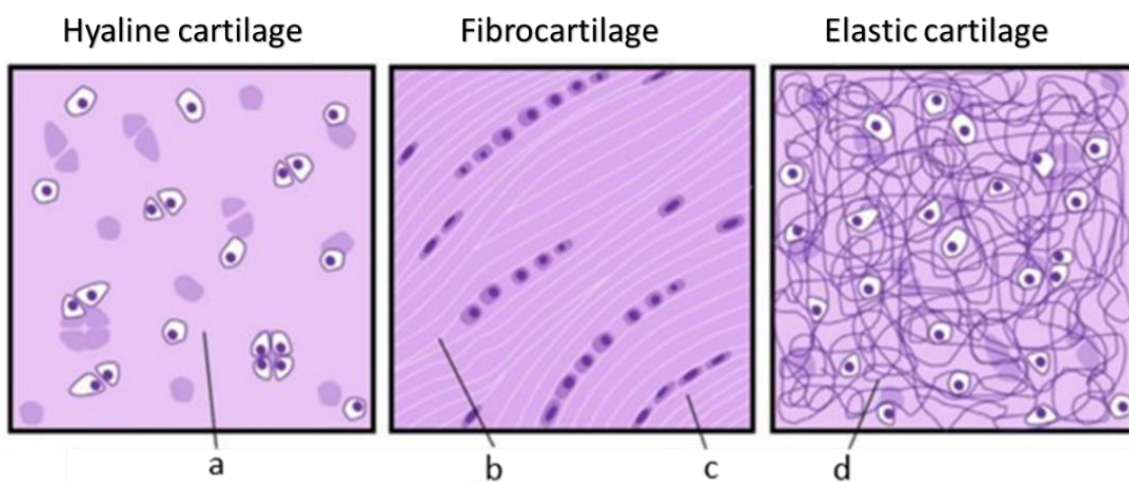
Figure 3 – Histological differences between the three types of cartilage, schematization adapted from the literature [17]. *Hyaline cartilage presents a crisp ground substance (a); fibrocartilage exhibits densely layered collagen fibers (b), and flat organized cell rows (c); lastly elastic cartilage shows elastic fibers in the ECM.*

The present work focuses on hyaline cartilage, the main target of research into new therapies for cartilage repair in the field of regenerative medicine. Hyaline cartilage's matrix consists mostly of three classes of macromolecules: collagens (predominantly type II fibrils, and other cartilage-specific collagen molecules), proteoglycan aggregates containing GAGs, and multiadhesive glycoproteins (noncollagenous proteins) (Table 1) [1].

Table 1 – Summary of the most representative molecular components present in hyaline cartilage.

Cartilaginous ECM composition			
Molecular component	Most representative examples	Structure	Reference
Collagen fibrils	Collagen types II, IX, X and XI	Fibrillar network	[16,18]
Proteoglycans	Aggrecan	Brush-like molecule with GAG side chains	[18]
GAGs	Chondroitin sulfate, Dermatan sulfate, Hyaluronan, and Keratan sulfate	Linear polymerized chains	[16,18]
Multiadhesive proteins	Anchorin CII, Chondronectin, and Lubricin	Mucin glycoproteins composed of a core protein with N- and O-linked oligosaccharide side chains	[16,18]

In hyaline cartilage, aggrecan is the most representative proteoglycan monomer, playing a crucial role in hyaline cartilage, consisting of 90% of chondroitin sulfate aggregates (Figure 4) [16,19]. Due to their sulfate groups, aggrecan molecules have a large negative charge with high affinity for water molecules [19].
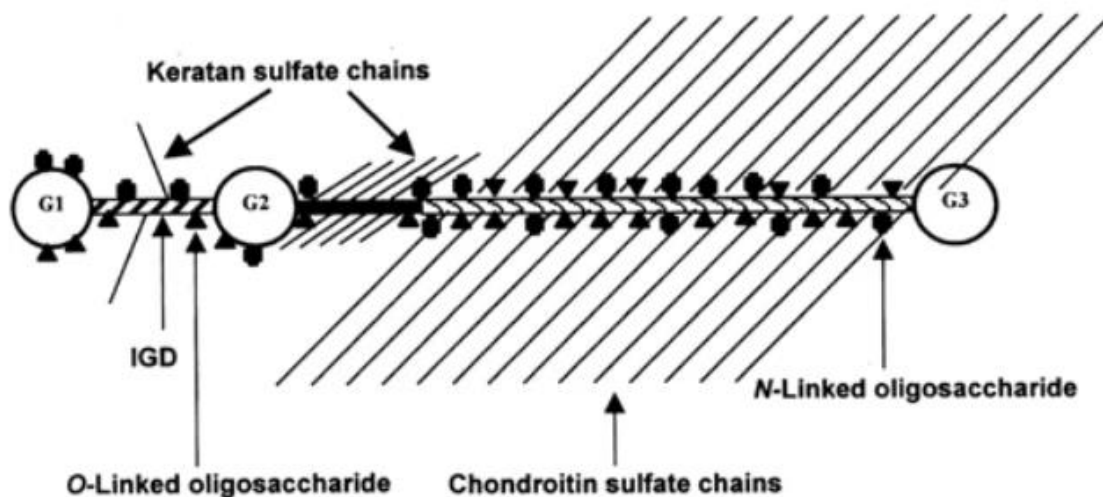
*Figure 4 – Aggrecan structure composed of globular protein domains attached to GAG side chains. Aggrecan presents three protein globular domains (G1, G2, and G3) in addition to three other domains: **Inter-globular domain** (IGD), that connects G1 and G2; and a large sequence of modified **Keratan sulfate** and **Chondroitin sulfate** side chains [19].*

Each linear hyaluronan molecule is associated with a large number of aggrecan molecules; aggrecan is bound to the hyaluronan by linker proteins at the N terminus of the molecule, giving rise to large proteoglycan aggregates (Figure 5). Each molecule of hyaluronic acid associates with a large number of aggrecan molecules (more than 300) to form large agglomerations of proteoglycans [10]. Other proteoglycans such as syndecan, glypican and perlican, located in the pericellular matrix, are produced in smaller amounts [10,12].
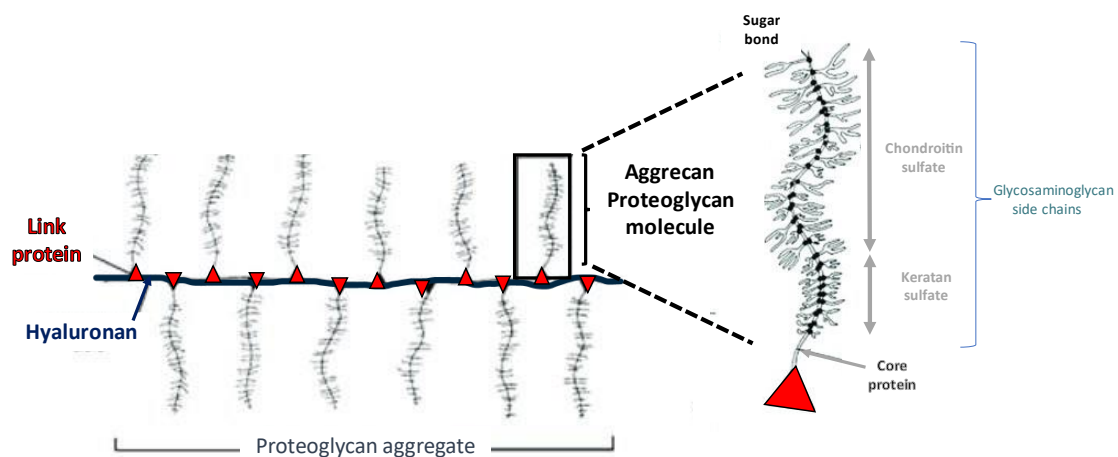
Figure 5 – General structure of a proteoglycan aggregate adapted from literature [13].

These highly charged proteoglycan aggregates, for instance, bind to the collagen matrix fibrils and to multiadhesive glycoproteins by electrostatic interactions [16][11]. This entrapment of molecules is the main reason for hyaline cartilage's unique biomechanical properties [19]. Some of the proteoglycans that do not form aggregates are also able to bind to other molecules, assisting the matrix stabilization [11].

1.2. Articular Cartilage and the need for cartilage repair

Problems in articular cartilage represent a huge burden to society because of the health care costs involved in addition to the discomfort and limitations carried to the patients. Articular cartilage loss of function results in a progressive reduction of mobility and increased pain with joint movement, shortening the number of healthy years of life, and increases mortality and comorbidities, such as depression [20,21]. Cartilage problems

bring out the inherent need to develop new and increasingly effective regenerative therapies.

Articular Cartilage (AC) is hyaline cartilage with a thickness of 2–4 mm, mainly composed of chondrocytes and ECM [4–6]. This specialized connective tissue provides support, load-transmission endurance and joint lubrication; lining the articular surface of bones within the arthrodial joints makes AC able to respond to tensile and compressive forces [22–24].

AC's regenerative capacity after damage or disease is limited by the lack of blood supply, nerve tissues, or lymphatic vessels, in combination with low chondrocyte density and extremely slow metabolic rate [4–6]. Therefore, once injury occurs, cartilage can quickly deteriorate, leading to articular lesions prone to progress to osteoarthritis (OA) and long-term joint instability [24,25].

Damage of articular cartilage can be triggered either by trauma, aging or degenerative joint disease [25,26]. As previously mentioned, cartilage has little capacity for renewal and spontaneous repair, due to poor cellularization, and the absence of vascularization [27,28]. This tissue's intrinsic low healing potential can lead to the formation of fibrocartilaginous tissue, eligible to overtime failure, which may lead to impaired joint function and disability [29]. Amongst the pathologies associated with damage or loss of function of the cartilaginous tissue, osteoarthritis (OA) and rheumatoid arthritis (RA) are the most prevalent [25].

Osteoarthritis (OA) is one of the most common types of degenerative joint diseases. The pathogenesis of this disease is unknown to its full extent. However, the disease is characterized by chronic joint pain with various degrees of joint deformity and destruction of the articular cartilage [16,20,21]. Despite the unknown full extent of the pathogenesis, some aspects have already been established; it has been associated with a decrease in proteoglycan content, culminating with the reduction in intercellular water content in the ECM [20,21].

In the early stages of the disease, the superficial layer of the articular cartilage is disrupted. With the time course, the destruction of the cartilage extends to the bone, where the exposed subchondral bone becomes a new articular surface (Figure 6)

[20,21]. To this day, OA still has no cure, and the available treatments focus only on relieving pain and stiffness, improving the joint's range of movement [11].
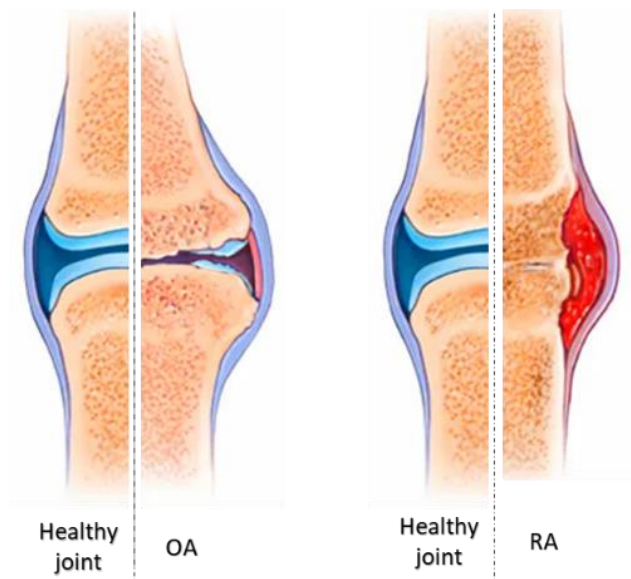
Figure 6 – Comparison of the most concerning cartilaginous pathologies with healthy joints: Osteoarthritis (OA) on the left, and Rheumatoid Arthritis (RA) on the right, illustration adapted from Mayo Clinic website [30]. *OA is characterized by a thinned cartilage layer, often culminating in bone grinding together. RA portrays swollen inflamed synovial membrane, and bone erosion.*

Rheumatoid arthritis (RA) is a chronic systemic autoimmune disease mainly diagnosed in the elderly, being more frequent in women. RA commences by the activation of synovial tissue lining the joint capsule, which can lead to the invasion of cartilage and bone (Figure 6). This condition can result in progressive disability and dysfunction, premature death, and socioeconomic burdens. Typical clinical manifestations include arthralgia, swelling, redness, and even limiting the range of motion. Similarly to OA, there is currently no cure for RA, the treatment strategy aims to expedite diagnosis and rapidly achieve a low disease activity state [31,32].

Articular cartilage defects' traditional therapies are very limited. Some of the most common clinical methods include microfracture, autologous chondrocyte implantation (ACI), and also matrix-assisted ACI [25].

Microfracture induction consists of a marrow stimulation technique to establish communication between cartilage and subchondral bone plate with microfracture awls or drill bits, or by a general abrasion of the subchondral bone with burrs; stimulating bone marrow from the subchondral compartment to fill the defect (Figure 7) [22].
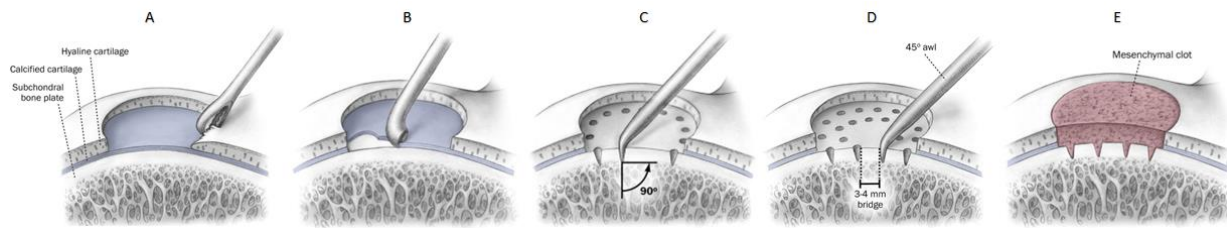
Figure 7 – Microfracture surgery steps, scheme adapted from literature [33]. *This surgical technique begins with the debridement of stable hyaline cartilage (A) to reach the calcified cartilage layer. This calcified layer is then carefully removed (B). After injured layer's exposure, homogeneous microfracture penetrations are placed within the defect (C). The resultant final defect (C) will be filled by a strongly anchored mesenchymal clot (E).*

Amongst the currently available cell-based therapies, **ACI and matrix-assisted ACI (MACI)** are the most common. **ACI** is a two-step surgical procedure that primarily involves the isolation of autologous articular chondrocytes from a non-weight bearing region, and its *in vitro* expansion and subsequent reinjection into the defect site (Figure 8) [24].
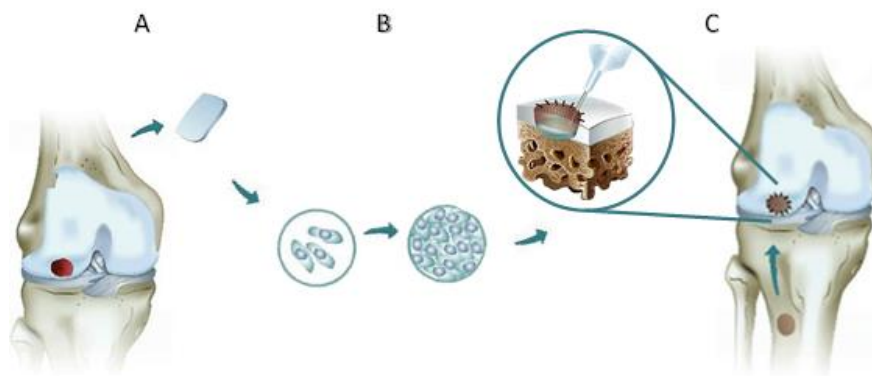
Figure 8 – ACI cartilage regeneration approach. Scheme adapted from the International Cartilage Regeneration & Joint Preservation Society [34]. *The process begins with a biopsy from a healthy zone of the cartilage's own patient (A); then chondrocytes are multiplied in vitro (B); afterwards a periosteal flap is harvested from a healthy site, being fixed over the defect site, in the end the injection of the autologous chondrocyte suspension takes place under the periosteal flap (C).*

The **matrix-assisted ACI (MACI)** is an improved variation of the aforementioned ACI with a twist. This therapeutic approach requires an *ex vivo* engineered hybrid construct, resultant from the seeding of autologous chondrocytes onto a 3D biomaterial matrix prior to implantation (Figure 9) [23,24]. Both approaches have been proved to lead to quite satisfactory results, however the harvest procedure results in donor-site morbidity. This associated with the fact that the 2D expansion can induce phenotypic changes in the differentiated cells, are presented as major disadvantages [24].
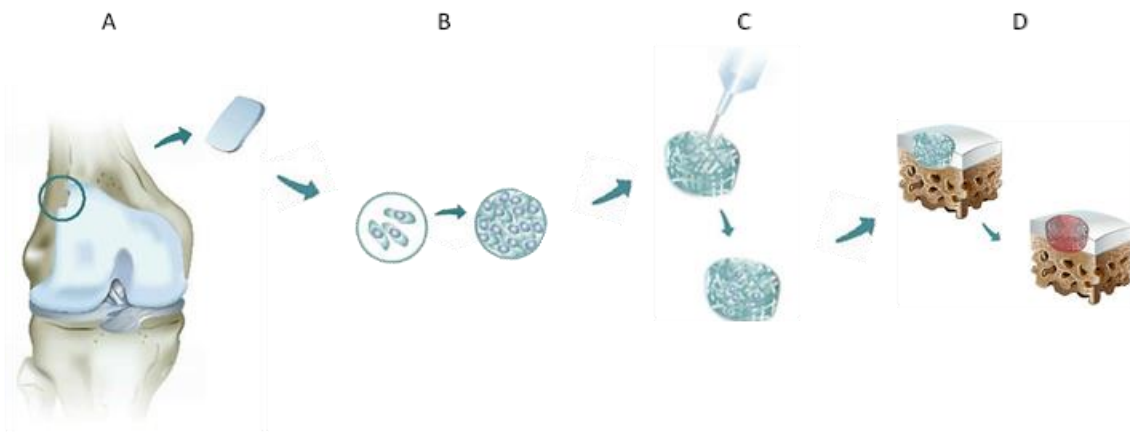
Figure 9 – MACI cartilage regeneration approach. Scheme adapted from the International Cartilage Regeneration & Joint Preservation Society [35]. This method commences in a similar way to the ACI, with a biopsy and chondrocyte culture in vitro (A and B); then the autologous chondrocyte suspension is seeded onto an absorbable 3D matrix prior to implantation (C). In the final step of this clinical approach, the cell-seeded scaffold is fibrin-bound to the defect site, inducing cartilage cells to grow and re-establish the damaged tissue.

Currently used clinical treatment procedures fail to restore the native structure and function of damaged articular cartilage, along with the possibility of donor site morbidity [28,36]. The latest generation of MACI using chondrocyte pellets has shown promise in the treatment of large chondral defects [37–39]. Since previous studies reported in the literature indicate that high cell density and cell-cell communication encountered by cells in multicellular aggregates are sufficient to maintain the chondrocyte phenotype [40,41].

1.3. Mesenchymal Stem Cells and regenerative medicine

1.3.1. Characterization and therapeutic properties

Mesenchymal stem/stromal cell (MSCs) are pursued as cell sources for regenerative medicine (RM), due to their ability to self-renew and differentiate into mesenchymal lineage cells: adipocytes, osteocytes, and chondrocytes. These multipotent non-hematopoietic cells can be harvested from multiple tissues like the umbilical cord, bone marrow, and fat tissue [42,43]. These cells are responsible for ensuring tissues' growth and maintenance, bearing a crucial role in the self-renewal process [3]. MSCs exist within their *in vivo* niches as part of heterogeneous cell populations, exhibiting variable stemness potential and supportive functionalities [11].

Chondrocytes are usually obtained autologously or generated *in vitro* from adult stem cells [24]. Autologous chondrocytes display a limited availability, reduced expansion capacity *in vitro,* and tendency to lose the differentiated phenotype; ergo MSCs arise as a promising alternative to autologous chondrocytes [23,24]. In contrast, MSCs are easily obtained, expand rapidly *in vitro*, and are able to differentiate into chondrocytes when exposed to appropriate growth factors (GFs) and transcription factors (TFs) [23]. The perceived advantage of resorting to MSC as novel cell therapy approaches is also associated with their high proliferative capacity in addition to the ease of isolation. MSCs are capable of retaining their stemness *in vitro*, while also displaying paracrine immunomodulatory and trophic (i.e., angiogenic, anti-fibrotic, anti-apoptotic, and mitogenic) actions *in vivo* [16,21,44].

1.3.2. MSCs differentiation towards the chondrogenic lineage

Most cartilage arises from mesenchyme during chondrogenesis. Chondrogenesis consists of the process of cartilage development, beginning with the aggregation of chondroprogenitor mesenchymal cells to form a mass of rounded, closely apposed cells [16,23].

Hyaline cartilage formation is firstly recognized by an aggregate of mesenchymal cells known as a chondrogenic nodule [16,23]. The expression of sex-determining region Y (SRY) − Box Transcription Factor 9 (SOX-9) triggers the differentiation of MSC into chondroblasts [16,23].

Chondroblasts secrete cartilage matrix and progressively move apart as they deposit matrix; when surrounded by matrix material, the cells are called chondrocytes [11,16]. The mesenchymal tissue immediately surrounding the chondrogenic nodule gives rise to the perichondrium [16,23]. Chondrocytes found in articular cartilage are responsible for the synthesis of ECM proteins such as Collagen Type II (Col II) and proteoglycans [45].

Chondrogenesis is regulated by many molecules, including extracellular ligands, nuclear receptors, transcription factors, adhesion molecules, and matrix proteins [1,11,16]. Likewise, the growth and development of the cartilage skeleton are influenced

by biomechanical forces that not only regulate the shape, regeneration, and aging of cartilage, but also modify cell–ECM interactions within the cartilage [11,16].

MSCs differentiation into chondrocytes requires a certain degree of homeostasis between various promoters and inhibitors. Precursor cells' microenvironment is enriched with soluble cytokines, surrounding matrix, nearby cells, and physical stimuli, that altogether play an important role in determining the cellular fates and chondrogenic differentiation of MSCs [46]. However, after differentiating into mature chondrocytes, MSCs may undergo cellular hypertrophy (Figure 10) [46]. This hypertrophic stage is undesirable in view of biomedical applications for cartilage regeneration.
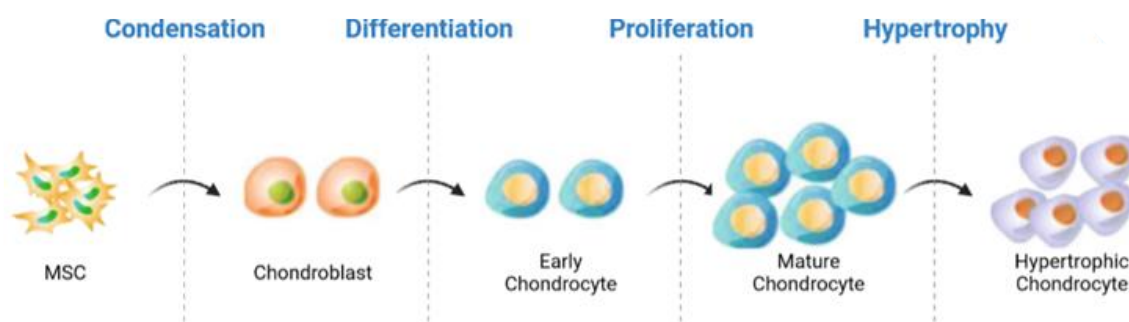
Figure 10 – Chondrogenesis process of MSCs, illustration adapted from literature using BioRender website (biorender.com) [46]*. The differentiation is perceived as following, including condensation, differentiation, proliferation, and hypertrophy as the main stages.*

During the differentiation, a cascade of events takes place within the MSC, that induces both phenotypic and metabolic transformations. The differentiation is revealed by the reduction of the expression of stemness genes, and the activation of genes related to the specialized cells' phenotype [47].

MSC-based Tissue Engineering (TE) products have been associated with qualitative variability that opposes a challenge for their therapeutic efficacy. To bypass these limitations, various *in vitro*/*ex vivo* techniques have been used to manufacturing protocols to induce specific features, attributes, and functions in expanding cells [44].

1.4. MSCs' spheroid models

1.4.1. Formation and structure

Currently, the treatment for degenerative morbidities associated with locomotion is fundamentally symptomatic; therapeutic actions are therefore exclusively of a palliative and social care nature. Furthermore, it is necessary to consider **new therapeutic strategies** that address some of the key elements of the physiopathology of these diseases.

Cells produce certain components of ECM responsible for organizing their own 3D structure, giving rise to spontaneous approximately spherical cellular aggregates called spheroids [48,49]. Within a spheroid, gradients of oxygen and nutrients develop, as well as of metabolic waste products, mimicking the *in vivo* situation better than standard cell culture techniques [50]. MSCs' remarkable ability to coalesce and assemble in tri-dimensional (3D) structures, is reminiscent of their innate aggregation as limb cell precursors in the mesenchymal condensation during early skeletogenesis [44].

Regarding 3D culture strategies, spheroid culture of MSCs is a promising therapeutic alternative, preventing replicative senescence and contributing to stemness preservation [43].

The cell aggregation process that gives rise to multicellular spheroid formation processes involves three phases. Initially, cells form loose aggregates through tight binding of ECM arginine–glycine–aspartate (RGD) motifs with membrane-bound integrin [16,44,51,52]. As a result of the increased cell-cell interactions, cadherin gene expression is upregulated, and cadherin protein accumulates on the cell membrane [44,51,52]. During the later phase, homophilic cadherin-to-cadherin binding induces the formation of compact cell spheroids (Figure 11) [53].
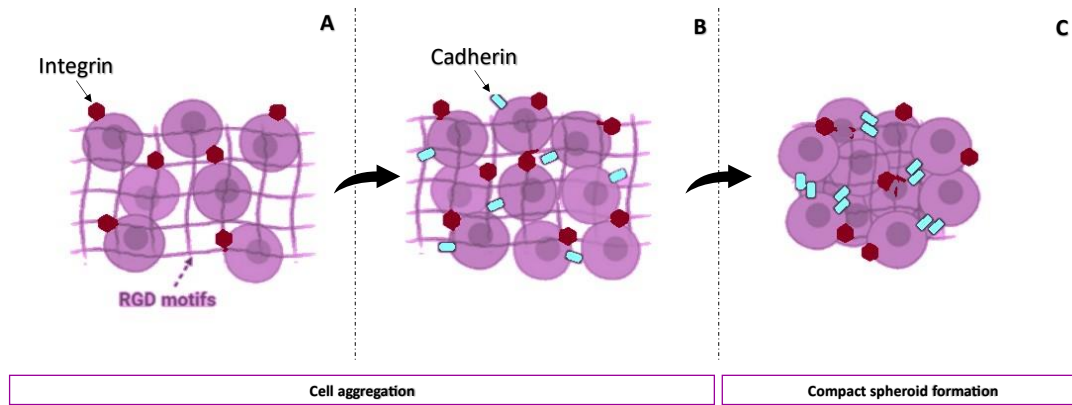
Figure 11 – Simplified spheroid formation mechanism, adapted from the literature [53]. *Spheroid formation process begins with cell aggregation; initially, cells form loose aggregates via the tight binding of extracellular matrix arginine–glycine–aspartate (RGD) motifs with membrane-bound integrin (A). Due to increased cell–cell interactions,* cadherin *gene expression levels are upregulated, and cadherin starts being accumulated on the cell membrane (B). In the later phase, compact cell spheroids are formed as a consequence of the establishment of homophilic cadherin-to-cadherin binding.*

Other intercellular proteins such as connexin, pannexins, and actin cytoskeleton filaments have also been proven to be essential in cell-cell interactions and subsequent multicellular cell spheroid formation [53].

Structurally, most multicellular spheroids can be divided into three zones: proliferative zone, intermediate zone and necrotic zone/core (Figure 12), according to cell size and abundance of both nutrients and oxygen. The outer asynchronously **proliferative zone** includes metabolically active proliferating cells with intact nuclei that are proliferative. Whilst the **intermediate zone** comprises shrunk nuclei cells in a quiescent state, that display basal metabolic activity. Usually, in the function of spheroid size, the inner **necrotic zone** is formed by the gradual retention of metabolic waste within the core, resulting in senescent/apoptotic cells with disintegrated nuclei on account of the limited nutrient and oxygen influx (hypoxia) [53].
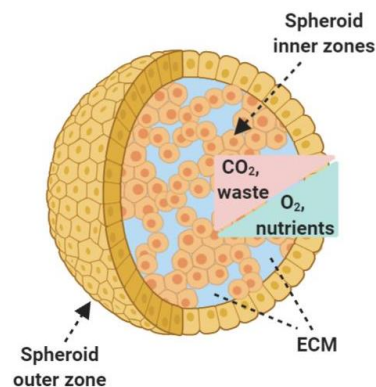
Figure 12 – MSC spheroid construct structure and ECM network composition. Nutrients, oxygen, and waste rates within the spheroid achieve increased functionality "in vivo-like" settings. Image adapted from the literature [53].

1.4.2. Applications in cartilage regeneration

In **two-dimensional (2D) culture conditions**, cells seeded as a cell suspension in the culture dish, becoming adherent cells, forming a monolayer cellular display [43]. This arrangement induces changes in adhesion, feeding rate and motility, consequently altering cellular phenotype and behaviour [43]. When disposed in a monolayer, it is presumed that only half of the cell surface is in contact with the media and that only a reduced percentage of the cells interact with each other, in other words, an artificial environment is introduced. The reduction in cell-cell and cell-ECM interactions affects negatively both the differentiation and the proliferation capacities; while also preventing the establishment of colonies, culminating in replicative senescence and reduced multipotency [43].

Ergo, a **three-dimensional (3D) environment** shows great potential to bring further the understanding of complex biological processes, revealing crucial cues related to physiological context. The 3D disposition creates relevant microenvironments; that display complicated cell–cell and cell–matrix interactions and complex transport dynamics for nutrients and cells can reconstitute conditions similar to that in an *in vivo* microenvironment [21,42,49,54]. This assembly of cells enables the establishment of context-dependent motility, closely resembling the complexity of native tissues, generating differences in the phenotype, behaviour and therapeutic [43,55]. This complex network of interactions plays a significant role in various cellular mechanisms, maintaining the cellular properties, while also enhancing cell differentiation [24].

Tissue Engineering (TE) strives to develop replacement biological tissues and organs for a wide range of medical conditions, related to tissue loss or dysfunction [8]. An additional *in vitro* maturation step may be included, allowing for newly seeded cells to differentiate, deposit functional ECM, and/or attach to a scaffold [8]. TE emerges as the solution to the development of newly *in vitro* formed tissue-material constructs that mimic the biological and mechanical characteristics of the native tissue appropriately [21,23]. TE offers a promising therapeutic option for the repair of traumatic and degenerative articular cartilage injuries, particularly focusing on the development of spheroids made of differentiated cells towards the chondrogenic lineage, the chondrospheres [10]. It has been proven that chondrospheres naturally adhere to

cartilage defect sites after injection, assembling and fusing in a random pattern [24]. Therefore, the implantation of MSCs spheroids provides a viable therapeutic option [25].

In this line of thought, the chondrogenic lineage phenotype induction has been reported by many differentiation protocols, mentioning the major importance of applying a chondrogenic culture medium containing growth factors, such as transforming growth factors (TGF) and/or bone morphogenetic protein (BMP) [23,24]. BMPs were originally known to be critical in the development of bone and cartilage [23,24]. TGF-β superfamily of proteins controls the architecture of various tissues by contributing to several processes such as proliferation, differentiation, and apoptosis [4–6,45]. Transforming growth factor-β (TGF-β) is known to play an important role in stimulating MSC chondrogenesis, promoting mesenchymal condensation, and enhancing cartilage ECM production [56]. Three isoforms (TGF-β1, TGF-β2, and TGF-β3) of this superfamily have been reported to induce chondrogenesis [43].

MSCs' spheroids application in tissue regeneration can be also achieved by *in vitro* 3D culturing techniques, in an effort to more closely recapitulate the *in vivo* MSC niche, and therefore, preserve or enhance cellular phenotypes that result in improved *in vivo* therapeutics, representing the bridge between current knowledge of the cell structure and metabolism to the extensive complexity of tissues and organs (Figure 13).
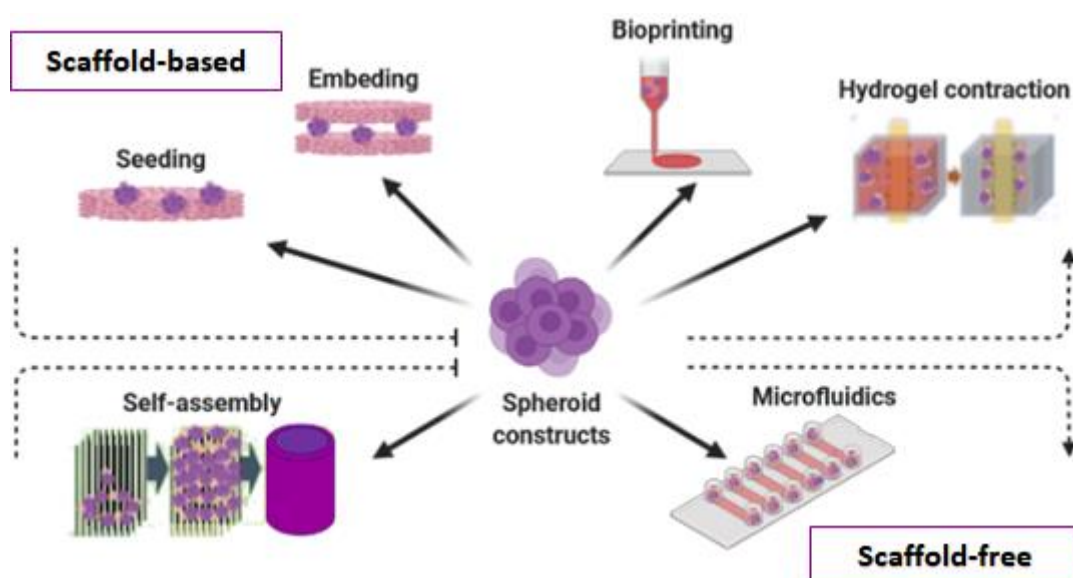
Figure 13 – Possible applications of spheroids with/without scaffold to replicate the complex geometry and physiological activities of three-dimensional tissues [57]. Illustration constructed using BioRender website (biorender.com).

The resulting spheroid structures provide spatial cell organization with increased cell–cell interactions, stable, or even enhanced phenotypic profiles [44,51,52]. The hMSC spheroid approach paves the way to the assembly of microtissues for biomedical applications to generate cartilage constructs, as well as offering potential 3D models to study the effect of certain biomaterials composition on cell alignment and migration before implantation [28,49,58,59].

Stem cell spheroids have also demonstrated enhanced therapeutic effects when transplanted into various disease models, such as in wound healing and ischemic injury models, due to their increased growth factor secretion, immunomodulation effects, and target tissue integration [58], hence these multipotent cells own the ability to modulate the immune system, decrease inflammation and participate in wound healing processes [23].

The injection of spheroids is a promising alternative to single cell suspension injections, because spheroid maturation commences *in vitro*, allowing the establishment of tissue specific ECM, permitting the newly formed chondrospheres (spheroids in which cells are compromised towards the chondrogenic lineage) to naturally adhere to the cartilaginous defect site, assembling and fusing randomly [24]. Another approach to treat cartilage defects is based on tissue engineering cartilage constructs from stem cells *in vitro* before implantation into a cartilage defect [60].

1.4.3. *In vitro Spheroid culture systems*

In vitro studies investigating the MSC chondrogenic potential are limited mostly due to the low cell-cell contact in traditional cell cultures. The use of pre-cultured human mesenchymal stromal cells (hMSC) spheroids to study chondrogenesis as the first step in these studies takes advantage of the high cell-cell contact within each individual spheroid [28]. It has been shown that the pre-culture of hMSC spheroids might have a beneficial effect on hypertrophic gene expression without compromising chondrogenic differentiation, and extracellular matrix (ECM) production [61].

MSC spheroids' organization provides similar physiological environments, while also promoting stemness marker expression; this organization results in changes in cell

morphology, cytoskeleton rearrangement, and polarization by virtue of cell-cell and cell–ECM interactions within the 3D structure inherent to spheroid culture systems [59]. Cadherins are crucial in the proliferation, migration, and differentiation process of MSC cultures; E-cadherin activation and cell-cell interactions regulates proliferative and paracrine activity [53]. Hereinafter, the inherent increased cadherin levels upon MSC spheroid constructs can be associated with the increased MSC spheroid functionality *in vitro* and *in vivo*, offering an advantage over 2D MSC cultures [53,59]. 3D MSC spheroids have shown enhanced "medicinal signalling" activities and increased homing and survival capacities upon transplantation *in vivo* [44,51,52].

The culture matrix to which cells are exposed is the crucial first step to develop successful culture systems for spheroids. The ECM is the key component to generate a microenvironment that resembles the *in vivo* environment well enough to stimulate proper cell behaviour, influencing cell growth and signalling pathways [49]. However, the establishment of diffusion gradients is difficulted with increased spheroid size, being the lack of nutrients in the core of the spheroid a consequence [59].

To date, various methods have been used to generate MSC spheroids including the "classic" hanging drop technique, and other improved methods such as the application of ultra-low adhesive substrates, scaffold-based aggregation or forced aggregation techniques (Figure 14).
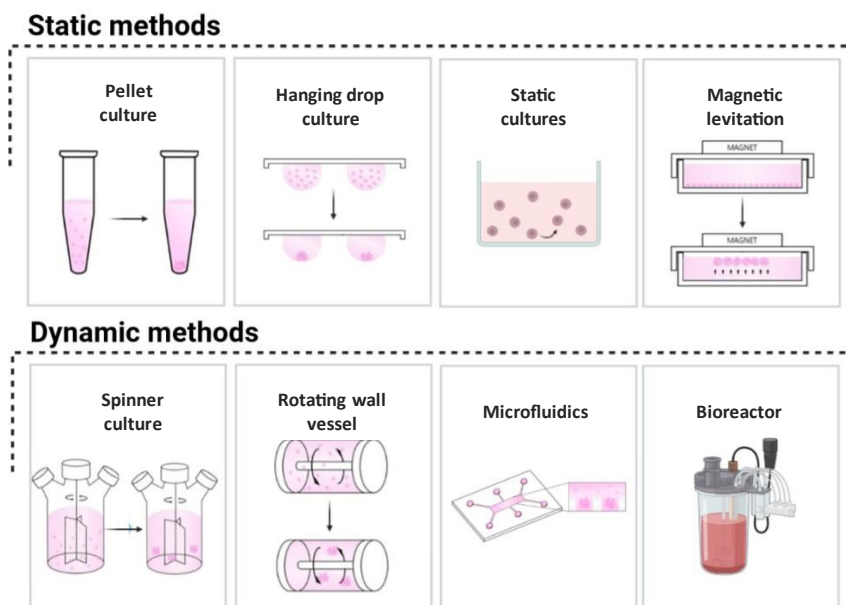
Figure 14 – Schematization set of some technical methods to produce spheroids. Scheme adapted from the literature [62].

Scaffold-free approaches

Spheroids exhibit morphological and functional similarities to native tissues, which makes their formation of particular interest. Along those lines, MSCs' spheroids provide a good platform to study endogenous ECM more thoroughly. Matrix-free techniques include liquid overlay (generation of ultra-low attachment/adhesive surfaces), hanging drop, spinner flask and magnetic levitation [48].

Static culture methods

Forced aggregation technique (or pellet culture) is also used to generate scaffold-free MSC aggregates by gravitational force, the generated spheroids are further induced toward 3D differentiation protocols such as high-density MSC chondrogenic pellet culture centrifugal force is used to concentrate cells to the bottom of a tube maximizing the opportunity for cell-to-cell adhesions to form [44,51,52].

In the **Hanging Drop** (HD) method MSCs are aggregated by gravitational force as well. But, this time, due to the absence of direct contact with solid surfaces; in this case, the composition of ECM proteins is the main factor for the regulation of spheroid microenvironment [44,51]. MSCs quickly aggregate, coalescing into a single central sphere in the apex of the drop [44]. No specialized and expensive equipment is required (for experimental and small animal model scale work) as large amounts of spheres can be formed easily using multichannel pipettors and harvested conveniently [44]. This method offers MSC spheroids of controlled size and number; at the cost of a laborious preparation of the 3D cultures that significantly limits the large-scale production of spheroids for in vivo applications [51].

A less burdensome and more practical technique is the use of low-attachment or ultra-low attachment/adhesion (ULA) surfaces [53]. The use of non-adhesive plastic surfaces or functionalizing the surfaces of tissue culture well plates with a non-adhesive coating layer (hydrophilic polymer) eliminates cell–surface interactions, giving rise to increased cell-cell interactions, stimulating spheroids formation. This method presents itself as a **static suspension culture** technique [59]. The coating of the culture ware is often accomplished by a cost effective, easy to handle and scale-up prone technique, the liquid overlay technique (LOT); being the major drawback the time-consuming plate-

coating pre-step [63,64]. Agar, agarose and Poly(2-hydroxyethyl)methacrylate (Poly-HEMA) polymers are frequently used for this purpose due to their low cost and easy manipulation [63–65].

Magnetic levitation is another method used to generate MSC spheroids *in vitro* by mixing the cells in culture with magnetic particles that are incorporated, thus diminishing gravitational force by application of an exogenous magnetic field, inducing cell aggregation. Although some studies report spheroid formation reproducibility, others have reported that abnormal gravity induces phenotypic changes, apoptotic alterations such as cell size reduction and cell membrane blebbing, reduced cell viability, and nuclear chromatin condensation, as well as margination [53].

Dynamic culture methods

Various dynamic approaches have been studied to generate MSC spheroids. Amongst them, the most common techniques are spinner flask culture and rotating wall vessels. **Spinner culture** technique pends on a spinner flask bioreactor system where cells are continuously in motion by stirring, whereas the **rotating wall vessel** technique generates a microgravity field by constant circular motion, keeping cells in suspension [53].

A comparative study between dynamic and 2D MSC cultures reported in the literature indicates that both spinner and rotating wall vessel dynamic cultures can form viable compact MSC spheroids, showing altered cell size, and altered phenotypic and molecular profiles at the same time, while also enhancing some lineages differentiation potential [53].

Although all different scaffold-free technical approaches previously mentioned rely on the basis principle of cell-aggregation (stimulating cell-cell interactions in detriment of cell-substrate interactions), an ideal method for the generation of 3D multicellular spheroids models should produce consistent aggregates with reproducible sizes and uniform shape; to obtain spheroids with the desired properties, researchers must choose a method that meets the needs of the desired outcome.

The main principles, benefits, and troubleshooting of the main scaffold-free approaches are described in Table 2.

Table 2 – Conventional scaffold-free techniques used for spheroid generation.

Scaffold-free spheroid culture systems					
Approach	Technical method	Basic principle	Advantages	Disadvantages	References
Static cultures	**Pellet culture by centrifugation**	Force cell aggregates to form through centrifugation	Less laborious, standardized technique	Increased variability in size and morphology	[43,53,64]
	Hanging drop culture	Take advantage of surface tension and gravitational forces at the same time	Cheap; Does not require specialized equipment; Tailored shape and sized spheroids	Laborious preparation, that limits scale-up production	[43,53,64]
	Ultra-low attachment surfaces	Resort to non-adhesive materials to inhibit cell attachment	Cheap, easy maintenance; Does not require specialized equipment; Low shear stress; High accessibility to the spheroids; Scale-up prone; High reproducibility	Size, shape, and spheroid number variability, when spheroids are generated on flat non-adhesive surfaces; The plate-pre-coating step may be laborious	[43,53,64]
	Magnetic levitation	Use magnetic forces to induce cells' levitation	Facilitates multi-cellular co-cultures; Reproducible; Reduces necrosis in spheroid core	Geometry and cell mass changes' induction; The artificial gravity can lead to changes in cell structures, resulting in apoptosis	[43,53,62]
Dynamic cultures	**Spinner culture**	Convective force generation by using a stirring bar	Generation of multiple spheroids, prone to long-term cultures; Dynamic control of culture conditions (pH, nutrient and glucose concentrations, and oxygenation); Easy accessibility to the 3D constructs	Spheroid size heterogeneity; requires specialized equipment; Shear stress exposure; spheroids lack individual compartments	[43,53,64]
	Rotating wall vessel	Constant circular rotation of the culture vessel			

Scaffold-based approaches

Recently, cell-based tissue engineering techniques for cartilage regeneration using three-dimensional scaffolds have been reported, being based on a mixture of cells (such as chondrocytes or MSCs) with biomaterials (such as alginate, fibrin, hyaluronic acid and collagen membranes, among others) [4–6]. Scaffold's topography allows seeded MSCs to form a microstructured matrix within the 3D spheroid microenvironment [44,51,52].

In TE, scaffolds can assume multiple forms, varying between solid, fibrous and hydrogel form. The precise control over scaffolds' architecture is a main advantage when it comes to regenerative medicine, enabling the development of TE devices that fit a certain shape, dimension and biological needs of individual defect sites [8]. Natural or synthetic scaffolds that are biocompatible, biodegradable, and biomimetic are key components, being their association with growth factors "the lock" component in cartilage TE [56]. To overcome the possibility of rapid release and inactivation rates, dynamic growth factor release profiles are likely to provide more leverage over cell behaviour [8].

Hydrogel-based scaffolds are frequently used in cellular-based treatments to treat cartilage morbidities; they work as a pro-chondrogenic environment, mimicking the biological and physiological properties of the native ECM [24]. In addition to the hydrogel itself, the ability to functionalise bioinert polymers allowing for the sustained release of bioactive molecules can take advantage of biomimetic principles to evoke regenerative responses from transplanted or host cells, using technically and commercially feasible means [8].

1.4.4. *Clinical perspectives of hMSC spheroids' role in cartilage repair*

3D cultures using hMSC fall into the category of promising novel cell-based therapy approaches in TE. An optimization of the culture conditions could significantly impact the field of regenerative medicine. Finding more reproducible clinical outcomes may be achieved without requiring extensive *ex vivo* MSC manipulation and MSC stimulatory regimes.

Recent studies have shown that MSC spheroid cultures with or without the usage of biomaterials not only preserve MSC phenotypic and molecular profiles, but also

reinforce MSC functionality related to their immunomodulatory, anti-fibrotic, angiogenic, and trophic properties. 3D spheroid formation closely mimics the natural *in vivo* MSC niche, protecting MSC viability, while working as a "vehicle" for their effective homing to the affected tissues upon further implantation *in vivo* at the same time. Adapting high-throughput regulatory-compliant and reproducible methods for MSC spheroid production would allow their use in clinical settings and contribute to an improved MSC-based product for safer and more effective therapeutic applications [66].

1.5. Objectives of the Thesis

This thesis appears as a preliminary study aiming to implement the research in the area of spheroids for cartilage regeneration in CQM's laboratories. In this context, hMSCs were used and several studies were performed with the following main objectives:

(a) To select the most efficient and practical methodology for the preparation of stable spheroids, homogeneous in size and with high spheroidicity; the pellet and hanging drop techniques, as well as self-aggregation of cells in ultra-low adhesion (ULA) cell plates (all of them static methodologies) were compared. Furthermore, within these studies, to assess the effect of the addition of carboxymethylcellulose (CMC) (in the case of the last two techniques) on spheroid formation and to test agarose and poly-2-hydroxyethyl methacrylate (polyHEMA) as surface coatings for the obtention of ULA cell culture plates.

(b) To evaluate the effect of the presence of TGF-β1 on cell behaviour in the cell culture medium; and also the effect of medium supplementation with glutamine, glucose and insulin, using 2D cell cultures. In particular, the metabolic activity of cells was determined (by the resazurin reduction assays), which can be correlated with cell viability/proliferation, and by qualitatively assessing chondrogenesis (by histochemical staining).

(c) Based on the results obtained for the assays done to reach objectives (a) and (b), the ultimate goal was to obtain chondrospheres (spheroids containing viable cells committed with the chondrogenic differentiation process). In more detail, to prepare optimized spheroids, to expose them to chondrogenic medium (CM), and to characterize them in terms of morphology (using optical microscopy and scanning electron microscopy), cell viability (using fluorescence microscopy through the live/dead assay), dsDNA content (by UV-visible spectroscopy), and the chondrogenesis process through histochemical staining (detection of proteoglycans), and also by ELISA techniques (detection of collagen type II and aggrecan in culture).

2. Materials and methods

2.1. Cells, materials, reagents, and general equipment

All hMSCs batches used in the present work were obtained from human trabecular bone samples collected during surgical interventions at Dr. Nélio Mendonça Hospital (Funchal). The whole process had the consent of the Hospital Ethics Committee. The bone marrow held to the trabecular bone fragments was collected to obtain the primary culture of adherent hMSCs, and the cell number was then expanded by performing several cell passages.

Cells from several passages were cryopreserved in liquid nitrogen. For both 2D and 3D cell culture experiments, α-minimal essential medium (α-MEM, Gibco), phosphate buffered saline solution (PBS, Sigma-Aldrich), 100x antibiotic/antimycotic solution (AA, Gibco), and fetal bovine serum (FBS, Gibco) were used.

In the preparation of the 3D spheroid models, commonly used materials and reagents were 100 mm tissue culture dishes, 96-well flat bottom plates (VWR), 96-well round bottom plates (Corning, Costar®), agarose (Sigma-Aldrich), poly 2-hydroxyethyl methacrylate (polyHEMA, ChemCruz), and sodium carboxymethyl cellulose (NaCMC, Sigma-Aldrich).

For the chondrogenesis potential evaluation, some reagents have often been used, such as bovine serum albumin (BSA) (Sigma-Aldrich), bicinchoninic acid (BCA) solution (Sigma-Aldrich), copper (II) sulphate solution ($CuSO_4$, Sigma-Aldrich), sodium hydrogen carbonate ($NaHCO_3$, Merck), sodium carbonate (Na_2CO_3, Sigma-Aldrich), and magnesium chloride-6-hydrate ($MgCl_2 \cdot 6H_2O$, Riedel-de Haën). All the remaining reagents were purchased from Sigma-Aldrich, unless stated otherwise.

Cells and media were manipulated in a Nuaire Laminar Flow Hood (Model NU-425 class II type). Cell suspensions were centrifuged in a superspeed refrigerated centrifuge (Sigma, Model 3-30K). Cell culture in 2D and 3D environments was always conducted in a DH Autoflow Automatic CO_2 Air Jacked Incubator (Nuaire) at 37 °C, in a humidified atmosphere with 5 % CO_2. Cell and spheroid imaging throughout this work used a Nikon Eclipse TE 2000E inverted fluorescence microscope. The microscope was equipped with a Nikon camera, and all digital image recordings were performed with the NIS Elements

Advanced Research (version 2.31) software. All image treatment and spheroid morphology characterization indexes were determined using Image J software (NIH, Bethesda, MD, USA).

2.2. Spheroids' generation and characterization methods

2.2.1. Cell culture

For the preparation of 3D spheroids, hMSCs from several cell passages (P4 – P6), and at different cell seeding densities, were used. First, cryopreserved hMSC cells were thawed, and centrifuged at 300 g for 5 min at 20 °C. The pelleted cells were resuspended in 1 mL of complete cell culture medium (α-MEM containing 10% [v/v] FBS, and 1% [v/v] AA) henceforth also referred to as basal medium.

Cells were cultured in 100 mm culture dishes with 10 mL of complete culture medium and maintained in the incubator. The medium was changed 3 times a week. Before maximum confluency, cells were trypsinized. Succinctly, the culture medium was removed, and the cells were washed with PBS. After that, 1 mL trypsin solution (0.25% [v/v] trypsin-EDTA, ThermoFisher™ LIFEtechnologies) was added to each culture dish, followed by culture's incubation in at 37°C for 3 min. After cells detachment, 2 mL of complete medium was added to stop trypsin action. Viability and cell density were determined in a cell suspension aliquot using 0.2% [w/v] trypan blue (Sigma-Aldrich) staining and a haematocytometer (Neubauer chamber). These cell suspensions were then used for spheroid preparation. For each spheroid generation method, specific guidelines will be addressed in the respective sections thereunder.

2.2.2. Preparation of spheroids by the pellet method

To quickly obtain hMSC spheroids through forced aggregation, an adaptation of the classic pellet culture method proposed by several different protocols found in literature (such as in Zhang *et al.* (2010) and Muraglia *et al.* (2003) [67,68]) was made.

Expanded hMSC were trypsinized and counted using TrypanBlue as previously mentioned. Cells at three different cell densities were seeded on 15 mL centrifuge tubes

with 1.5 mL of basal medium. Three replicates were prepared for each seeding density. All different cell suspension samples (ultimately having 1.2×10^5, 2.4×10^5 and 3.6×10^5 cells/pellet) were centrifuged at 500 g, for 5 min at 20 °C. After that, the pellet cultures were incubated in the tubes with loosened caps to ensure adequate gas exchange. After 72h, cell pellets became compact aggregates, and culture media was changed twice a week by removing 50% [v/v] of the supernatant of each tube and restoring the same volume with fresh medium.

2.2.3. *Preparation of spheroids by the hanging drop method*

Different cell densities were tested to generate 3D spheroid models of hMSC using the hanging drop method. This method began with the removal of the lid from 100 mm tissue culture dishes, and the placement of 12 mL of PBS on the bottom of those dishes. This step is crucial to avoid the desiccation of the hanging drops, acting as a hydration chamber. On the inverted lid of each dish, 20 µL drops of each cell suspension were deposited (sufficiently apart to avoid the contact with the liquid of the surrounding drops) to generate cell aggregate models containing 2×10^4 and 2.6×10^4 cells per spheroid. Afterwards, the lids were carefully inverted onto the PBS-filled bottom chamber, and the hanging drop cultures were incubated in the usual conditions. Cell aggregation was assessed by microscopy, and after 17 days the hanging drop cultures were transferred to ultra-low attachment (ULA) U-bottom 96-well culture plates (coated with 1.5% [w/v] agarose; the coating process will be explained in detail in a following section.

2.2.4. *Preparation of spheroids by self-aggregation using ultra-low attachment surfaces*

In this approach, an ultra-low attachment surface is generated in the bottom of cell culture wells (the coating process will be explained in detail in a following section). Then, spontaneous aggregation of the cells is promoted, as the cells are prevented from adhering to the coating layer. Thus, by seeding the desired cell densities per well, as previously explained for the hanging drop approach, it was possible to control the number of cells per spheroid [69].

2.2.5. Ultra-Low attachment surfaces: fabrication of non-adhesive microwells

In the present work, two different coatings were evaluated to fabricate non-adhesive microwells: agarose coating, and poly-HEMA coating. Both coatings were performed using the LOT technique. Agarose-coating was used in the preliminary studies on flat-well plates, and, later on, using round-bottom plates; while poly-HEMA-coating was only carried out on round-bottom plates.

Agarose has been used to create spheroids due to its hydrophobic nature [69]. The agarose coated microwells used in this project were used by preparing the desired solutions of agarose (1 and 1.5% [w/v]) in distilled water. The powder was mixed with the water and heated until boiling in a microwave. The solution was autoclaved for about 20 minutes at 120 °C, 2 bar. After sterilization, the solution was transferred to a water bath at 65 °C for half an hour, not being allowed to solidify. After that, a final volume of 50 µL of the two agarose solutions were pipetted into the cell culture plates of choice. The plates were sat for 20 min at room temperature and, once the prepared ULA plates have cooled down, a coating layer was visible on the bottom of the plate. The plates were then sealed with parafilm and stored at 4 °C until cell seeding.

Regarding **Poly-HEMA,** the coating process began with the preparation of a 2% [w/v] solution of this polymer in 96% ethanol (EtOH). The solution was left to stir for four hours in a water bath at 65 °C. Afterwards, each microwell was covered with 100 µL of the solution. The plates were left at 37 °C for 72h, to promote solvent evaporation. After drying, the plates were sterilized using UV-light for 20 minutes, sealed with parafilm, and stored at 4 °C until further use.

2.2.6. Addition of carboxymethyl cellulose (CMC) to the media

In order to obtain cohesive multicellular aggregates with increased spheroidicity, cellulose-based supplements can be added to cell environment, increasing the viscosity of the growth media, stabilizing spheroids. Both the static suspension and the hanging drop culture approaches were tested with and without the addition of carboxymethyl cellulose (CMC) to the media.

For the spontaneously aggregated spheroids on the static cultures, the CMC polymer was only introduced after a 5-day spheroid stabilization period as, before that,

spheroid construct's environment should not be disrupted. When it comes to the spheroids generated on hanging drops, the polymer was introduced upon their collecting and transferring to the previously prepared ultra-low attachment treated plates. For both approaches 25, 50 and 100 ng/mL of CMC was added the culture final volume to the media. The CMC solution was previously prepared by the stepwise addition of 1g of Carboxymethyl cellulose sodium salt to 100 mL basal medium, the polymer was left to hydrate for at least 72h prior to its use.

To examine cell aggregates evolution and spheroid growth over time, for each cell seeding concentration, spheroids were imaged on different time points using optical microscopy.

2.2.7. Long-term spheroid cultures viability assessment

Cell viability within the spheroid constructs was determined using the Live/Dead Cell Assay. This assay was used to visually determine if cells within multicellular aggregates remained viable after spheroid formation and maintenance in static suspension cultures for long periods.

After their removal from the microwells, the spheroids were incubated with a solution containing 2 µg/mL of fluorescein diacetate (FDA, Sigma-Aldrich) and 50 µg/mL propidium iodide (PI, Thermo Scientific^{TM}) in α-MEM, at 37°C, for 10 min, protected from light. After double washing the samples with PBS, spheroids were resuspended on basal medium. Samples were immediately imaged using the inverted fluorescence microscope under both green (λ_{ex} = 450 nm; λ_{em} = 500 nm), and red (λ_{ex} = 510 nm; λ_{em} = 590 nm) excitation radiations. Stacked images were obtained resorting to ImageJ software.

2.2.8. Optimization of spheroid formation in ULA microplates

Similarly to the previously described methods, expanded P4 hMSC were trypsinized and counted. After that, the desired cell suspension aliquot was centrifuged at 300 g, for 5 min, at 20 °C. The resulting pellet was resuspended in a previously prepared high glucose (4.5 g/L) basal medium, and 3×10^4 cells were placed in each individual non-adhesive microwell of 2% [w/v] poly-HEMA-coated round bottom plates.

The newly prepared static suspension cultures were also incubated in a humidified atmosphere at 37°C with 5% CO_2 throughout the assay. Feeding was skipped until day 5, and cells were left to spontaneously aggregate due to the combined action of gravity and forced cell-cell interaction resulting from the coating-induced repulsion. Spheroids were visible on the apex of the round bottoms since day 2. After day 5, media was changed every 3 to 4 days with the presence of 50 ng/mL of CMC in basal medium.

2.2.9. Spheroids characterization by optical microscopy

Spheroids diameter was measured over time using optical microscopy and the previously mentioned ImageJ software (NIH, Bethesda, MD, USA).

Spheroid circularity index was measured using ImageJ, applying a known scale as calibration. As an indication of spheroid density, the solidity index was also recorded using the same software. For circularity and spheroidicity measurements, the "*analyze particles*" setting of the program software was used; firstly, this command requires images to be "thresholded", then the software scans the selection of the image until the edge of the spheroid is found. The formula for circularity is $4\pi \frac{Area}{Perimeter^2}$, where a value of 1 indicates a perfect circle [70]. As for solidity (measurement of the overall concavity of a particle), the software calculates this particle shape describer indicator as the area of a particle divided by its convex hull area. Thus, as the particle becomes more solid, the image area and convex hull area approach each other, resulting in a solidity value of 1 [71].

2.3. Experiments in 2D cell cultures: influence of TGF-β1, glutamine/glucose, and glucose/insulin in cell behaviour

2.3.1. Definition of media composition

Two different assays were performed using P4 hMSCs: the first to test TGF-β1 and glutamine and glucose supplementation (alone and in combination); the second to test TGF-β1 and glucose and insulin supplementation (alone and in combination).

Confluent cells were trypsinized, counted and used to prepare suitable cell suspensions for both assays. For both test settings cells were seeded in 24-well plates with 500 μL of basal medium per well. After 24 h, adherent cells were exposed to the chondrogenesis assay conditions. The control groups consisted of cells only exposed to basal medium, whilst the experimental groups (chondrogenic groups) were exposed to a cocktail of supplements. For the first study, 4×10^4 cells were seeded onto each well to maximize cell-cell interactions, known to have an important role in chondrogenesis. In this assay, the chondrogenic medium consisted of basal medium supplemented with 4 mM proline (Gibco), 200 μM ascorbic acid (Sigma-Aldrich), 1% Insulin-Transferrin-Selenium (ITS, Gibco), 1mM sodium pyruvate (Sigma-Aldrich), 100 nM dexamethasone (Sigma-Aldrich), and 10 ng/mL of TGF-β1 (BioRad). Along with these known supplements usually present in commercially available chondrogenic media [72], the influence of the presence of 2 mM glutamine (Gibco) and 2.5 mM glucose (Sigma-Aldrich) was also evaluated.

For the second assay, the experience was carried out along the previous lines, but now with seeding of 3×10^4 cells per well. This time, all samples maintained in chondrogenic media were exposed to 4 mM proline, 200 μM ascorbic acid, 1% [v/v] ITS, 1mM sodium pyruvate, 100 nM dexamethasone, 2 mM glutamine, and 10 ng/mL of TGF-β1. Simultaneously, the influence of glucose (2.5 mM), insulin (5 μg/mL) and the combination of both supplements were also evaluated.

2.3.2. hMSCs metabolic activity evaluation by the resazurin reduction assay

The resazurin reduction assay considers that only living cells are metabolically active and capable of transforming resazurin into resorufin, a fluorescent compound [73]. For both the hMSC seeded in 24-well plates at a density of 4×10^4 cells/well or 3×10^4 cells/well

in 500 μL of either basal medium, or chondrogenic medium, this assay was performed at 21 and 28 days of culture.

At the desired time periods, the medium was replaced with fresh complete medium containing 10% [v/v] of a resazurin solution (0.1% [w/v] in PBS, Sigma-Aldrich), followed by incubation for 4 h. Then, 100 μL of the supernatant was transferred to an opaque 96-well plate and the resorufin fluorescence was measured in a microplate reader at λ_{ex} = 530 nm and λ_{em} = 590 nm. Medium incubated in wells without cells were used as the blank in fluorescence measurements.

2.3.3. Histochemical staining

Cell samples were fixed with 3.7% [v/v] formaldehyde solution (Sigma-Aldrich) for 20 min and rinsed with distilled water. The cells were then stained for proteoglycan and glycosaminoglycan detection through histochemical staining and observed using an inverted optical microscope.

For Toluidine Blue O staining, cells were washed twice with PBS; a 0.3% ([w/v], Sigma-Aldrich) aqueous toluidine blue solution was added, and cells were left to incubate for 30 min; the cultures were then washed for 5 min with running distilled water. The washing step was repeated as many times as needed, to remove all unbound dye.

For the Safranin O/Fast green staining, the cultures were first incubated with a 0.05% [w/v] solution of Fast Green (Sigma-Aldrich), prepared in distilled water, for 10 min; followed by a quick rinsing with 1% [v/v] alcohol acetic acid solution for 15 s. Samples were then stained with a 0.01% [w/v] Safranin O (Sigma-Aldrich) aqueous solution for 3 min, and rinsed, firstly with 96% EtOH, and lastly with distilled water.

As for the Alcian Blue/NFR staining, cells were stained with a 1% [w/v] Alcian blue 8GX (Sigma-Aldrich) solution (prepared in 3% acetic acid alcoholic solution, pH 2.5) for 30 minutes; after incubation, samples were quickly washed with 1% alcohol-acetic acid solution and rewashed with 70% EtOH. After that, cells were incubated for 5 minutes with NFR dye (Sigma-Aldrich), and thoroughly washed with distilled water.

2.3.4. Total protein quantification and alkaline phosphatase (ALP) activity measurement

The ALP activity was determined using a colorimetric assay based on the hydrolysis of p-nitrophenyl phosphate to p-nitrophenol. At each timepoint, the cell supernatant was removed, cells were washed with PBS, 100 µL of Lysis Buffer (Pierce^{TM}) was added to each well and the plates were stored at -20 °C until analysis.

At the time of the assay, the cells were lysed using thee freezing-thaw cycles of 30 min at room temperature, intercalated with 30 min at -20 °C. Then, 20 µL of the lysates were transferred to a 96-well plate, and 200 µL of ALP substrate (2 mM p-nitrophenyl phosphate, Sigma-Aldrich) prepared in sodium bicarbonate buffer (pH 10.0) containing 15 mM of magnesium chloride ($MgCl_2$) was added. The plates were incubated for 60 min in the dark at 37°C. After incubation, 10 µL of 0.02 M sodium hydroxide (NaOH) was added to each well to stop the reaction and develop colour. A calibration curve was performed with serial dilutions of a stock solution of 10 µmol/mL p-nitrophenol (Sigma-Aldrich) with 0.02M NaOH. The absorbance was read at 405 nm using a microplate reader. The total protein content in the cell lysates was determined by the bicinchoninic acid assay (BCA) assay, using 10 µL of each sample. The results of ALP activity were expressed as nmol of p-nitrophenol produced per min and per mg of protein.

2.4. Chondrogenesis studies in spheroids

2.4.1. hMSC spheroid constructs generation and chondrogenesis induction

P4 hMSCs were seeded in Poly-HEMA-coated (2% [w/v]) U-bottom 96-well plates, using high glucose 4.5 g/L) Basal Medium (BM), to generate 3D constructs of 3.0 x 10^4 cells/spheroid. Cells were left to self-aggregate for 5 days. After cohesive spheroids were formed, CMC (50 ng/mL) was added to the culture medium. Spheroids were left to mature for a total of 14 days prior to the differentiation induction.

After the initial maturation period the 3D chondrogenesis assay lasted for 28 additional days, counting with a control group, and an experimental group. The control group consisted of spheroids maintained in high glucose BM supplemented with CMC (50 ng/mL), while the experimental group consisted of spheroids exposed to the

Chondrogenic Medium (CM), composed of the high glucose BM with the chondrogenesis inducing supplements, supplemented with CMC as well.

2.4.2. *Morphology monitoring by optical and electron microscopy, and cell viability assessment*

Spheroids were imaged on different time points of their maturation and of the chondrogenesis process using optical microscopy. Spheroid average diameter, circularity and solidity indexes were determined as previously explained.

Spheroids were fixed with 3.7 % Formaldehyde (Sigma-Aldrich) prepared in PBS (Sigma-Aldrich) for 72h at 4°C. After fixation, samples were washed three times with cold PBS at room temperature for 5 minutes. Afterwards, they were subjected to gradient dehydration using 30%, 50%, 70%, 80%, 90%, and 96% (twice in the last case) ethanol solutions (EtOH, Sigma-Aldrich) for 3 minutes each. Samples were stored in 96% EtOH at 4°C until the analysis. The day before the analysis, spheroid suspensions were placed onto carbon tapes, due to the sample's lack of conductivity, having been left to dry. Spheroids were then fully dried in hexamethyldisilazane (HMDS, Sigma-Aldrich) for 15 min, and left to air drying under a fume hood for 15-20 minutes. Scanning Electron Microscopy (SEM) images of the collected spheroids were obtained with a Bench SEM Microscope Phenom - Pro X, and acquired using different magnifications (1000 and 3000x) with an acceleration voltage of 10 keV.

Cell viability in spheroids was assessed by fluorescence microscopy using the Live/Dead assay following the same procedure steps previously mentioned.

2.4.3. *dsDNA quantification*

For both CTRL and CM conditions 6 replicates were considered, having the spheroids been collected individually. For each sample, 1.0 ml of sodium citrate buffer solution, containing 100 mM NaCl (Sigma-Aldrich) and 50 mM sodium citrate (Chem-Lab) (1:1), was added. Spheroids were then stored at -80°C until further analysis.

For the DNA quantification, spheroids were disaggregated, and cells were lysed with sonication in sodium citrate solution for 5 minutes. After the samples were lysed, an

aliquot of 2 µL from each replicate was used to measure the concentration of dsDNA using the NanoDrop™ One Microvolume UV-Vis Spectrophotometer (Thermo Scientific™). Shortly, this microvolume spectrophotometer allowed for the nucleic acid samples' quantification resorting the preprogrammed application for dsDNA. To deduce each sample's concentration, the NanoDrop One software uses the measured absorbance at 260 nm, the mass extinction coefficient for dsDNA (50 ng/µL cm^{-1}) and Beer's Law, while providing two purity ratios based on the absorbances of 230, 260 and 280 nm : A $_{260\,nm/280\,nm}$ and A $_{260\,nm/230\,nm}$ [71].

2.4.4. *Histochemical staining*

Alcian Blue, Safranin O/Fast green, and Toluidine Blue O staining of the CTRL and CM spheroids collected during the chondrogenesis induction assay was performed as previously described for 2D cultures, increasing the number and durability of the washing steps.

2.4.5. *Total protein content and alkaline phosphatase (ALP) activity per spheroid*

Spheroids were collected at 21 and 28 days of chondrogenesis induction for total protein quantification and ALP activity determination. For both CTRL and CM conditions, 6 replicates were considered, having the spheroids been collected individually. Each sample was washed with PBS and preserved in 100 µL of Lysis Buffer at -20 °C until analysis. For the afore mentioned analysis, spheroids were thawed and lysed by sonication for 5 minutes. After, lysates were prepared and treated in the same way as explained before for 2D cultures.

2.4.6. *Chondrogenic ECM markers specific detection and quantification*

Spheroids were collected at days 21 and 28 after chondrogenic induction. Enzyme-Linked Immunosorbent Assay (ELISA) analysis was performed to detect the content of human collagen type II (COL II) and aggrecan (ACAN), using specific ELISA kits (Human

Collagen Type II (COL 2) ELISA kit and ACAN ELISA Kit PicoKine®, respectively) following the manufacturer's instructions.

Briefly, the collected spheroids were disaggregated through centrifugation (10 000 rpm, for 10 min), and each supernatant was individually collected for testing. Both ELISA kits employed the "Double Antibody Sandwich" technique, in which the analyte of interest is immobilized by analyte-specific capture antibodies onto the pre-coated plate, while the detection antibody is a biotinylated antibody. After the antibody-antigen-antibody complex is formed, the avidin-peroxidase conjugates are added to the wells for color development, forming a blue product due to the peroxidase activity, that then becomes yellow upon the addition of the stop solution to the mix. To quantify the analyte of interest, the quantity of target in the sample is computed, being positively correlated with coloration intensity, using a reference curve.

2.5. Statistical Analysis

Statistical analysis was performed using GraphPad Prims 9.4.1 for Windows. The results are presented in the form of mean ± s.d. One-way ANOVA with Bonferroni's multiple comparisons test was used to compare the results obtained for the spheroid models preparation, in Figures 19, 22 and 29; and two-way ANOVA with Tukey's multiple comparisons test was used in Figure 31. Two-way ANOVA with Bonferroni's test was used to determine statistical differences regarding both 2D and 3D chondrogenesis results in Figures 23, 25, 27, 33, 36 and 37.

3. Results and discussion

The main goal of this thesis was the development of reproducible cohesive hMSCs 3D spheroid models to subsequently induce their differentiation towards the chondrogenic lineage for future biomedical applications in the field of cartilage regeneration.

In a first step, three different methods do generate multicellular aggregate spheroid models were studied to determine the best method to generate viable cells within cohesive structures in long term cultures. For this first study task, higher passages of cells (up to Passage 6, P6) were used since their stemness was not a critical requirement for the development/optimization of the 3D models.

As a second task, an optimized chemical formulation for the chondrogenic medium was developed by testing the effects of different "cocktails" of supplements on 2D cultures of hMSCs, using a lower cell passage (Passage 4, P4).

Then, the chondrogenic potential of the optimized spheroid models (using P4 hMSC) when exposed to a chemically defined chondrogenic medium was evaluated at two different time points of the differentiation assay.

3.1. Spheroid generation methods evaluation

3.1.1. Study of the reproducibility of three different methods to generate hMSCs-based spheroids

Spheroids were engineered having in view the fabrication of structurally and functionally reliable *in vitro* artificial 3D tissues. For this purpose, several different cell seeding densities and three different methods to generate hMSC spheroidal constructs of the desired shape and size were tested. Using spheroid culture methods allows for maximum cohesion among cells, taking advantage of different physical forces to guide their spontaneous assembly while minimizing cellular interactions with substrates.

Pellet cultures are the current gold standard practice to generate spheroids that are furtherly induced to *in vitro* differentiation towards the chondrogenic lineage and were first tested in this work. The three cellular densities tested (1.2×10^5, 2.4×10^5 and 3.6×10^5 cells/spheroid) yielded morphological different spheroids even starting from

the same primary cells (Figure 15). In this case, the extremely high cellular density of the most concentrated cell suspension was the only one to present a satisfactory construct.

| 1.2 x 10^5 cells/spheroid | 2.4 x 10^5 cells/spheroid | 3.6 x 10^5 cells/spheroid |
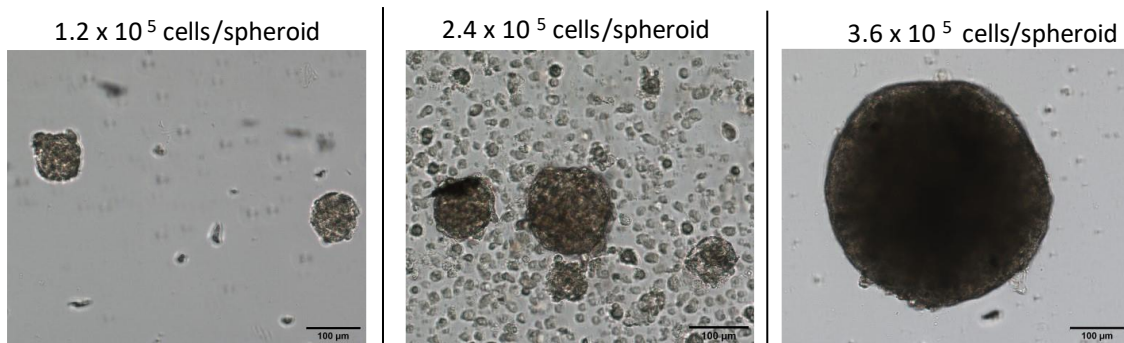
Figure 15 – 14-days-old P5 hMSC spheroids resulting from the pellet culture method with the initial seeding of 1.2 x 10^5, 2.4 x 10^5 and 3.6 x 10^5 cells/spheroid. Representation of the morphology of the different cell aggregates (scale bar 100 µm).

For all cell densities, approximately spherical models were obtained. However, it would have been expected that only a single spheroid would form per pellet. This was only true for the highest cell density used, indicating that using 15 mL screw-cap centrifuge tubes to obtain the 3D cultures by forced aggregation is not the most appropriate choice for seeding cells at densities below 3.6 x 10^5 cells per spheroid. This may be related to the relatively large area at the conical bottom of each tube, which may be responsible for the cells not being able to communicate with each other equally, becoming more dispersed and distant. In addition to that, it is noticeable that the generated spheroids show increased variability in size and morphology. This method was soon discarded, as it proved extremely difficult and impractical to obtain reproducible spheroids as well as to maintain culture conditions, not envisaging a possible scale-up production. Furthermore, the literature mentions that this method presents several liabilities, mostly conveyed to the construct up-scaling and future hypertrophic differentiation of hMSCs, followed by pre-mineralization of the generated cartilage tissue [28].

Another of the three techniques tested was the hanging drop (HD) method. In this case, two similar cell seeding densities were tested – 2 x 10^4 and 2.6 x 10^4 cells/spheroid (Figure 16). As promised in the literature, the hanging drop method allowed for a large number of spheroids to be obtained in a quick, relatively easy, and effective process, requiring a considerably reduced number of cells per spheroid when

compared to the first method tested. Moreover, the size of the spheroid could easily be manipulated by changing the size of the drop or the cell concentration.
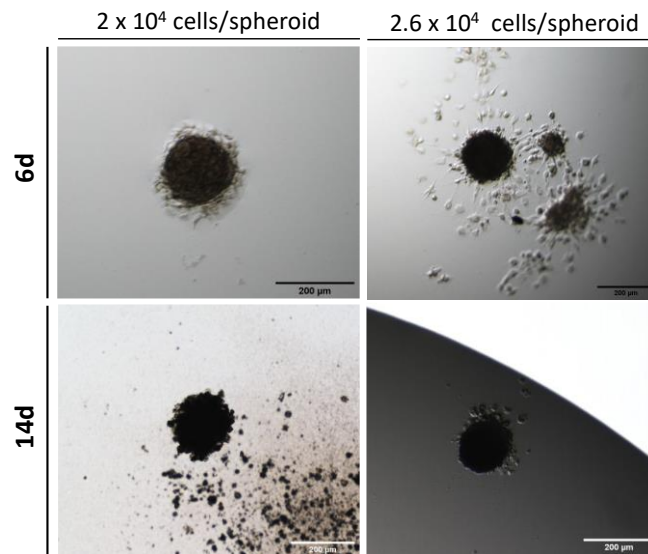
Figure 16 - P6 hMSC spheroids obtained through the HD method using 20 µL drops with 2.0×10^4 and 2.6×10^4 cells each. Spheroids monitoring between 6 and 14 days (scale bar 200 µm).

In the hanging drop technique, cells are aggregated by gravitational force and it is reported that, due to the absence of direct contact with solid surfaces, the composition of ECM proteins is the main factor for the regulation of spheroid microenvironment [53]. Therefore, the hanging drop technique can generate MSC spheroids of controlled size and number. However, its main limitations are the laborious preparation of the 3D cultures that significantly limits the large-scale production of spheroids for *in vivo* applications [44,51,52], alongside with the long-term desiccation of the drops, even with the hydration chamber with PBS at the bottom of the culture plate, and with increasing O_2 and nutrient deprivation throughout the assay. This last factor leads to the fact that each drop must be transferred to an individual well of a desired culture plate if the spheroids are to be kept viable in long-term cultures, so that the culture medium can be renewed, without the danger of disrupting the surface tension of each drop. Because of that, after 17 days, the pre-HD originated spheroids were transferred to ultra-low attachment round-bottom (U-bottom) 96-well plates coated with agarose (1.5% [w/v]). The idea was to monitor their growth and also improve their spheroidicity by using different gradients of carboxymethylcellulose (CMC) supplementation (Figure 17).
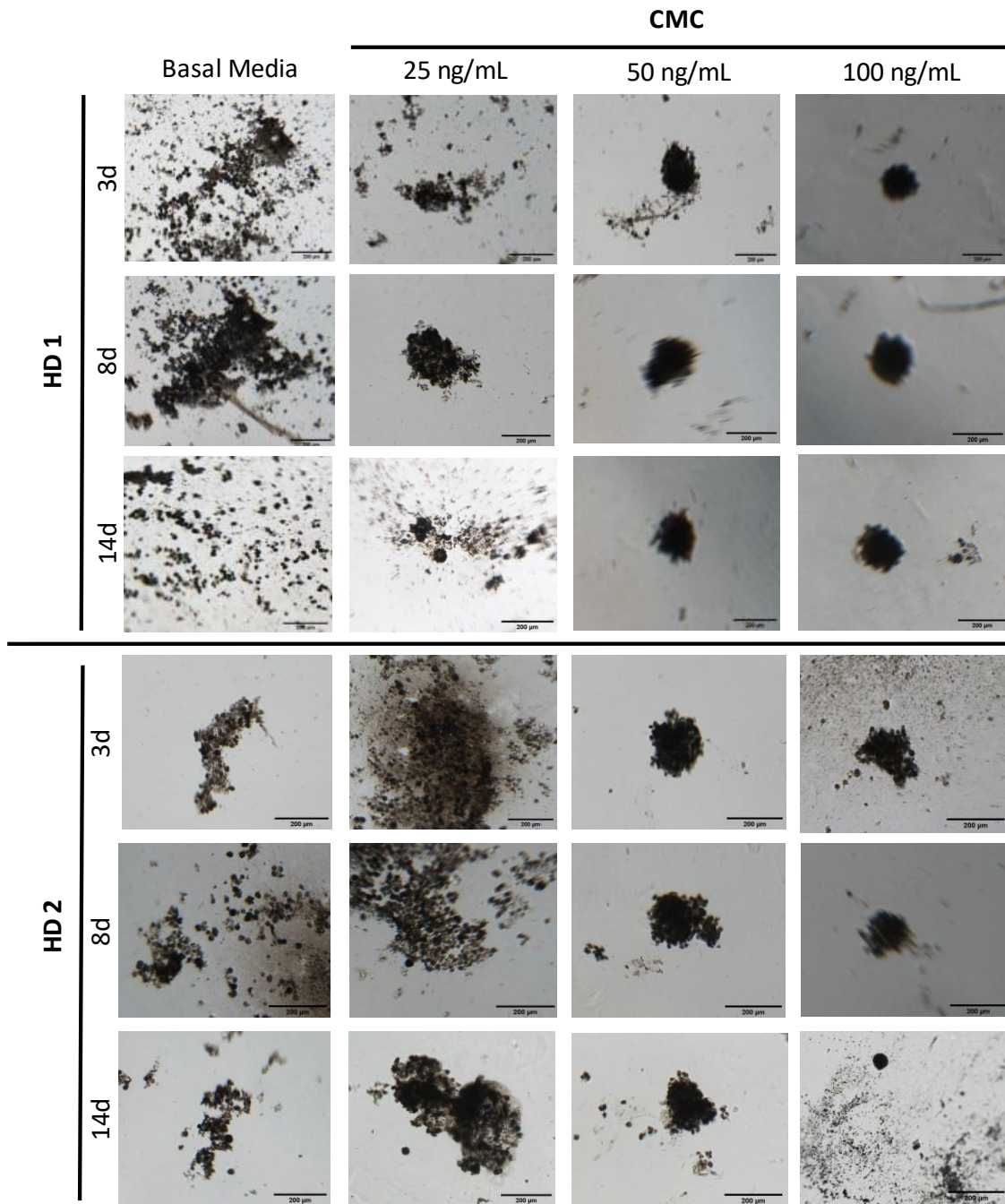
*Figure 17 – Previously generated HD spheroids of P6 hMSC transferred to 1.5% [w/v] agarose-coated U-bottom 96-well plates after their maturation for 17 days (scale bar 200 µm). Cellular aggregates' behaviour was monitored both in the absence, as well as in the presence of CMC in media. The results are presented as a function of the number of days after spheroids' transfer. **HD 1** – initial 2.0 x 10^4 cells/drop; **HD 2** – initial 2.6 x 10^4 cells/drop.*

After transferring the pre-HD generated spheroids to the ultra-low attachment (ULA) plates, the rupture of the vast majority of spheroids was soon noticeable, resulting in the presence of heterogeneous cell suspension flakes, which highlights another limitation of this technique: the need to submit the spheroids to external pressures for their transfer.

Namely, subjecting the "newly-formed" 3D models to this extra pipetting-step leads to their disintegration and loss of spheroidicity. However, in the few cases where it was possible to transfer a complete cell aggregate with a pseudospherical morphology, it was found that the higher concentrations of CMC in the culture medium allowed this same morphology to be preserved to some extent.

Although the hanging drop technique works well for primary hMSCs, the spontaneous aggregation of cells in liquid medium only using ultra-low attachment surfaces reveals itself as a more appropriate mean for spheroid further analyses, and downstream differentiation studies. For these future studies, the integrity of the spheroids is necessary. In addition to that, the handling is easier and the volume of medium higher, which prevents starvation and dehydration in long-term cultures [74]. Indeed, MSCs spheroid preparation in a non- or ultra-low adherent environment is usually more rapid, and low-cost [44,51,52]. Having this in mind, this spheroid generation method was tested in long term cultures using 1.8×10^4 and 2×10^4 cells per spheroid (Figure 18), simultaneously evaluating the influence of the presence of the CMC polymer supplement in the medium.
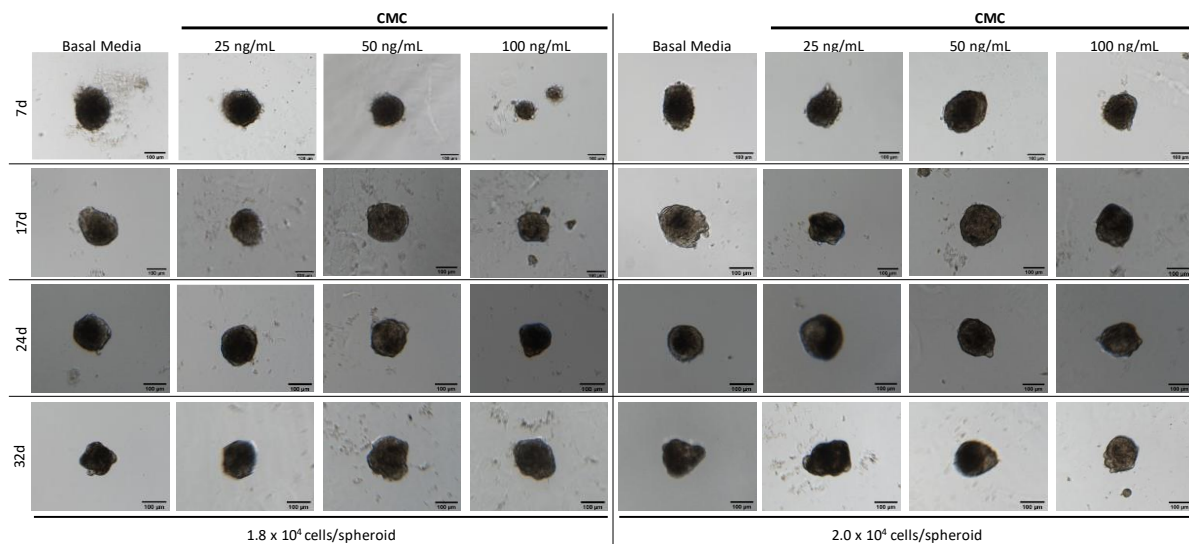
Figure 18 – P5 hMSC spheroids monitoring over 32 days after spontaneous aggregation of different cell densities through static suspension cultures on U-bottomed 96-well Agarose-coated (1.5% [w/v]) plates using α-MEM supplemented with CMC at 25, 50 and 100 ng/mL (scale bar 100 μm).

Cellulose is the most abundant polysaccharide in nature, displaying a regular and linear polymer of D-glucose units linked by glycosidic bonds. The hydroxyl groups

present in the monomers of this polymer create intra- and intermolecular hydrogen bonds, granting a stiff structure, forming crystalline regions due to the low accessibility to reactants [75]. Therefore, cellulose and its derivatives, such as sodium carboxymethyl cellulose (NaCMC) and methylcellulose (MC), are often presented in the literature as semi-solidification agents in 3D cell culture media. NaCMC is known to be less viscous than MC, presenting better dissolution rate and solubility profile, providing an homogeneous environment for cells. This cellulose derivative also possesses deflocculating properties because of the anionic carboxyl groups [75].

For these reasons, CMC (NaCMC) was used in these assays. The addition of the CMC polymer to the cell culture medium leads to an increased viscosity of the medium, preventing the cells from sedimenting and adhering to any possible breaches in the coating layer. This polymer is expected to induce cells to promptly form aggregates, leading to cohesive spheroids with improved spheroidicity [76]. Recent reported research papers have associated a significant modulating role with cellulose polymers viscosity, influencing cell morphology, paving the way to generate uniform spheroids [75].

To determine the influence of CMC on the growth and appearance of the spheroids, different concentrations of the polymer in cell culture medium were tested and control experiments were performed without the polymer addition. To determine the best concentration of this polymer in the culture medium, three different values were tested: 25, 50, and 100 ng/mL. In addition to morphological monitoring of the generated spheroids using brightfield optical microscopy (Figure 18), measurements of the average diameter of the spheroids were taken throughout the assays (Figure 19).
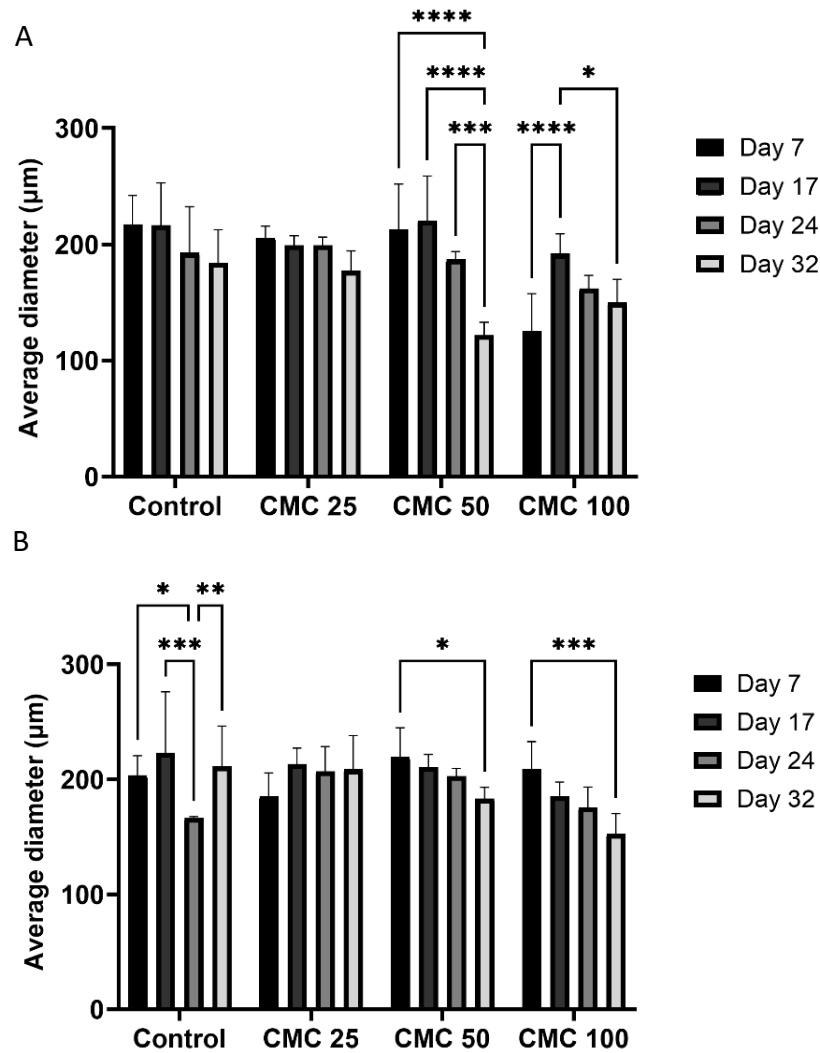
Figure 19 – P5 hMSC spheroids average diameter measurements using the software ImageJ over 32 days after spontaneous aggregation of cells in static suspension cultures on U-bottom 96-well Agarose-coated (1.5% [w/v]) plates. Culture medium supplemented with 25, 50 and 100 ng/mL of CMC was tested. Initial seeding of 1.8×10^4 cells/spheroid (A), and of 2.0×10^4 cells/spheroid (B). The results are expressed as mean of six replicates ± s.d. *p ≤ 0.05; **p ≤ 0.01; ***p ≤ 0.001 ; ****p ≤ 0.0001.

Spheroids were spontaneously formed by cell aggregation when using the ultra-low attachment cell culture dishes. Focusing on the micrographs taken (Figure 18), for both cell densities, the influence of CMC is almost unnoticeable to an inattentive eye; however, paying closer attention, one can observe a higher spheroidicity when it is present. When analysing the average diameter of the spheroids (Figure 19), one can see that some shrinking generally occurred and that the presence of CMC had no effect on the process. However, it is also possible to verify that the higher the cell concentration, the more decelerated this shrinking phenomenon seems to be, even if the tested difference in cell concentration was relatively small (about 10%). Shrinking especially

occurred after 24 and 32 days of culture. This suggests that shrinking might be an intrinsic property of the extracellular matrix (ECM) that cells are producing as time progress, and not exclusively related to cell proliferation. When the highest cell density was used, the best results were obtained with CMC concentrations of 25 and 50 ng/mL (CMC 25 and CMC 50). In fact, for these CMC concentrations, the size of the spheroids remained stable (the significantly different value of average diameter observed for CMC 50 at day 32 is not relevant compared with the initial size of the construct) and CMC presence clearly contributed for the improvement of spheroidicity.

Once the effectiveness of CMC supplementation in controlling the size and morphology of the spheroids was proven, it was necessary to determine whether this polymer interfered in any way with cell viability in the generated 3D models. Therefore, spheroids were collected from static suspensions after 40 days in culture to perform the Live/Dead Assay (Figure 20). This assay, allows a gross internal architecture evaluation, allowing to detect eventual external proliferative and inner necrotic zones in the generated spheroids, through the spatial distribution of live (green) and dead (red) cells.[1]
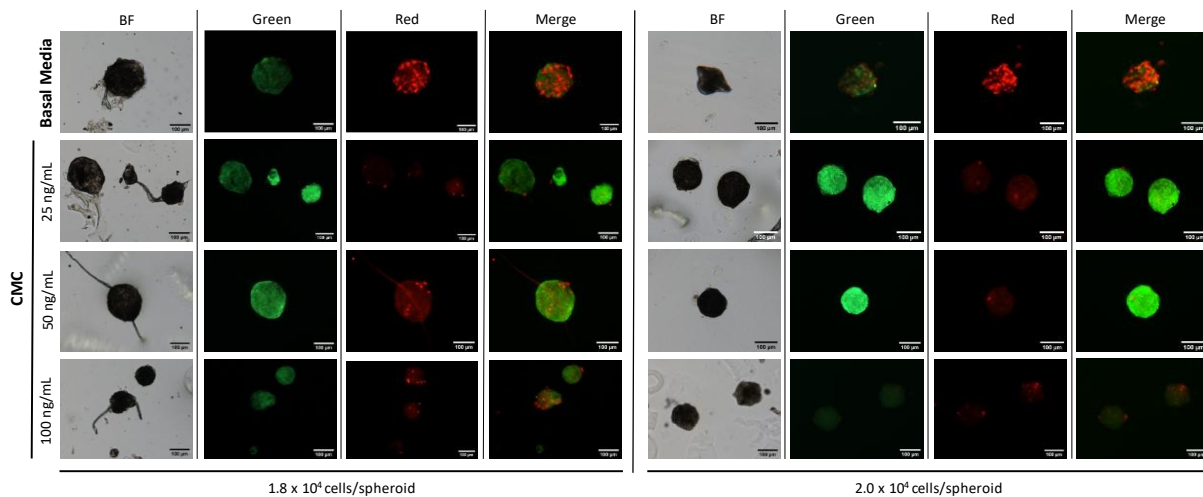
Figure 20 – Live/Dead staining with FDA/PI of P5 hMSC spheroids 40 days after spontaneous aggregation on static suspension cultures on U-bottom 96-well Agarose-coated (1.5% [w/v]) plates using Basal Media as the control experiment, as well as medium supplemented with CMC at 25, 50 and 100 ng/mL (scale bar 100 µm). Initial seeding of 1.8 x 10⁴ cells/spheroid and 2.0 x 10⁴ cells/spheroid.

[1] During the experimental work, it was possible to verify the existence of a necrotic core and a proliferative zone in the periphery of the spheroids using z-stacking (*data not shown*).

Through the Live/Dead assay, it was possible to determine that the decrease in spheroid size observed for the control groups was accompanied by the loss of cell viability, since almost no viable cells were detected. Once again, the best results were associated with 25 and 50 ng/mL CMC in the media. For both cases, an external viable shell (green) was detected, as well as a lower detection of dead cells (red). The unstained areas present can be attributed to the presence of ECM. CMC revealed not only to be crucial in terms of spheroid morphology, but also improved cell viability, probably due to its intrinsic ability to retain water as well as to retain and stepwise release the nutrients present in the culture medium [77].

3.1.2. Cell viability and spheroidicity enhancement

Based on the previous results, from here forward, it was decided to prepare spheroids by cell aggregation only using ultra-low attachment cell culture dishes and to include CMC in the medium at a concentration of 50 ng/mL.

As such, a set of additional experiments were performed having in view the enhancement of cell viability inside the spheroids and the improvement of their spheroidicity. ULA plates were used to prepare the static suspensions, but this time with a poly-HEMA coating instead of the agarose-coating used before.

The method of ULA preparation using poly-HEMA is less labour intensive and faster to obtain, allowing for a thinner coating layer to be obtained, which repels cells from the bottom of the well, preventing their adhesion, at the same time that allows for better imaging, consenting higher magnifications to be used without the inconvenient focusing difficulty that can arise when the agarose-coating layer is used (it is too thick). It should also be mentioned that the use of round-bottom (U-bottom) plates combines the advantageous characteristics of using surface tension and gravitational force with the ease and practicality of using ULA plates (the use of non-adhesive materials to inhibit cell attachment to the substrate), forcing cell aggregation at the apex of each well.

Having in view that spheroids applicability can be in tissue engineering, where hMSCs are aimed at chondrogenesis induction and a high-cell density is required, 3.0×10^4 cells were seeded per each spheroid in these new experiments. Due to the size of the spheroids generated, they were generated and maintained in a high glucose medium

to increase the viability of the spheroids, to maintain an active outer proliferative zone throughout the entire assay, and to decrease the necrotic core as much as possible [77]. An additional supplementation of 4.5 g of glucose per litre of medium was then used in an attempt to mimic commercially available culture media, commonly used to generate organoid models, and to subject the spheroids to chondrogenic differentiation.

As previously discussed, in order to generate reproducibly homogeneous spheroids with a controlled size and enhanced spheroidicity, 50 ng/mL of the CMC polymer were also added to the culture medium after cohesive spheroid models were formed, being added to the culture medium after 7 days. The evolution of the spheroids was monitored over 15 days, being several parameters associated with their morphology evaluated, namely their diameter, circularity and solidity indexes (Figures 21 and 22).
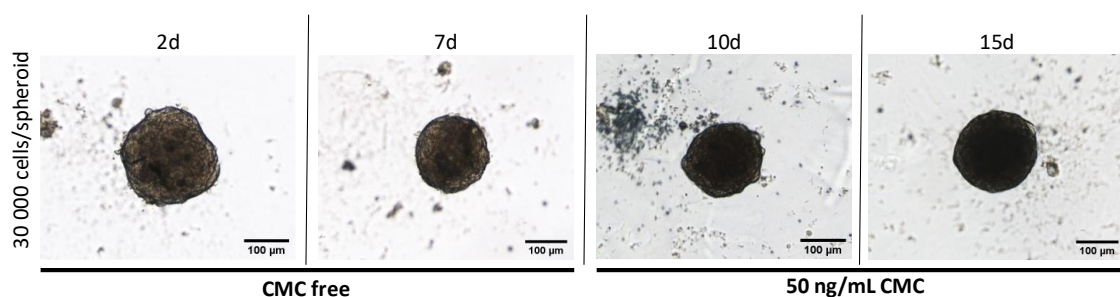
Figure 21 – P4 hMSC spheroids formation and monitoring between 2 and 15 days after spontaneous aggregation in static suspension cultures on U-bottom 96-well p-HEMA coated (2% [w/v]) plates, with the initial seeding of 3.0 x 10⁴ cells/spheroid. 50 ng/mL of CMC was added to enhance spheroidicity and control spheroid growth since day 7 (scale bar 100 μm).

Self-aggregation and spheroid formation was very uniform and reproducible, and all spheroids condensed to a stable size. In the initial stage, cell aggregates began to fuse, being driven by intercellular interactions and contacts, and early formed spheroid-like loose aggregates that were visible since day 2. From day 2 to day 7, spheroids suffered a slight shrinking, displaying a more cohesive appearance, and having smooth and continuous surfaces (day 2–7). After that, the border of the spheroids became a bit more ruffled, suggesting cell proliferation at the spheroid periphery (day 7–10), and individual cells were no longer distinguishable, similar to what was observed by other authors [78].
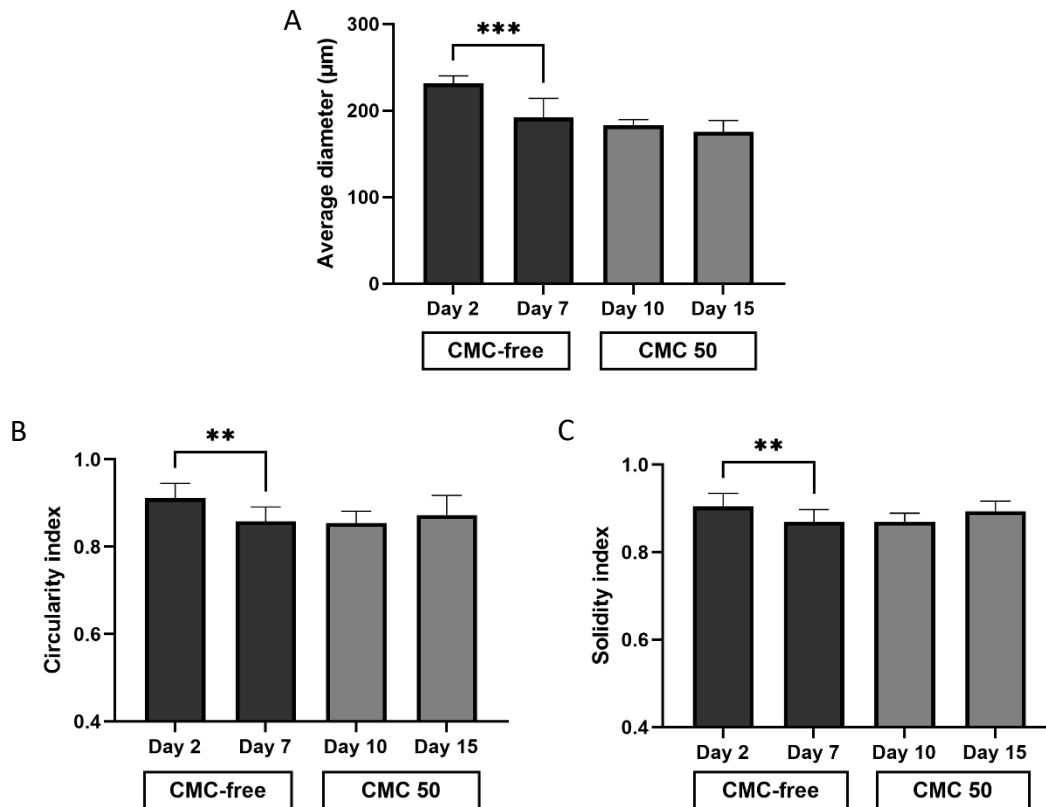
Figure 22 – P4 hMSC spheroids average diameter measurements (A), circularity (B) and solidity (C) indexes determination using the software ImageJ (n=6) over 15 days after their spontaneous aggregation o static suspension cultures with the initial cell seeding of 3.0×10^4 cells/spheroid on U-bottomed 96-well pHEMA-coated (2% [w/v]) plates. Spheroidicity enhancement and spheroid growth control was achieved by supplementing the medium with 50 ng/mL of CMC (CMC 50). The results are expressed as mean of six replicates ± s.d. $**p \leq 0.01$; $***p \leq 0.001$.

Indeed, after day 7 and addition of CMC as supplement, all evaluated parameters reached a plateau, remaining at a reasonably constant level throughout the 15 days of monitoring. The use of the stated concentration of CMC, high glucose in the medium, and round-bottomed ultra-low adhesion wells in 96-well plates was critical for the formation of highly uniform 3D multicellular spheroid models. The increased viscosity of the cell environment provided by the cellulose derivative added to the cell culture medium likely moderated the extrinsic vibration, and decreased the number of forces given to the spheroid, thus resulting in improved stability [79]. The solidity and circularity values shown were always high and were in line with the microscopy observations. The values of solidity and circularity stabilized after an initial decrease, which can be explained by possible cellular reorganization and ECM secretion processes [78].

3.2. Optimization of the chondrogenic medium using 2D cultures

Before studying chondrogenesis in spheroids, a study was performed in 2D cultures to assess the effect of the medium composition on cell behaviour (metabolic activity/cell viability and chondrogenesis). In particular, the influence on cells of the presence of TGF-β1 in the medium was evaluated, as well as of the presence of glutamine, glucose, and insulin.

The resazurin reduction assay gives information about the metabolic activity of cells and is often used as an indirect measure of cell viability [80]. As such, it was performed in hMSCs cultured in media of differing composition after 21 and 28 days (Figure 23).

The main objective behind this assessment of cell viability, was to determine if cells were healthy and retained their proliferative ability when exposed to certain supplements that are usually used in the formulation of chondrogenic media. In a first assay, and since chondrogenesis requires high cell densities, a seeding of 4×10^4 cells per well was used. The isolated effect of TGF-β1 (BM + TGF-β1) and its effect in conjunction with glutamine and glucose as extra supplements in the chondrogenic medium was evaluated (Figure 23).

It should be noted that the basal medium (BM) is composed of α-MEM with antibiotic/antimycotic and fetal bovine serum (complete medium), whereas the chondrogenic medium (CM) is prepared by adding to the basal medium several other constituents, namely proline, ascorbic acid, insulin-transferrin-selenium (ITS) supplement, sodium pyruvate, dexamethasone and TGF-β1.

*Figure 23 – Effect of medium composition (TGF-β1, glutamine, and glucose presence) on cell metabolic activity assessed by the Resazurin Reduction Assay after 21 and 28 days of culture (initial seeding of 4.0 x 10^4 cells/well, BM= basal medium, CM= chondrogenic medium). Concentrations: TGF-β1 (10 ng/mL), glutamine (2 mM), glucose (2.5 mM). The results are expressed as mean of four replicates ± s.d. *p ≤ 0.05; ****p ≤ 0.0001*

Mostly, there are no significant differences between the metabolic activity on 21 and 28 days. Thus, assuming that the metabolic activity and the number of viable cells are proportional, we can assume that cell proliferation reached a stationary stage.

The presence of TGF-β1 lead to an increased cell proliferation, since the metabolic activity in the presence of basal medium and the referred supplement (BM+TGF-β1) is higher than the control group (cells kept only in basal medium, BM) both at 21 and 28 days of chondrogenesis. Indeed, TGF-β1 lives up to its name (growth factor), promoting marked cell proliferation that translates into increased metabolic activity as already reported by others [81]. The chondrogenic medium also led to an increased cell proliferation, not only when compared to the control group (BM), but also when compared with the basal medium supplemented only with TGF-β1 (BM+TGF-β1).

Because of this finding, one can conclude that there are other components in the chondrogenic medium responsible for this proliferative effect. This is not surprising as it is reported that dexamethasone negatively regulates the transcription of genes associated to apoptosis, and positively regulates genes linked to cell proliferation [82]. Relatively to the presence of glutamine and glucose in the chondrogenic medium, these appear not to induce any significant changes in cell proliferation, even when combined.

The cultures made in a 2D environment in media with different composition were also analysed for chondrogenesis using histochemical assays. For this, cells were submitted to histochemical staining with Toluidine Blue O, also known as tolonium chloride (Figure 24). This is an acidophilic metachromatic dye that selectively stains acidic tissue components (sulphates, carboxylates, and phosphate radicals) [83].
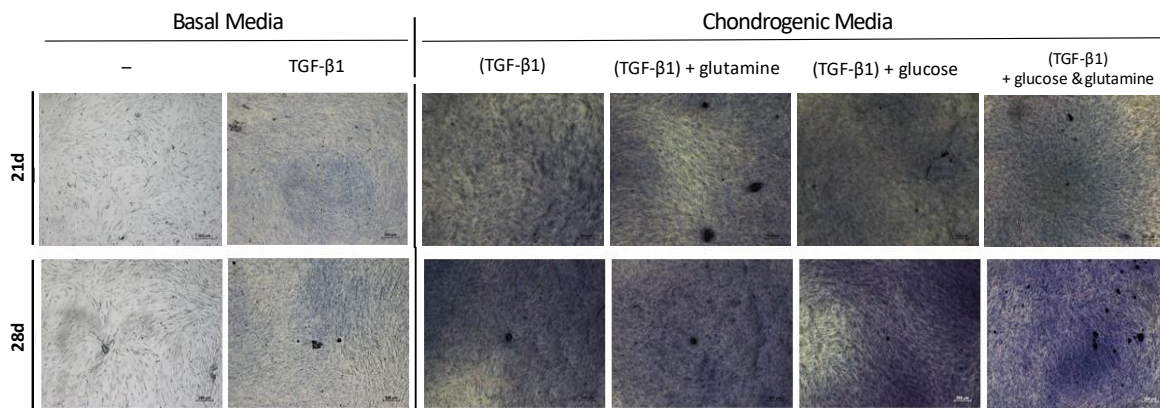
Figure 24 – Toluidine Blue O staining of P4 hMSCs cultured for 21 and 28 days (initial seeding of 4.0 x 10^4 cells/well) (scale bar 200 µm) in Basal and in Chondrogenic media containing different supplements: TGF-β1 (10 ng/mL), 2.0 mM glutamine and 2.5 mM glucose.

Staining tissues using this metachromatic dye is a well-established procedure for the histological assessment of cartilaginous and chondrogenic tissues; being a cationic dye, toluidine blue staining allows for proteoglycan detection in a tissue because of its high affinity for the sulphate groups in this constituents of the ECM [84]. A slight blue colour appeared in the cultures under the influence of TGF-β1 alone (BM+TGF-β1). But the clear presence of cartilaginous ECM is undeniable for all cultures induced to differentiate by all chondrogenic media formulations, with and without the extra supplements of glutamine and glucose, when compared with the basal medium. As such, not only the chondrogenic medium leads to an increase in cell number, but it also promotes the differentiation process (as expected). The purplish/blue colour obtained

after staining the cultures with Toluidine Blue O also increased in intensity from day 21 to day 28, thus showing the progress of differentiation. This is in agreement with the previous metabolic activity results as cells undergoing differentiation usually decrease their rate of proliferation.

In addition, it was also observed that there is an increase in cartilaginous ECM deposition from day 21 to 28 of the differentiation assay, and this deposition is more pronounced in cultures subjected to chondrogenic medium with the extra glucose supplement. These results are coherent with the information stated in the literature, since glucose is a well-known critical energy supply and key metabolite for most cells, playing a crucial role in cell fate and cell differentiation [85]. Some studies demonstrate the effect of glucose concentration in the enhancement of hMSC chondrogenic potential, claiming that glucose availability in cell microenvironment regulates TGF-β signalling, priming precursor hMSC for subsequent chondrogenesis [85]. It is described that pre-chondrogenic cells aggregate to form pre-cartilaginous condensates, and that the cells within the centre of these condensates subsequently begin their differentiation process, turning into chondroblasts, being this in association with the acquisition of a more ovoid/round shape and the elaboration of a chondrocytic matrix rich in proteoglycans [86]. The proteoglycan detection in the chondrogenesis induced cultures in association with the presence of pre-chondrogenic nodules (the dark cell agglomerates) visible in the micrographs unravels the chondrogenic potential of the different chondrogenic media formulations tested.

3.2.1. Influence of glucose vs insulin supplements

There is scientific evidence regarding the role of insulin-like growth factor-I (IGF-I) in chondrogenic differentiation induction, that is, chondrogenic differentiation can be induced when exposing cells to physiological concentrations of IGF-I [87]. Moreover, some studies report a stimulation of differentiation upon exposure to insulin, referring that this supplement can work as a mild substitute for IGF-I signalling in cellular pathways [87].

As such, it was also decided to evaluate the influence of insulin on cell behaviour. This time the influence of glucose, insulin, and the combination of these two extra

supplements in hMSCs was the main focus. These assays counted, once again, with control cultures maintained in basal medium. In turn, the basis of the chondrogenic media consisted of the previous primary composition now with 2 mM glutamine as well. First, the metabolic activity of cells exposed to the media containing different supplements was studied (Figure 25).
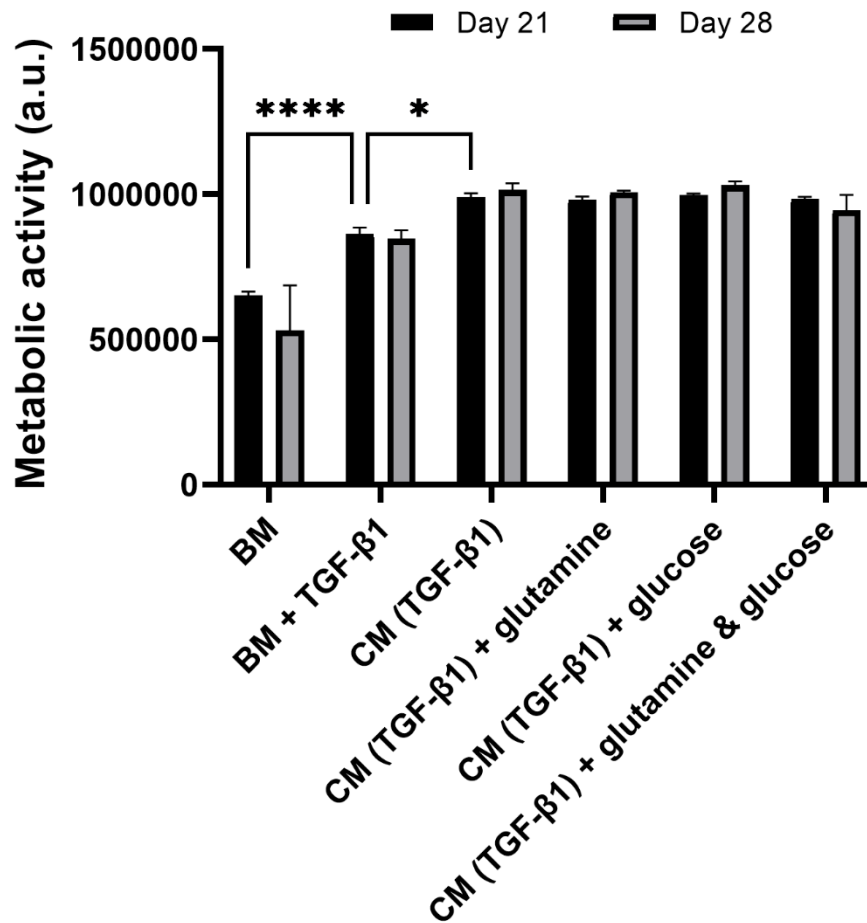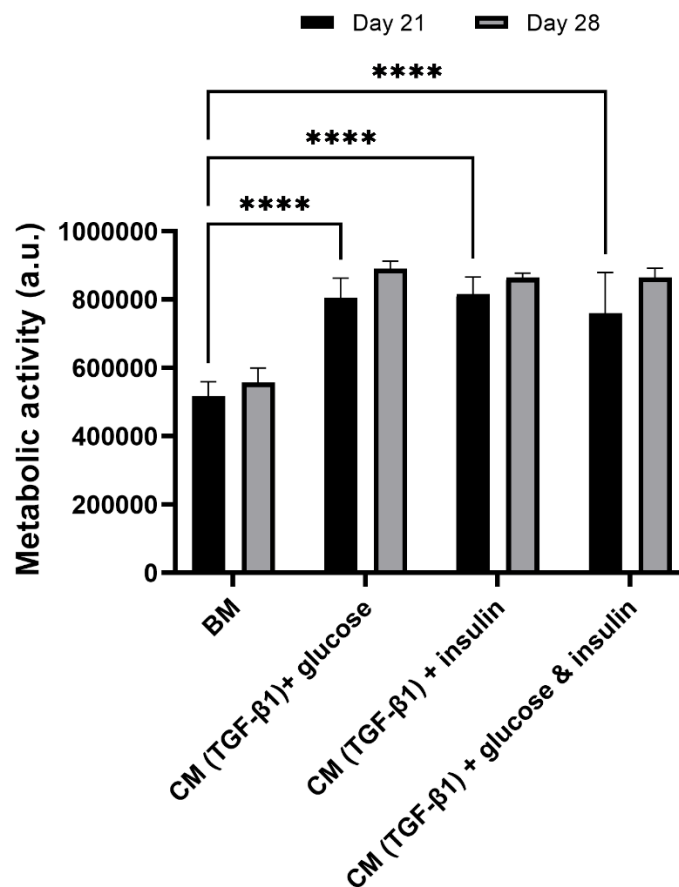

Figure 25 – Effect of medium composition (TGF-β1, glucose, and insulin presence) on cell metabolic activity assessed by the Resazurin Reduction Assay after 21 and 28 days of culture (initial seeding of 3.0 x 10⁴ cells/well, BM= basal medium, CM= chondrogenic medium). Concentrations: TGF-β1 10 ng/mL, glucose 2.5 mM, and insulin 5 µg/mL. The results are expressed as mean of six replicates ± s.d. ∗∗∗∗p ≤ 0.0001.

Even if this experiment was performed using an inferior cell number than the previous one (3.0 x 10⁴ cells instead of the 4.0 x 10⁴ used in the previous one), once again it was possible to conclude that the proliferation rate of cells was higher in chondrogenic media (with or without glucose). Moreover, not only glucose, but also insulin, had no effect on cell proliferation. Again, cell proliferation between 21 and 28 days of culture time was very low in all cases.

Considering the previous studies, the differentiation potential after 21 and 28 days was evaluated, performing histochemical stanning with two other dye combos: Fast Green/Safranin O, and Alcian Blue/Nuclear Fast Red (NFR), besides the Toluidine Blue O staining already tested. For the monitoring of the chondrogenesis, samples were submitted to histochemical stanning to detect the presence of cartilaginous ECM (Figure 26).
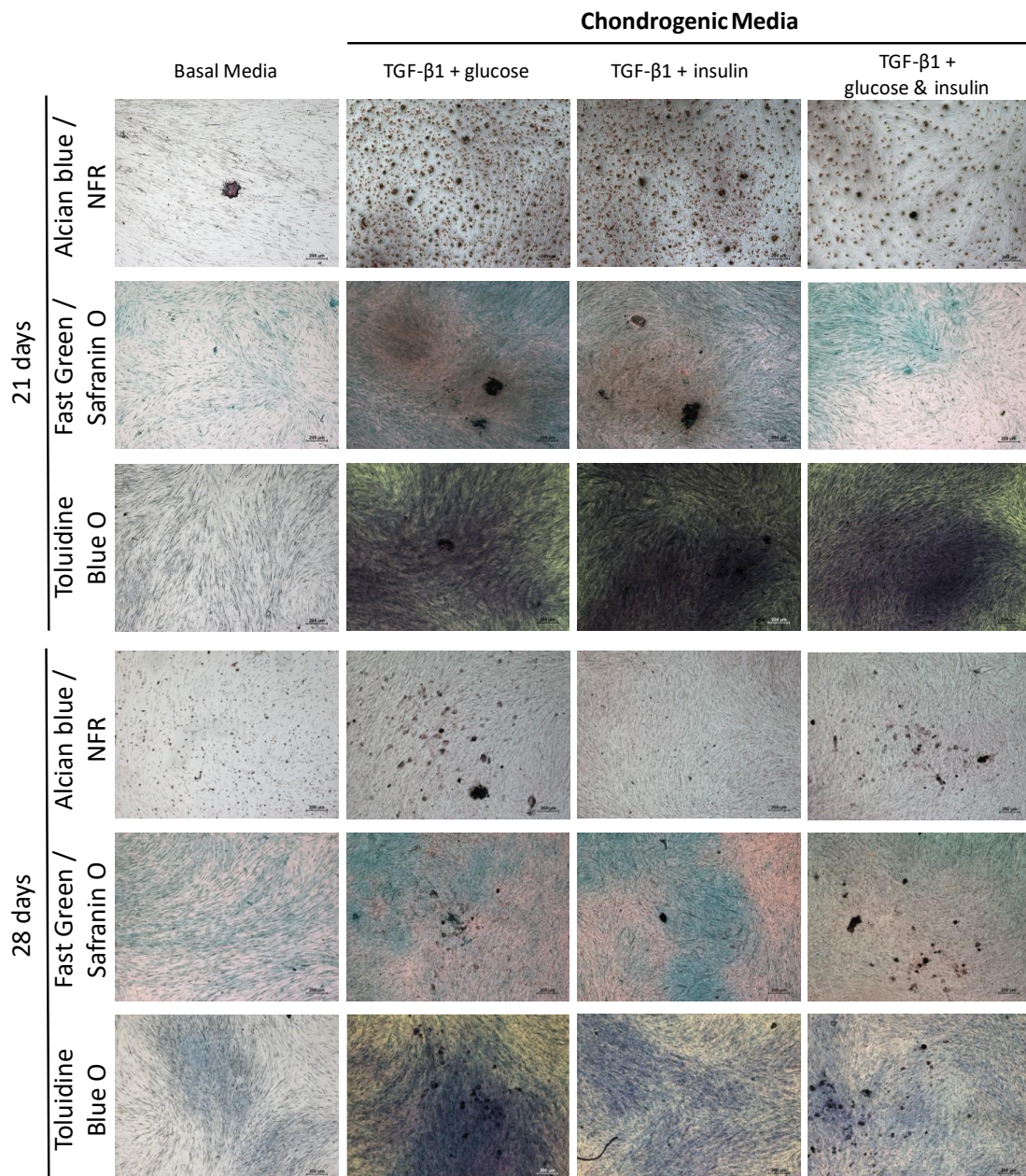
Figure 26 – Alcian Blue 8G/Nuclear Fast Red (I), Fast Green/Safranin O (II) and Toluidine Blue O (III) staining of P4 hMSCs cultured for 21 and 28 days (initial seeding of 3.0 x 10⁴ cells/well) (scale bar 200 μm) in Basal and in Chondrogenic medium containing different supplements: glucose (2.5 mM), insulin (5 μg/mL) and the combination of both.

Both Safranin O and Toluidine Blue O are cationic dyes that stain proteoglycans as well as glycosaminoglycans. Toluidine Blue O has been reported to provide more intense staining, due to the fact that it has a higher affinity for the sulphur in cartilage compared to Safranin O [88]. Safranin is mostly used for the identification of cartilage, mucin, and mast cell granules. Its staining works by binding to acidic proteoglycans in cartilage tissues with a high affinity forming a reddish to orange complexes. Safranin O is a basic dye that stains growth plate cartilage and articular cartilage (proteoglycans, chondrocytes, and type II collagen) with varying shades of red. The intensity of Safranin O staining is proportional to the proteoglycan content in the cartilage tissue [89,90]. Fast green is a green dye vastly used in optical microscopy that stains cellulose, cytoplasm, collagen, and mucilaginous tissues green; this dye is frequently used with safranin as a counterstain [91].

Alcian Blue is often used to identify chondrocytes from differentiated cultures of both human and rodent mesenchymal stem cells. Alcian blues are a family of polyvalent basic dyes, of which, the Alcian Blue 8G has been historically documented as the most common and the most reliable member, being commonly used to stain acidic polysaccharides such as glycosaminoglycans (GAGs) in cartilage [92]. NFR is used as a counterstain to allow some contrast with the blue dye. NFR is an optimized nuclear counterstain solution that produces an intense nuclear stain requiring only one step and staining the nucleus in just five minutes [93]. This stain is composed of an anionic anthraquinone dye, used in conjunction with a mordant, usually an aluminum salt; and can also be called as Kernechtrot or Calcium Red. This versatile dye selectively stains nuclear chromatin red, while the nonspecific signals display pink tones. This staining solution offers a faster, optimized, intense and simpler multi-labeling nuclear counterstain alternative in comparison to the traditional use of hematoxylin [94].

Globally, analysing the obtained histochemically stained micrographs, it is quite noticeable that, in general, cell morphology changed in the presence of the chondrogenic medium, going from fusiform-like cells to cells with a rounder appearance. These rounder cell aggregates (condensation nodules, as described in literature regarding chondrogenesis [95]) are associated to the chondrogenic process. On the contrary, for the control experiments, cell morphology remained virtually unchanged,

and there was no staining indicative of the presence of cartilaginous ECM, indicating that the adherent cells preserved their stemness.

Just based on the histochemical experiments, it was not possible to distinguish the effect of glucose or insulin (alone or in combination) on the extent of cell differentiation.

Regarding Alcian Blue colour staining, it is only possible to detect a slight bluish tone for all cultures kept in chondrogenic media. However, NFR allowed for a clear detection of the conformational changes that occurred during the differentiation process with the cells in culture going from the typical adherent fusiform shape to a rounded morphology (the rounded cells condensed into pre-cartilaginous nodules).

The abundant deposition of GAGs and proteoglycans is flagrant in the presence of the chondrogenic media and extra supplements of glucose and insulin as well (orange for the Safranin O staining, and purple for the Toluidine Blue O staining). The intense bluish-green colour staining of Fast Green revealed de deposition of collagen as well.

Total protein content and ALP activity were also assayed to evaluate the behaviour of the hMSCs when exposed to all chondrogenic media formulations (Figure 27). Samples maintained in basal medium were used as reference controls.

The total protein content in culture has a similar trend to that observed for the metabolic activity (Figure 25), that is, protein values are higher when cells are exposed to chondrogenic media than when basal medium is used. Yet, sharper differences are noticed between days 21 and 28 in the case of total protein quantification, with much higher levels of protein on day 28 than on day 21 (regarding metabolic activity, that is usually well correlated with cell proliferation, these differences were comparatively much smaller).

Having in mind that the total protein in culture is the sum of the cells' constituent protein and the extracellular protein (ECM), it appears that the cells, after attaining the stationary phase of their growth, are actively depositing matrix. This deposition was also confirmed by the analysis of the micrographs obtained during the histochemistry studies. Clearly, taking into account both the histochemical analysis and the quantification of the total protein content, for the different cultures maintained in chondrogenic medium, it is possible to infer that this protein content is due to increased

collagen synthesis (also detectable by Fast Green staining) and increased synthesis of proteoglycans (Safranin O and Toluidine Blue staining).
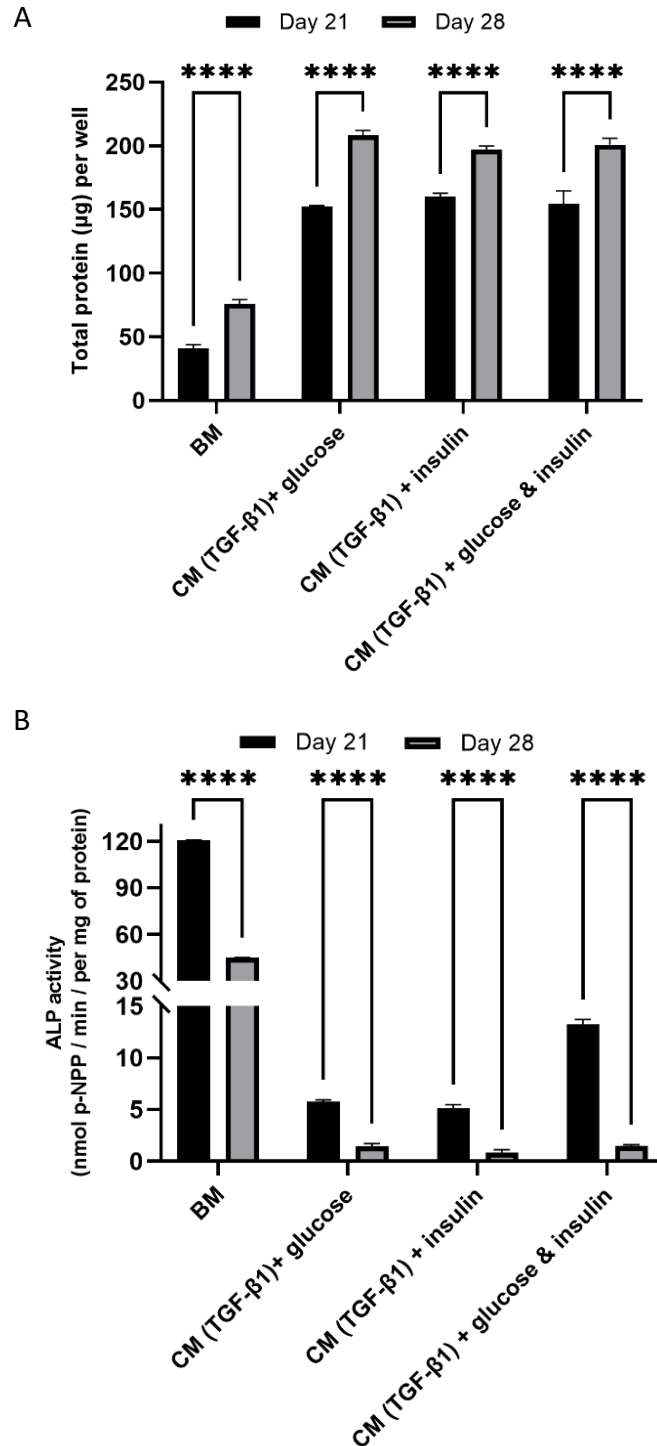
*Figure 27 – (A) Total protein content (µg) assessed by the BCA assay and (B) alkaline phosphatase activity measured at days 21 and 28 of hMSCs culture (initial seeding of 3.0 x 10⁴ hMSC per well). BM= basal medium, CM= chondrogenic medium. The results are expressed as mean of six replicates ± s.d. ****p ≤ 0.0001.*

ALP activity was determined at 21 and 28 days of culture and its values are normalized for the protein content. The assessment of ALP activity in culture is important as it is a marker of the hypertrophic phase of chondrogenic differentiation [11,60]. Although not desired, it is known that MSCs may follow an "endochondral" differentiation [96]. In the experiments performed, after 21 and 28 days in culture, the cells cultured in chondrogenic medium did not show significant ALP levels, in other words, the cultures did not reach the hypertrophic phase. Moreover, all cultures exposed to the chondrogenic media displayed a decrease in enzyme activity between 21 and 28 days. In fact, TGF-β1 is known to inhibit the growth of hypertrophic chondrocytes in culture plates, which is a plausible reason for the absence of the expected ALP activity rise at the end of the chondrogenesis process [60]. Surprisingly, cells cultured in basal medium (BM; without chondrogenesis or even osteogenesis inducing supplements) show much higher ALP levels at 21 and 28 days (with 21-day values lower than 28-day values). Possibly, in the absence of chondrogenesis inducers, these cells followed an osteogenic differentiation *in vitro*. In this case, it is known that ALP levels reach peaks between 2 and 3 weeks in culture [97].

3.3. Chondrogenesis in 3D cultures

Multicellular systems have earned great significance over time in the fields of tissue engineering and regenerative medicine. However, the recreation of complex tissue architectures is very challenging, being very time consuming, and often relying on expensive techniques. In this section, a practical, relatively cheap, fast, and reproducible technique for spheroid preparation was followed based on the experience gained in the previous experiments.

Here, hMSC spheroidal constructs were spontaneously generated and maintained in static suspensions, aiming to generate cohesive, high-density models of chondrospheres. First, 3D multicellular spheroids were obtained by spontaneous aggregation on ULA U-bottom 96-well plates coated with PolyHEMA 2% [w/v] (initial seeding of 30 000 cells/spheroid). After, spheroids were allowed to mature until 14 days in the presence of high glucose concentration (as a guarantee of improved cell viability). CMC was added to the medium since day 5 to stabilize spheroids' morphology throughout the assay (Figure 28).

As expected, the hMSCs self-assembled spontaneously into slightly irregular shaped spheroids after 3 days of culture when seeded onto polyHEMA-coated U-bottom wells, resulting from a combination of different factors, among which the repulsion caused by the polymer coating layer and the gravitational forces that cooperate with the round-bottom wells (Figure 28). As the culture time increased, spheroids became rounder and more compact, exhibiting a more dense and cohesive appearance, accompanied by a significant reduction in diameter from day 3 to day 14.

| 3d | 5d | 7d | 10d | 14d |

CMC free   **CMC 50 ng/mL**
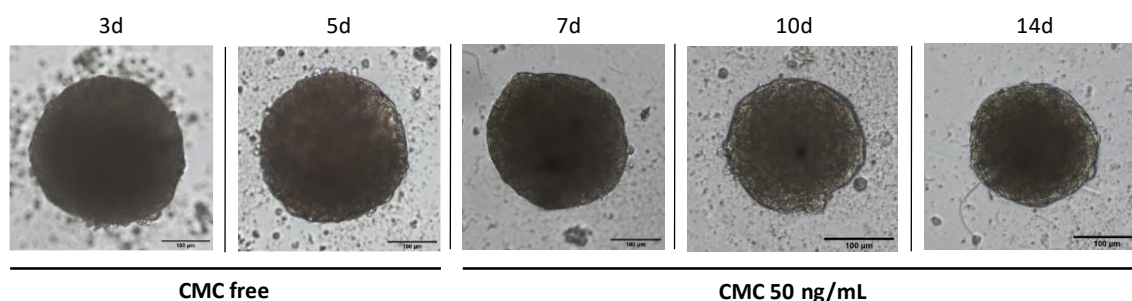
Figure 28 – P4 hMSC spheroids formation and monitoring between 3 and 14 days after spontaneous aggregation through static suspension cultures on U-bottomed 96-well pHEMA-coated (2% [w/v]) ULA plates, with the initial seeding of 3.0×10^4 cells/spheroid. 50 ng/mL of CMC were added to enhance spheroidicity and control spheroid growth since day 5 (scale bar 100 μm).

The scaffold-free approach used allowed to obtain spheroid architectures resulting only from spontaneous natural cell-cell interactions, due to gravity and the repelling-coated surface. Like also shown in the previous 3D construct models' optimization section, cells condensed and suffered shrinking over time, having stabilized since day 10 (Figures 28 and 29 – A). The addition of CMC polymer to the culture medium led to size and morphology stabilization, which was visible not only by microscopy, but also through the circularity and solidity indexes determined (Figures 28 and 29). These features are of great interest since small diameter spheroids with uniform shapes and sizes may be necessary for compatibility with the needle used for injection in certain biomedical applications.

Figure 29 – P4 hMSC spheroids average diameter measurements (A), circularity (B) and solidity (C) indexes determination using the software ImageJ (n=8) over 15 days after their spontaneous aggregation o static suspension cultures with the initial cell seeding of 3.0×10^4 cells/spheroid on U-bottomed 96-well pHEMA-coated (2% [w/v]) plates. Spheroidicity enhancement and spheroid growth control was achieved by supplementing the medium with 50 ng/mL of CMC (CMC 50). The results are expressed as mean of eight replicates ± s.d. ∗∗p ≤ 0.01, ∗∗∗∗p ≤ 0.0001.

The appealing aspect of resorting to scaffold-free approaches is partially derived from the successful outcomes of some reported 3D autologous chondrocyte transplantation, carrying out significant improvements in patients' life quality and health [98]. The generated chondrospheres represent a biofabricated microtissue construct that mimics the main structural and ECM biomechanical properties usually absent during the typical 2D chondrogenic maturation *in vitro* [98].

The injection of spheroids on injured patients can be used as a potential mean to treat cartilage defects, overcoming the challenges inherent to the injection of single cells. Single cells suspensions are often subjected to dedifferentiation, leading to inferior fibrous tissue deposition; while spheroid maturation commences *in vitro*, establishing tissue specific ECM prior to implantation/injection, due to their high cellularity and cell density [24]. Some clinical trials have proven the efficacy of chondrospheres, proving that these differentiated spheroids naturally adhere to cartilage defects after injection [24]. For this matter, the usage of hMSC is advantageous due to their inherent proliferative capacity, avoiding the invasion of the joint for the initial harvest of autologous chondrocytes [26]. In this scope, it is important to check if cells in the 3D constructs prepared in this thesis were able to differentiate towards the chondrogenic lineage when applying a chemically defined chondrogenic medium, similar to what was achieved in other works [24]. For this aim, the spheroids pass through 28 days of chondrogenesis induction after an initial 14 day maturation period.

To determine the chondrogenic potential of the 3D models generated, the mature spheroid constructs were exposed to a previously defined chondrogenic medium composed of high glucose basal medium supplemented with 4mM proline, 200 µM ascorbic acid 2-phosphate, 1mM sodium pyruvate, 100 nM dexamethasone, 1%[v/v] ITS + premix, 2 mM glutamine, 10ng/mL TGF-β1. Spheroids cultured in high glucose (4.5 g/L) basal medium (BM) were used as control experiments (a high glucose content was used to improve cell viability during the assays). All spheroids were exposed to an additional supplementation of the media with 50 ng/mL CMC throughout the whole assay to preserve the 3D models integrity and stability (Figure 30).
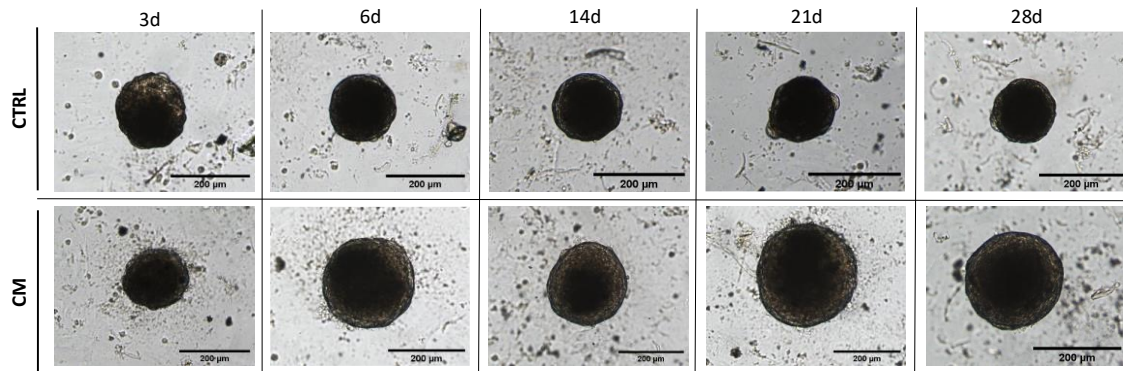
Figure 30 – Previously obtained P4 hMSC 14 days-old spheroids morphology monitoring along the chondrogenesis induction assay (28 days) in the presence of CMC polymer in the medium (50 ng/mL) (scale bar 200 µm). CRTL – control experiment: spheroids maintained in high glucose basal medium; CM – Chondrogenesis induction: spheroids maintained in chondrogenic medium.

This 3D spatial arrangement of cells into spheroids is known to enhance the differentiation process, mimics the natural environment, intensifying cell-communication and cell-ECM interactions [24]. The structural arrangement of the spheroids in conjunction with the supplements present in the chondrogenic medium clearly induced morphological changes in the cell behavior and fate. In the micrographs obtained throughout the assay (Figure 30), the differences are very obvious: spheroids in the control experiments continue to condense and suffer a mild and gradual shrinking, suggesting that cells reached a senescent phase; whilst the spheroids exposed to chondrogenic medium continue to grow until 21 days, just presenting a slight decrease in diameter between 21 and 28 days (Figure 31 – A). For the experimental spheroid models exposed to the cocktail of supplements that compose the chondrogenic medium, it was possible to distinguish a proliferative zone (lighter in color) and a necrotic core (darker center) (Figure 30). The proliferative zone increased until 21 days, proportionally to the diameter evolution, and this can be attributed mostly to dexamethasone and to TGF-β1, known to influence the synthesis of cartilaginous ECM [60]. Once again, it is clear that CMC does not influence cellular pathways, proving, however, to be an added value concerning stabilization of the morphology of the spheroid models. In this context, circularity and solidity indexes were maintained stable throughout the whole chondrogenesis assay (Figure 31 – B and C).
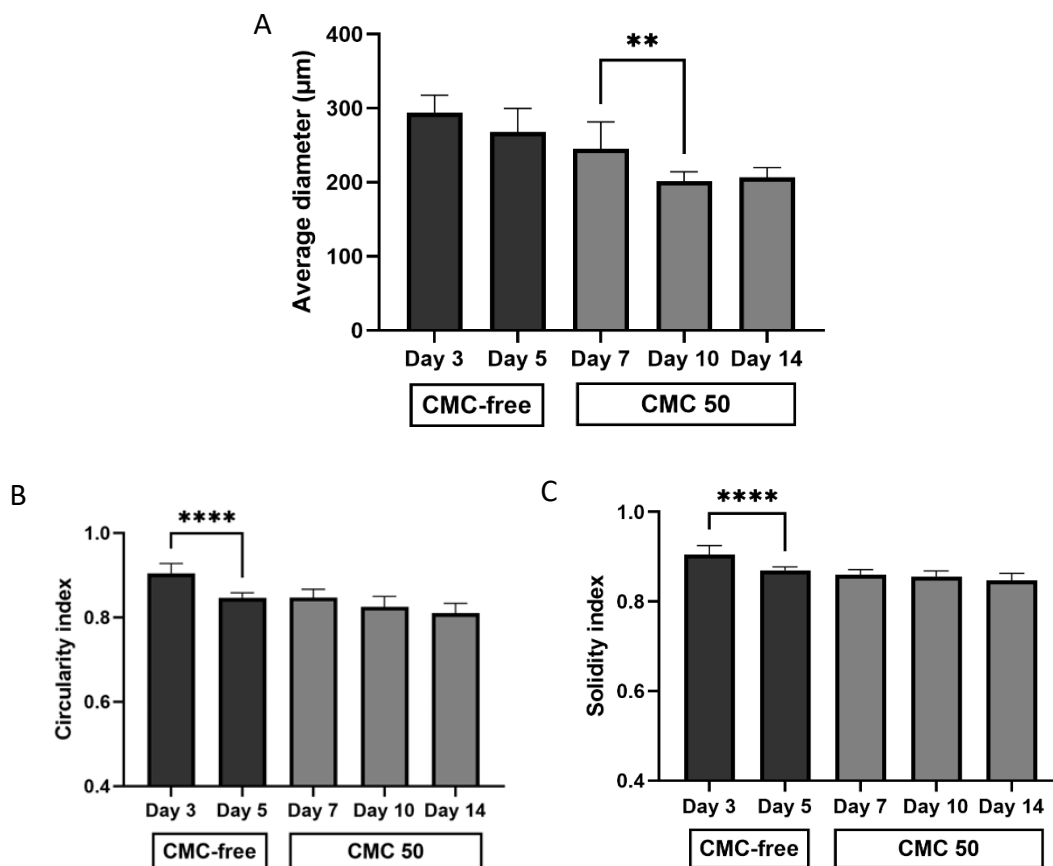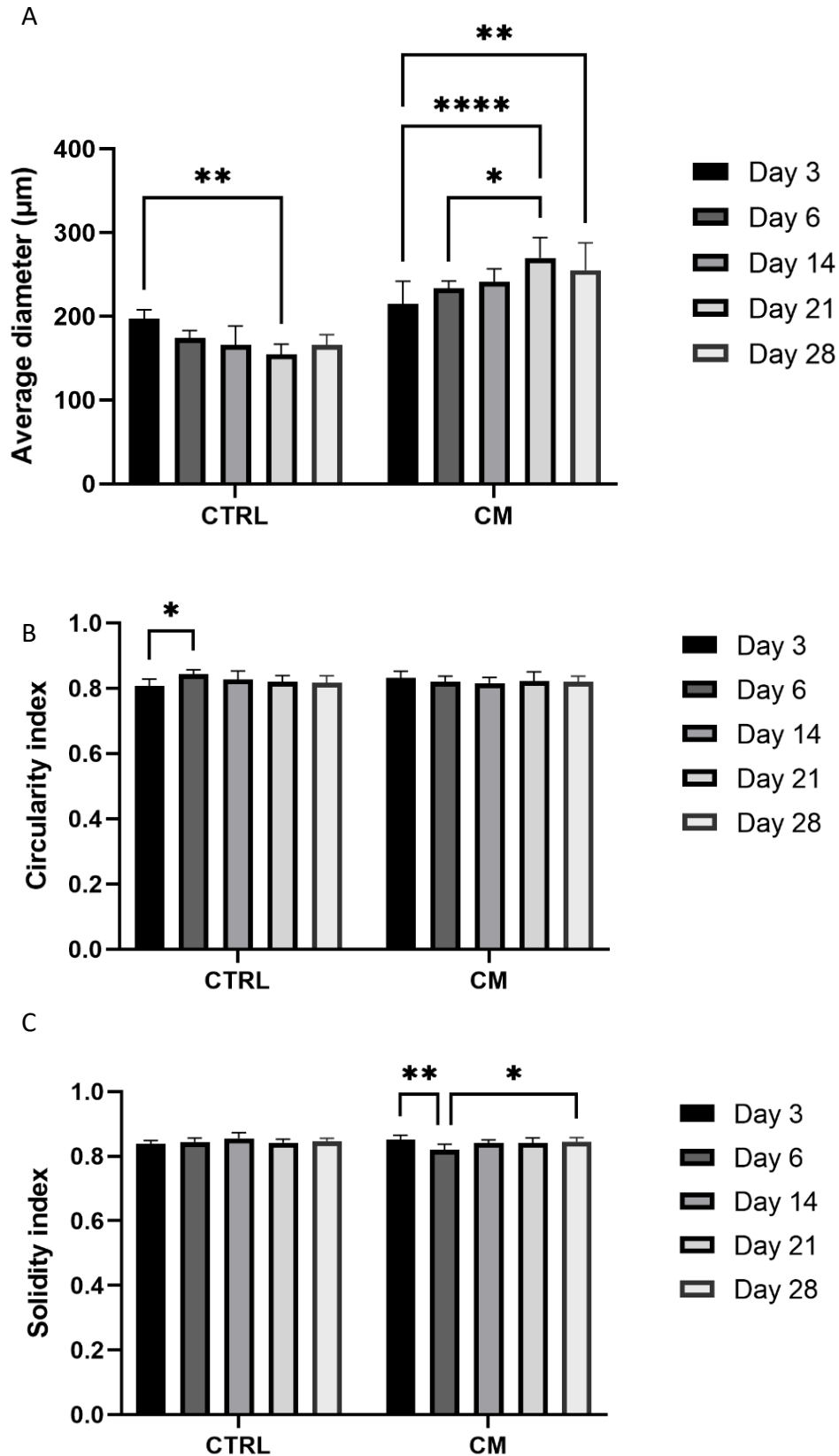
Figure 31 – P4 hMSC spheroids average diameter measurements (A), and circularity (B) and solidity index (C) determination using the software ImageJ (n=6) over the chondrogenic differentiation assay (28 days). CTRL – spheroids maintained on high glucose (4.5 g/L) basal medium; CM – spheroids maintained on chondrogenic medium. The results are expressed as mean of six replicates ± s.d. ∗p ≤ 0.05; ∗∗p ≤ 0.01.

The viability of the spheroid models generated was evaluated with the Live/Dead assay (Figure 32). The qualitative assessment of the chondrospheres' viability (CM spheroids) when compared to the CTRL spheroids revealed a satisfactory amount of living cells during prolonged cultures (28 days of chondrogenesis induction after a 14-days maturation period).

The majority of viable cells is mostly observed at the periphery of the spheroids, confirming the presence of a proliferative zone. This proliferative zone is much more prominent for the chondrospheres in the presence of the CM medium than for the CTRL spheroids.

For the samples exposed to the chondrogenic medium (CM), the population of nonviable cells increased at the latest stage of cultivation, between 21 and 28 days of the chondrogenesis induction assay, becoming the necrotic core more evident.
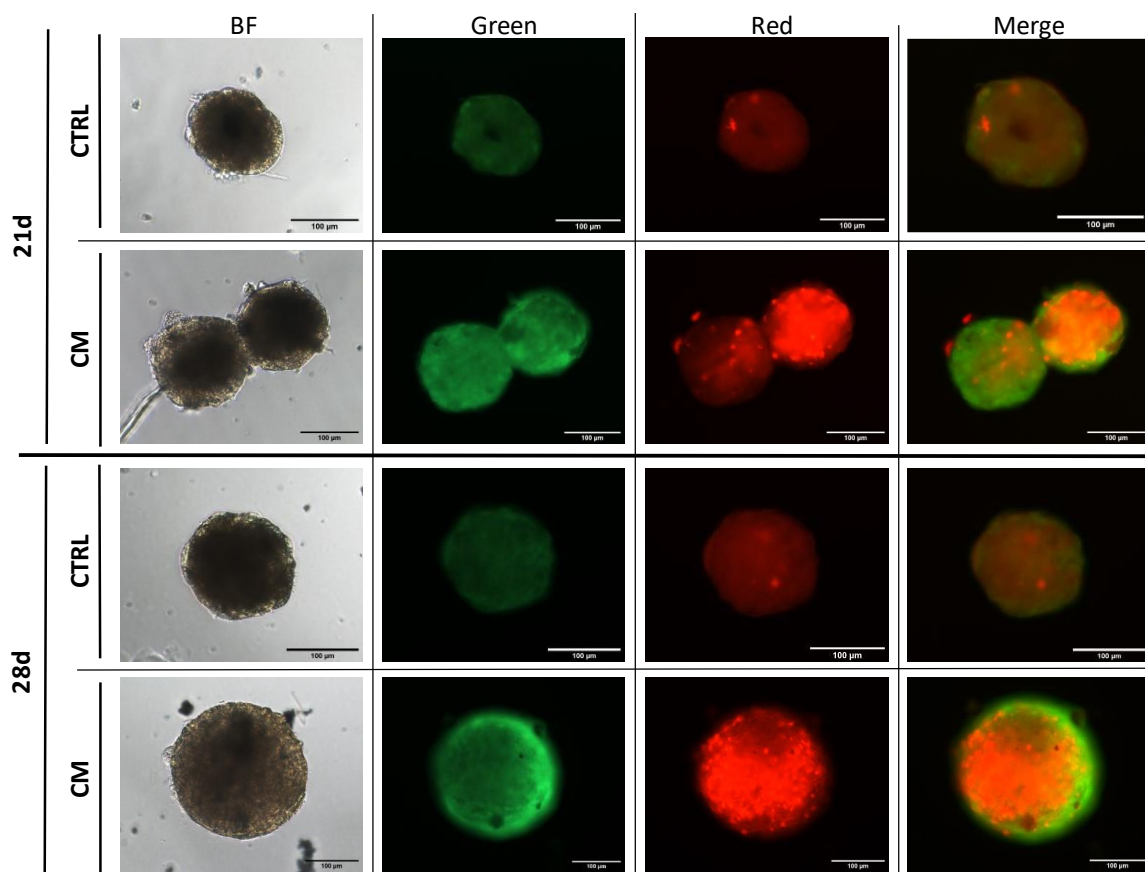
Figure 32 – Live/Dead staining with FDA/PI of P4 hMSC spheroids 21 and 28 days after chondrogenesis induction (after a maturation period of 14 days). Basal Media was used in the control experiments (CTRL). Differentiation experiments used chondrogenic medium (CM). Both media were supplemented with 50 ng/mL of CMC (scale bar 100 μm).

In addition, the dsDNA content was monitored at days 21 and 28 of chondrogenesis induction to trace cell proliferation, as shown in Figure 33. From day 21 to day 28, the DNA content of the spheroids rapidly declined, possibly associated with apoptotic and necrotic events within the spheroids during the prolonged culture period [78]. These events can be associated with the increase in the necrotic cores' size detected through the Propidium iodide (red) staining in the Live/Dead Assay.
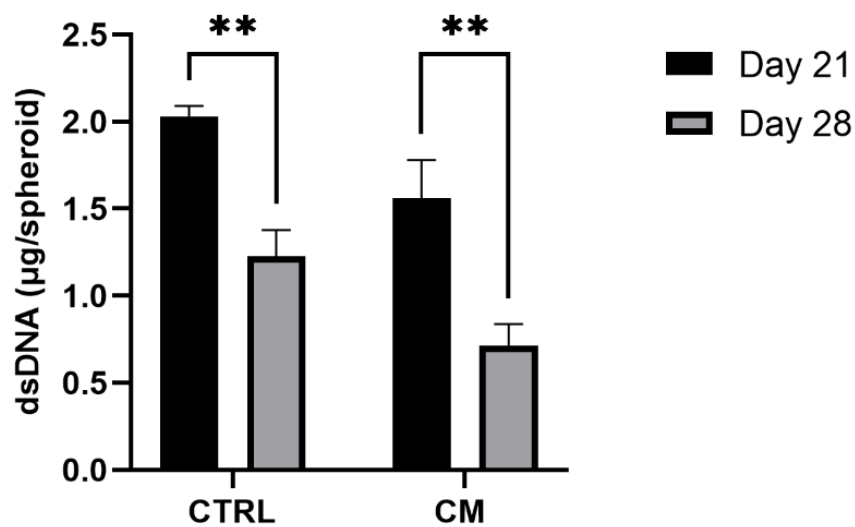
Figure 33 – dsDNA average quantification for an individual P4 hMSC spheroid, 21 and 28 days after chondrogenesis induction . The 14 days-old spheroids were maintained in static suspension cultures on U-bottomed 96-well PolyHEMA-coated (2% [w/v]) plates using high glucose (4.5 g/L) basal medium as the control experiment (CTRL), as well as a chemically defined chondrogenic medium (CM), both supplemented with 50 ng/mL of CMC. The results are expressed as mean of six replicates ± s.d. $**p \leq 0.01$.

The hMSC spheroids submitted to the chondrogenesis induction assay were collected at the desired times of differentiation (days 21 and 28) and stained with different histochemical dyes to detect the presence of cartilaginous ECM (Figure 34). The opacity of the spheroid constructs prevented the detection of the cartilaginous ECM characteristic molecules when using the majority of the assayed dyes, thus turning impossible to get conclusions. The histochemistry experiments were only successful for the spheroids stained with Fast Green/Safranin O. In this case, the spheroids exposed to chondrogenesis inducing medium (CM samples) exhibited an evident orange to red coloration, reporting the presence of proteoglycans.
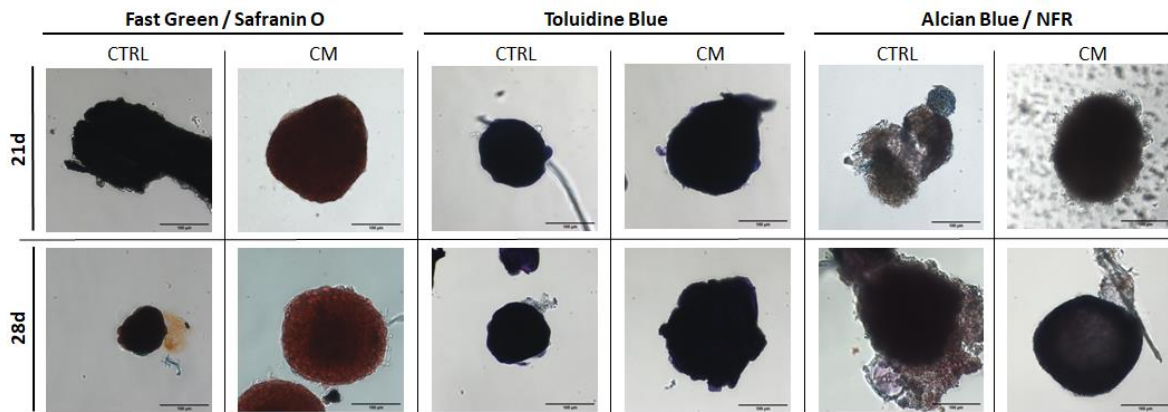
Figure 34 – Fast Green/Safranin O, Toluidine Blue O and Alcian Blue 8G/NFR staining relative to 21 and 28 days of 3D chondrogenesis induction using 14 days-old P4 hMSC spheroids (scale bar 100 µm) in Basal (CTRL) and in Chondrogenic medium (CM).

The observation of the spheroid constructs' morphology by Scanning Electron Microscopy (SEM) (Figure 35) showed that the size of control spheroids was lower than that of spheroids cultured in chondrogenic medium, in accordance with the diameters assessed by optical microscopy (Figure 31).

However, since sample preparation for SEM analysis imply dehydration steps that cause sample shrinking (in part due to the collapse of the ECM), spheroid diameters measured in SEM are substantially lower than in the hydrated samples. Interestingly, this phenomenon was observed but was much more pronounced in the control spheroids (CTRL) than in the spheroids subjected to the chondrogenesis-inducing medium (CM). This may be an indication that we are effectively in the presence of chondrospheres as the ECM in chondrospheres is expected to have a vastly superior robustness and to better resist to the forces inherent to the dehydration process.

Moreover, for both cases (control samples and samples exposed to chondrogenic medium) this shrinking due to sample dehydration occurred in a greater extent for samples collected at day 21 than for those collected at day 28. This should be also associated with ECM development (maturation) that grows with time and helps avoiding the collapse of the spheroid structure.
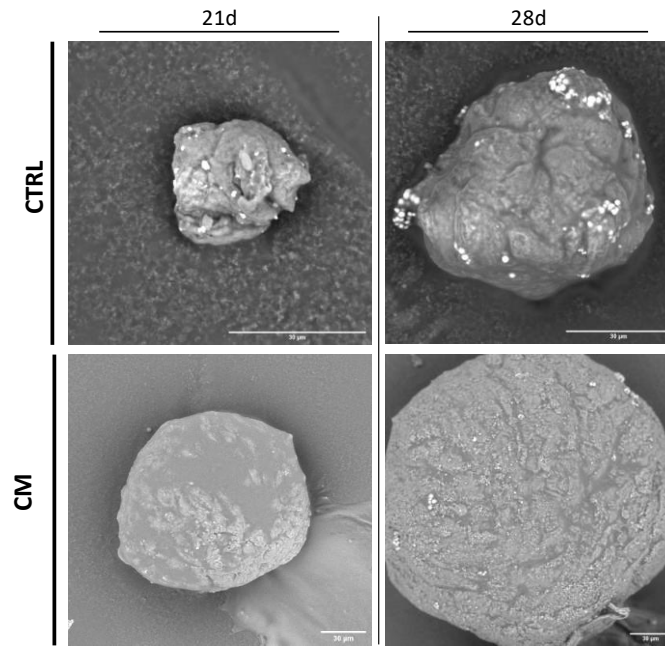
Figure 35 – SEM images relative to 21 and 28 days of 3D chondrogenesis induction using 14 days-old P4 hMSC spheroids in Basal (CTRL) and in Chondrogenic medium (CM) (scale bar 30 µm).

In addition, SEM images revealed that the generated spheroid models from hMSCs are highly cohesive, showing tight intercellular connections forming a predominantly flat surface. ECM deposition was visible for both control and chondrogenic groups (darker grey areas).

The spheroids were also characterized in terms of ALP activity at days 21 and 28 of chondrogenesis induction (Figure 36). The obtained results follow a similar trend to that found in the 2D assay performed with the same number of cells per well.

As previously mentioned, ALP activity is an important marker of the hypertrophic phase [11,60]. In one hand, the determined values indicate that the spheroids in chondrogenic media have not yet reached the hypertrophic phase. On the other hand, the control group (CTRL, spheroids in basal media) displayed an increase in ALP activity between 21 and 28 days, indicating that cells in these spheroids might be compromised with an osteogenic differentiation process due to the absence of hypertrophy delaying molecules such as TGF-β1 in culture media [60].
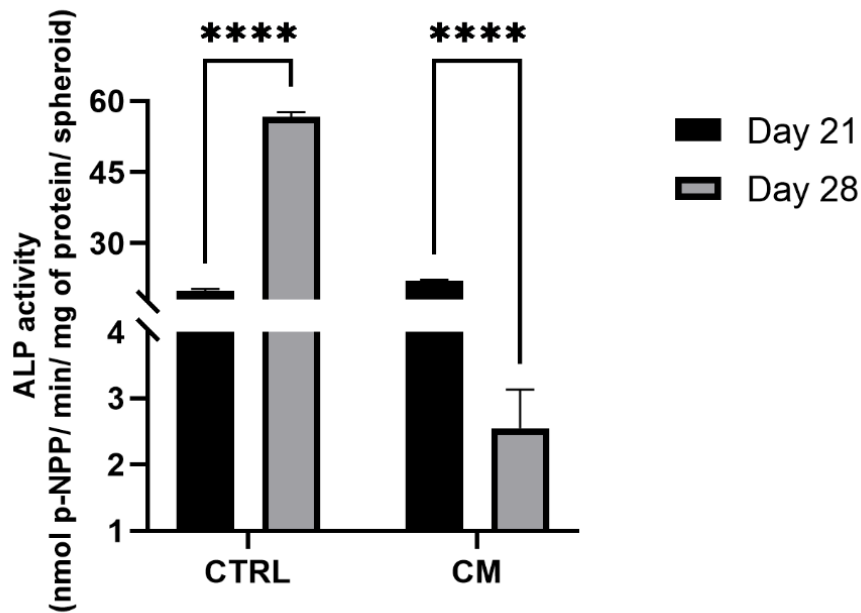
Figure 36 – ALP activity of spheroids (normalized for the total protein content) at days 21 and 28 of culture in Basal (CTRL) and in Chondrogenic medium (CM). The results are expressed as mean of six replicates ± s.d. ∗∗∗∗p ≤ 0.0001.

The occurrence of a cascade of events in hMSCs during differentiation is common knowledge. This process leads to morphologic and metabolic transformations, among which the reduction of the expression of stemness genes and the activation of genes related to the mature differentiated cells are the main distinctive features [47].

For this reason, in order to determine the chondrogenic potential of the 3D spheroid models in a more enlightening way, the expression of two of the major marker genes of chondrogenesis (collagen type II and aggrecan) was evaluated through their specific determination and quantification using Enzyme Linked-Immuno-Sorbent Assays (ELISA) (Figure 37).
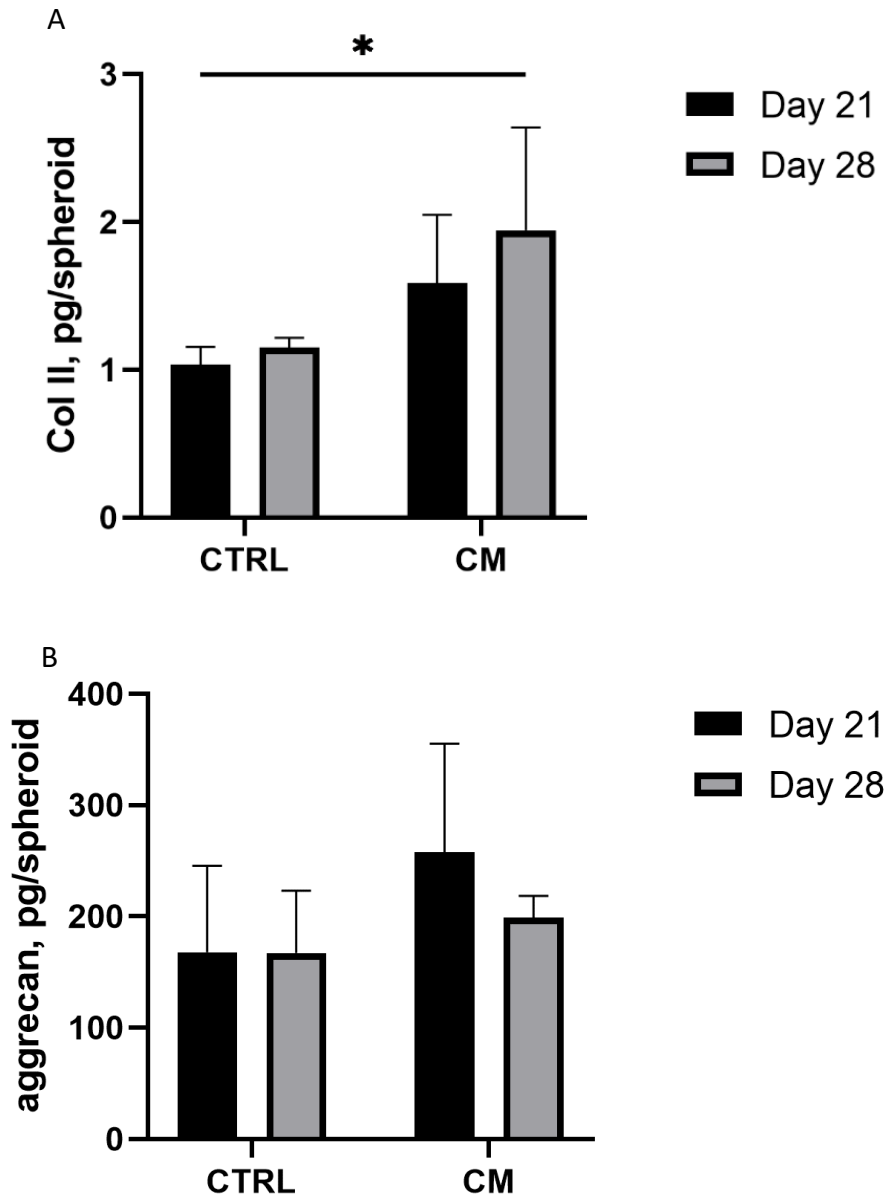
Figure 37 – Expression levels of collagen type II (col II) and aggrecan in spheroids by ELISA techniques at days 21 and 28 of chondrogenic induction. The results are expressed as mean of three replicates ± s.d. ∗p ≤ 0.05

Collagen type II (Col II) is the predominant form of collagen in cartilaginous ECM [99]. Thus, regarding the col II content present in the ECM of each spheroid (Figure 37 – A), the mean value determined for the spheroids kept in chondrogenic medium (CM) is significantly higher than for the spheroids of the control group kept in basal medium (CTRL). These findings provide evidence of the efficacy of the formulated chondrogenic media on 3D cultures and are in line with the drawn conclusions from the histochemical staining experiments (Figure 34).

It is noteworthy that the mean Col II content determined for the experimental group (CM spheroids) increased from 21 to 28 days of differentiation. However, the values determined for the control group (CTRL) did not significantly change after 21 days.

Aggrecan is representative of cartilaginous tissues [16,19], being a decisive marker of chondrogenesis; for this reason, and despite the absence of statistically significant differences between the control group (CTRL) and the group of spheroids exposed to chondrogenic media (CM), the average aggrecan content determined for the CM group was slightly superior. Thus, the results point out that the extent of chondrogenesis was higher in the spheroids cultured in chondrogenic medium.

72

4. Conclusion and future perspectives

Cartilage is a specialized connective tissue with the ability to support loads, and locomotion. Since this tissue has a very limited regenerative capacity, current therapies for degenerative cartilage diseases represent a huge burden to society because of the high health care costs involved, and the decreased quality of life for the patients. In addition to that, current therapies are mainly of palliative nature, bringing a growing demand for new and effective therapeutic strategies to light.

hMSCs have been successfully employed in different approaches of Regenerative Medicine to re-establish tissue homeostasis and promote repair in autoimmune and inflammatory disorders [100], having shown applicability in various fields, including in articular cartilage regeneration. These cells are responsible for tissue growth and maintenance.

Since hMSCs exist within their *in vivo* niches, exhibiting variable stemness potential and supportive functionalities [11], spheroid culture of hMSCs may be a promising therapeutic alternative for several clinical problems [41]. In fact, in the scope of cartilage regeneration/tissue engineering, spheroids can recreate relevant microenvironments where complex cell–cell and cell–matrix interactions, as well as complex transport dynamics for nutrients and gas, are established, mimicking natural *in vivo* conditions. It is well known that stem cell spheroids have demonstrated enhanced therapeutic effects when transplanted into various disease models [58], for this reason 3D cultures using hMSC fall into the category of promising novel cell-based therapy approaches. Thus, an optimization of the culture conditions could significantly impact the field of regenerative medicine.

In this thesis, several preliminary experiments were performed in an attempt to develop reproducible and cohesive spheroid models based on hMSCs and aimed at chondrogenic differentiation, representing the first set of experimental work in the research line using 3D cultures done at CQM – Centro de Química da Madeira.

Of the three methods assayed (pellet culture, hanging drop and cells self-aggregation in ultra-low attachment surfaces), the preparation of spheroids in ULA plates was shown to be most convinient and scale-up prone. This method allowed to prepare cohesive, homogeneous, stable and reproducible 3D spheroid constructs when

supplementing the culture mediu, with the CMC polymer (50 ng/mL) and culturing cells on agarose-coated plates.

Once the inherent advantages of this method had been verified, high cell-density spheroids were optimised using Poly-HEMA coated ULA-plates using high glucose levels in the culture medium (4.5 g/L). These spheroids were matured for 14 days upon the presence of the afore mentioned CMC supplementation (50 ng/mL, added since day 5), and then divided into a control group maintained in high glucose basal medium (BM), and a experimental group exposed to the previously optimized chondrogenic medium (CM), always adding CMC to the culture medium; this differentiation assay lasted for 28 days.

The CM lead to spheroid differentiation towards the chondrogenic lineage, forming chondrospheres, as an ECM of chondrogenic nature was detected by histochemical staining of the proteoglycans using Fast Green/Safranin O. Through SEM analyses it was possible to verify that the chondrospheres were more robust than the control group of spheroids kept in BM, as its ECM proved to be more resistant to the dehydration steps in the sample preparation. This higher stress resistance is consistent with what one would be expected in a cartilaginous tissue. In addition to the qualitative chondrogenic potential evaluation, the ELISA assays allowed to detect two of the most relevant chondrogenesis markers in the chondrospheres: collagen type II and aggrecan.

Therefore, taking into account future perspectives reflected in the CQM laboratories, it would be necessary to carry out studies in a more systematic way, repeating the differentiation tests several times, and even varying the cell densities seeded for preparing the spheroids (to determine if cellular density influences the chondrogenic potential). Furthermore, it would also be necessary to characterise in a more comprehensive and complete way the chondrogenic potential of spheroids. For this characterisation, it would be advantageous to use confocal microscopy to study the morphology of the spheroids taking into account different planes; a microtome to analyse stained sections of the spheroids (histochemistry and/or immunostaining); or even clearing kits to reduce the opacity of the spheroids, allowing them to be visualised as a complete specimen.

Ultimately, the major global application of the present work is directed towards regenerative medicine, specifically for cartilage degenerative diseases, aiming joint rehabilitation. By inducing the differentiation of hMSC 3D spheroids towards the chondrogenic lineage, and further *in vivo* implantation of the chondrospheres on the defect site, the impairments may be lessened in the damaged joints. However, as previously mentioned the application of this therapeutic approach requires further testing to optimize and validate hMSCs chondrogenic differentiation in 3D cultures before moving forward to more complex study models.

REFERENCES

[1]   Ross M, Pawlina W. Histology: A Text and Atlas: With Correlated Cell and Molecular Biology. vol. xvii. 2006.

[2]   Camarero-Espinosa S, Rothen-Rutishauser B, Foster EJ, Weder C. Articular cartilage: from formation to tissue engineering. Biomater Sci 2016;4:734–67. https://doi.org/10.1039/C6BM00068A.

[3]   Adriano GFF. Scaffolds de nanofibras termo-sensíveis para cultura de células estaminais. Master Thesis. Instituto Superior Técnico (Universidade de Lisboa). 2014.

[4]   Rim YA, Nam Y, Park N, Jung H, Lee K, Lee J, et al. Chondrogenic Differentiation from Induced Pluripotent Stem Cells Using Non-Viral Minicircle Vectors. Cells 2020;9:582. https://doi.org/10.3390/cells9030582.

[5]   Díaz-Payno PJ, Browe DC, Cunniffe GM, Kelly DJ. The identification of articular cartilage and growth plate extracellular matrix-specific proteins supportive of either osteogenesis or stable chondrogenesis of stem cells. Biochem Biophys Res Commun 2020;528:285–91. https://doi.org/10.1016/j.bbrc.2020.05.074.

[6]   Kim SA, Sur YJ, Cho M La, Go EJ, Kim YH, Shetty AA, et al. Atelocollagen promotes chondrogenic differentiation of human adipose-derived mesenchymal stem cells. Sci Rep 2020;10:1–18. https://doi.org/10.1038/s41598-020-67836-3.

[7]   Vinci M, Gowan S, Boxall F, Patterson L, Zimmermann M, Court W, et al. Advances in establishment and analysis of three-dimensional tumor spheroid-based functional assays for target validation and drug evaluation. BMC Biol 2012 101 2012;10:1–21. https://doi.org/10.1186/1741-7007-10-29.

[8]   Place ES. Bioactive hydrogels for tissue engineering. PhD Thesis. Imperial College London, 2011.

[9]   Eyre D. Collagen of articular cartilage. Arthritis Res 2002;4:30–5.

https://doi.org/10.1186/AR380.

[10]   Marañón VZ, Dra P, Isabel A, Varona A, Teodoro P, Casado P. Development of a cartilage tissue engineering construct based on hASCs spheroids differentiated under hypoxia in a chitosan / chitin nanocrystals 3D scaffold. 2019.

[11]   Somoza RA, Welter JF, Correa D, Caplan AI. Chondrogenic Differentiation of Mesenchymal Stem Cells: Challenges and Unfulfilled Expectations. Tissue Eng Part B Rev 2014;20:596. https://doi.org/10.1089/TEN.TEB.2013.0771.

[12]   Knudson CB, Knudson W. Cartilage proteoglycans. Semin Cell Dev Biol 2001;12:69–78. https://doi.org/10.1006/SCDB.2000.0243.

[13]   Couto MR, Rodrigues JL, Rodrigues LR. Heterologous production of chondroitin. Biotechnol Reports 2022;33. https://doi.org/10.1016/J.BTRE.2022.E00710.

[14]   Schumacher BL, Block JA, Schmid TM, Aydelotte MB, Kuettner KE. A novel proteoglycan synthesized and secreted by chondrocytes of the superficial zone of articular cartilage. Arch Biochem Biophys 1994;311:144–52. https://doi.org/10.1006/ABBI.1994.1219.

[15]   Flannery CR, Hughes CE, Schumacher BL, Tudor D, Aydelotte MB, Kuettner KE, et al. Articular cartilage superficial zone protein (SZP) is homologous to megakaryocyte stimulating factor precursor and Is a multifunctional proteoglycan with potential growth-promoting, cytoprotective, and lubricating properties in cartilage metabolism. Biochem Biophys Res Commun 1999;254:535–41. https://doi.org/10.1006/BBRC.1998.0104.

[16]   Ham AW (Arthur W, Cormack DH. Histology: A Text and Atlas, with Correlated Cell and Molecular Biology 1979:966.

[17]   Teixeira MA, Amorim MTP, Felgueiras HP. Poly(vinyl alcohol)-based nanofibrous electrospun scaffolds for tissue engineering applications. Polymers (Basel) 2020;12. https://doi.org/10.3390/POLYM12010007.

[18] Han L, Grodzinsky AJ, Ortiz C. Nanomechanics of the cartilage extracellular matrix. Annu Rev Mater Res 2011;41:133–68. https://doi.org/10.1146/ANNUREV-MATSCI-062910-100431.

[19] Kiani C, Chen L, Wu YJ, Yee AJ, Yang BB. Structure and function of aggrecan. Cell Res 2002;12:19–32. https://doi.org/10.1038/SJ.CR.7290106.

[20] Karsdal MA, Michaelis M, Ladel C, Siebuhr AS, Bihlet AR, Andersen JR, et al. Disease-modifying treatments for osteoarthritis (DMOADs) of the knee and hip: lessons learned from failures and opportunities for the future. Osteoarthr Cartil 2016;24:2013–21. https://doi.org/10.1016/J.JOCA.2016.07.017.

[21] Lanza R, Langer R, Vacanti J. Principles of Tissue Engineering. Fifth Edit. 2020. https://doi.org/10.1006/cryo.1999.2214.

[22] Gao L, Orth P, Cucchiarini M, Madry H. Effects of solid acellular type-I/III collagen biomaterials on in vitro and in vivo chondrogenesis of mesenchymal stem cells. Expert Rev Med Devices 2017;14:717–32. https://doi.org/10.1080/17434440.2017.1368386.

[23] Zubillaga V, Alonso-varona A, Fernandes SCM, Salaberria AM, Palomares T. Adipose-derived mesenchymal stem cell chondrospheroids cultured in hypoxia and a 3D porous chitosan/chitin nanocrystal scaffold as a platform for cartilage tissue engineering. Int J Mol Sci 2020;21:1–17. https://doi.org/10.3390/ijms21031004.

[24] De Moor L, Fernandez S, Vercruysse C, Tytgat L, Asadian M, De Geyter N, et al. Hybrid Bioprinting of Chondrogenically Induced Human Mesenchymal Stem Cell Spheroids. Front Bioeng Biotechnol 2020;0:484. https://doi.org/10.3389/FBIOE.2020.00484.

[25] Huang J, Huang Z, Liang Y, Yuan W, Bian L, Duan L, et al. 3D printed gelatin/hydroxyapatite scaffolds for stem cell chondrogenic differentiation and articular cartilage repair. Biomater Sci 2021;9:2620–30.

https://doi.org/10.1039/d0bm02103b.

[26] Medvedeva E V., Grebenik EA, Gornostaeva SN, Telpuhov VI, Lychagin A V., Timashev PS, et al. Repair of Damaged Articular Cartilage: Current Approaches and Future Directions. Int J Mol Sci 2018, Vol 19, Page 2366 2018;19:2366. https://doi.org/10.3390/IJMS19082366.

[27] Kessler MW, Grande DA. Tissue engineering and cartilage. Http://DxDoiOrg/104161/Org6116 2008;4:28–32. https://doi.org/10.4161/ORG.6116.

[28] Staubli F, Stoddart MJ, D'Este M, Schwab A. Pre-culture of human mesenchymal stromal cells in spheroids facilitates chondrogenesis at a low total cell count upon embedding in biomaterials to generate cartilage microtissues. Acta Biomater 2022. https://doi.org/10.1016/J.ACTBIO.2022.02.038.

[29] Liu Y, Zhou G, Cao Y. Recent Progress in Cartilage Tissue Engineering—Our Experience and Future Directions. Engineering 2017;3:28–35. https://doi.org/10.1016/J.ENG.2017.01.010.

[30] Osteoarthritis vs. rheumatoid arthritis - Mayo Clinic n.d. https://www.mayoclinic.org/diseases-conditions/arthritis/multimedia/osteoarthritis-vs-rheumatoid-arthritis/img-20008728 (accessed May 21, 2022).

[31] Laev SS, Salakhutdinov NF. Anti-arthritic agents: Progress and potential. Bioorganic Med Chem 2015;23:3059–80. https://doi.org/10.1016/j.bmc.2015.05.010.

[32] Guo Q, Wang Y, Xu D, Nossent J, Pavlos NJ, Xu J. Rheumatoid arthritis: pathological mechanisms and modern pharmacologic therapies. Bone Res 2018 61 2018;6:1–14. https://doi.org/10.1038/s41413-018-0016-9.

[33] Mithoefer K, Mcadams T, Williams RJ, Kreuz PC, Mandelbaum BR. Clinical efficacy of the microfracture technique for articular cartilage repair in the knee: An

evidence-based systematic analysis. Am J Sports Med 2009;37:2053–63. https://doi.org/10.1177/0363546508328414.

[34] Autologous Chondrocyte Implantation (ACI) | Patient Education n.d. https://cartilage.org/patient/about-cartilage/cartilage-repair/autologous-chondrocyte-implantation-aci/ (accessed May 21, 2022).

[35] New Scaffolds & Cells | Patient Education n.d. https://cartilage.org/patient/about-cartilage/cartilage-repair/new-scaffolds-cells/ (accessed May 21, 2022).

[36] Mobasheri A, Kalamegam G, Musumeci G, Batt ME. Chondrocyte and mesenchymal stem cell-based therapies for cartilage repair in osteoarthritis and related orthopaedic conditions. Maturitas 2014;78:188–98. https://doi.org/10.1016/J.MATURITAS.2014.04.017.

[37] Niemeyer P, Laute V, Zinser W, John T, Becher C, Diehl P, et al. Safety and efficacy of matrix-associated autologous chondrocyte implantation with spheroid technology is independent of spheroid dose after 4 years. Knee Surgery, Sport Traumatol Arthrosc 2020;28:1130–43. https://doi.org/10.1007/S00167-019-05786-8/TABLES/9.

[38] Schulte-Zweckel J, Rosi F, Sreenu D, Schröder H, Niemeyer CM, Triola G. Site-specific, Reversible and Fluorescent Immobilization of Proteins on CrAsH-modified surfaces. R Soc Chem 2014.

[39] Eschen C, Kaps C, Widuchowski W, Fickert S, Zinser W, Niemeyer P, et al. Clinical outcome is significantly better with spheroid-based autologous chondrocyte implantation manufactured with more stringent cell culture criteria. Osteoarthr Cartil Open 2020;2:100033. https://doi.org/10.1016/J.OCARTO.2020.100033.

[40] Caron MMJ, Emans PJ, Coolsen MME, Voss L, Surtel DAM, Cremers A, et al. Redifferentiation of dedifferentiated human articular chondrocytes: comparison of 2D and 3D cultures. Osteoarthr Cartil 2012;20:1170–8.

https://doi.org/10.1016/J.JOCA.2012.06.016.

[41]   Grigull NP, Redeker JI, Schmitt B, Saller MM, Schönitzer V, Mayer-Wagner S. Chondrogenic Potential of Pellet Culture Compared to High-Density Culture on a Bacterial Cellulose Hydrogel. Int J Mol Sci 2020, Vol 21, Page 2785 2020;21:2785. https://doi.org/10.3390/IJMS21082785.

[42]   Prockop DJ, Phinney DG, Bunnell BA. Mesenchymal stem cells : methods and protocols 2008:192.

[43]   Labusca LS. Scaffold Free 3D Culture of Mesenchymal Stem Cells; Implications for Regenerative Medicine. J Transplant Stem Cell Biol 2015;2:1–8. https://doi.org/10.13188/2374-9326.1000008.

[44]   Kouroupis D, Correa D. Increased Mesenchymal Stem Cell Functionalization in Three-Dimensional Manufacturing Settings for Enhanced Therapeutic Applications. Front Bioeng Biotechnol 2021;9. https://doi.org/10.3389/fbioe.2021.621748.

[45]   Sultan S, Alalmie A, Noorwali A, Alyamani A, Shaabad M, Alfakeeh S, et al. Resveratrol promotes chondrogenesis of human Wharton's jelly stem cells in a hyperglycemic state by modulating the expression of inflammation-related cytokines. All Life 2020;13:577–86. https://doi.org/10.1080/26895293.2020.1835739.

[46]   Zha K, Sun Z, Yang Y, Chen M, Gao C, Fu L, et al. Recent developed strategies for enhancing chondrogenic differentiation of MSC: Impact on MSC-based therapy for cartilage regeneration. Stem Cells Int 2021;2021. https://doi.org/10.1155/2021/8830834.

[47]   Robert AW, Marcon BH, Dallagiovanna B, Shigunov P. Adipogenesis, Osteogenesis, and Chondrogenesis of Human Mesenchymal Stem/Stromal Cells: A Comparative Transcriptome Approach. Front Cell Dev Biol 2020;8:561. https://doi.org/10.3389/fcell.2020.00561.

[48]   Kamatar A, Gunay G, Acar H. Natural and Synthetic Biomaterials for Engineering Multicellular Tumor Spheroids. Polym 2020, Vol 12, Page 2506 2020;12:2506. https://doi.org/10.3390/POLYM12112506.

[49]   ThermoFisher S. 3D cell culture handbook. 3D Cell Cult Handb 2020:124.

[50]   Metzger W, Sossong D, Bächle A, Pütz N, Wennemuth G, Pohlemann T, et al. The liquid overlay technique is the key to formation of co-culture spheroids consisting of primary osteoblasts, fibroblasts and endothelial cells. Cytotherapy 2011;13:1000–12. https://doi.org/10.3109/14653249.2011.583233.

[51]   Page H, Flood P, Reynaud EG. Three-dimensional tissue cultures: Current trends and beyond. Cell Tissue Res 2013;352:123–31. https://doi.org/10.1007/s00441-012-1441-5.

[52]   Cesarz Z, Tamama K. Spheroid Culture of Mesenchymal Stem Cells. Stem Cells Int 2016;2016. https://doi.org/10.1155/2016/9176357.

[53]   Kouroupis D, Correa D. Increased Mesenchymal Stem Cell Functionalization in Three-Dimensional Manufacturing Settings for Enhanced Therapeutic Applications. Front Bioeng Biotechnol 2021;9:22. https://doi.org/10.3389/FBIOE.2021.621748/BIBTEX.

[54]   Kim HJ, Castañeda R, Kang TH, Kimura S, Wada M, Kim U-J. Cellulose hydrogel film for spheroid formation of human adipose-derived stemcells. Cellul 2018 254 2018;25:2589–98. https://doi.org/10.1007/S10570-018-1732-4.

[55]   Zhang YS, Duchamp M, Oklu R, Ellisen LW, Langer R, Khademhosseini A. Bioprinting the Cancer Microenvironment. ACS Biomater Sci Eng 2016;2. https://doi.org/10.1021/acsbiomaterials.6b00246.

[56]   Shen H, Lin H, Sun AX, Song S, Wang B, Yang Y, et al. Acceleration of chondrogenic differentiation of human mesenchymal stem cells by sustained growth factor release in 3D graphene oxide incorporated hydrogels. Acta Biomater 2020;105:44–55. https://doi.org/10.1016/j.actbio.2020.01.048.

[57]   Chae SJ, Hong J, Hwangbo H, Kim GH. The utility of biomedical scaffolds laden with spheroids in various tissue engineering applications. Theranostics 2021;11:6818–32. https://doi.org/10.7150/THNO.58421.

[58]   Kim S, Kim EM, Yamamoto M, Park H, Shin H. Engineering Multi-Cellular Spheroids for Tissue Engineering and Regenerative Medicine. Adv Healthc Mater 2020;9:2000608. https://doi.org/10.1002/ADHM.202000608.

[59]   Ryu N-E, Lee S-H, Park H. Spheroid Culture System Methods and Applications for Mesenchymal Stem Cells. Cells 2019, Vol 8, Page 1620 2019;8:1620. https://doi.org/10.3390/CELLS8121620.

[60]   B J, TM H, AI C, VM G, JU Y. In vitro chondrogenesis of bone marrow-derived mesenchymal progenitor cells. Exp Cell Res 1998;238:265–72. https://doi.org/10.1006/EXCR.1997.3858.

[61]   Mueller MB, Tuan RS. Functional characterization of hypertrophy in chondrogenesis of human mesenchymal stem cells. Arthritis Rheum 2008;58:1377–88. https://doi.org/10.1002/ART.23370.

[62]   Ryu N-E, Lee S-H, Park H. Spheroid Culture System Methods and Applications for Mesenchymal Stem Cells. Cells 2019;8. https://doi.org/10.3390/CELLS8121620.

[63]   Gianpiero Lazzari, Patrick Couvreur, Simona Mura. Multicellular tumor spheroids: a relevant 3D model for the in vitro preclinical investigation of polymer nanomedicines. Polym Chem 2017;8:4947–69. https://doi.org/10.1039/C7PY00559H.

[64]   Costa EC, Melo-Diogo D de, Moreira AF, Carvalho MP, Correia IJ. Spheroids Formation on Non-Adhesive Surfaces by Liquid Overlay Technique: Considerations and Practical Approaches. Biotechnol J 2018;13:1700417. https://doi.org/10.1002/BIOT.201700417.

[65]   EC C, D de M-D, AF M, MP C, IJ C. Spheroids Formation on Non-Adhesive Surfaces by Liquid Overlay Technique: Considerations and Practical Approaches.

Biotechnol J 2018;13. https://doi.org/10.1002/BIOT.201700417.

[66]   Bartosh TJ, Ylöstalo JH, Mohammadipoor A, Bazhanov N, Coble K, Claypool K, et al. Aggregation of human mesenchymal stromal cells (MSCs) into 3D spheroids enhances their antiinflammatory properties. Proc Natl Acad Sci U S A 2010;107:13724–9. https://doi.org/10.1073/pnas.1008117107.

[67]   Liangming Zhang, Peiqiang Su, Caixia Xu, Junlin Yang, Weihua Yu, Dongsheng Huang. Chondrogenic differentiation of human mesenchymal stem cells: a comparison between micromass and pellet culture systems. Biotechnol Lett 2010;32:1339–46. https://doi.org/10.1007/S10529-010-0293-X.

[68]   Muraglia A, Corsi A, Riminucci M, Mastrogiacomo M, Cancedda R, Bianco P, et al. Formation of a chondro-osseous rudiment in micromass cultures of human bone-marrow stromal cells. J Cell Sci 2003;116:2949–55. https://doi.org/10.1242/JCS.00527.

[69]   J F, C S, R E, LA K-S. Spheroid-based drug screen: considerations and practical approach. Nat Protoc 2009;4:309–24. https://doi.org/10.1038/NPROT.2008.226.

[70]   Analyze Menu n.d. https://imagej.nih.gov/ij/docs/menus/analyze.html (accessed August 20, 2022).

[71]   RNA/DNA Quantification | Thermo Fisher Scientific - PT n.d. https://www.thermofisher.com/pt/en/home/life-science/dna-rna-purification-analysis/nucleic-acid-quantitation.html?gclid=Cj0KCQjwjIKYBhC6ARIsAGEds-IJqEPKa1WFv3Vlq8MXE7xJ9rvcnj4O99T-J9xuCTV17Eop5COTk9gaAmjFEALw_wcB&ef_id=Cj0KCQjwjIKYBhC6ARIsAGEds-IJqEPKa1WFv3Vlq8MXE7xJ9rvcnj4O99T-J9xuCTV17Eop5COTk9gaAmjFEALw_wcB:G:s&s_kwcid=AL!3652!3!537634827299!p!!g!!dsdna quantification&cid=bid_pca_aqb_r01_co_cp1359_pjt0000_bid00000_0se_gaw_nt_pur_con (accessed August 20, 2022).

[72]   Description P, Information P. MesenCult ™ -ACF Chondrogenic Differentiation Medium Pre paration of Complete MesenCult ™ -ACF Chondrogenic Differentiation Medium n.d.:5–6.

[73]   Resazurin Cell Viability Assay | Creative Bioarray n.d. https://www.creative-bioarray.com/support/resazurin-cell-viability-assay.htm (accessed August 20, 2022).

[74]   Deynoux M, Sunter N, Ducrocq E, Dakik H, Guibon R, Burlaud-Gaillard J, et al. A comparative study of the capacity of mesenchymal stromal cell lines to form spheroids. PLoS One 2020;15:e0225485. https://doi.org/10.1371/JOURNAL.PONE.0225485.

[75]   Abdolahinia ED, Jafari B, Parvizpour S, Barar J, Nadri S, Omidi Y. Role of cellulose family in fibril organization of collagen for forming 3D cancer spheroids: In vitro and in silico approach. BioImpacts 2020;11:111–7. https://doi.org/10.34172/BI.2021.18.

[76]   Metzger W, Sossong D, Bächle A, Pütz N, Wennemuth G, Pohlemann T, et al. The liquid overlay technique is the key to formation of co-culture spheroids consisting of primary osteoblasts, fibroblasts and endothelial cells. Cytotherapy 2011;13:1000–12. https://doi.org/10.3109/14653249.2011.583233.

[77]   Miehle E, Bader-Mittermaier S, Schweiggert-Weisz U, Hauner H, Eisner P. Effect of Physicochemical Properties of Carboxymethyl Cellulose on Diffusion of Glucose. Nutrients 2021;13. https://doi.org/10.3390/NU13051398.

[78]   Gong X, Lin C, Cheng J, Su J, Zhao H, Liu T, et al. Generation of Multicellular Tumor Spheroids with Microwell-Based Agarose Scaffolds for Drug Testing. PLoS One 2015;10:e0130348. https://doi.org/10.1371/JOURNAL.PONE.0130348.

[79]   Abdolahinia ED, Jafari B, Parvizpour S, Barar J, Nadri S, Omidi Y. Role of cellulose family in fibril organization of collagen for forming 3D cancer spheroids: In vitro and in silico approach. Bioimpacts 2021;11:111.

https://doi.org/10.34172/BI.2021.18.

[80]   Prokopiuk V, Globa N, Prokopiuk O, Shchedrov A, Musatova I. Characterization of Placental Mesenchymal Stem Cells Spheroids after Generation, Hypothermic and Subnormothermic Storage. Innov Biosyst Bioeng 2019;3:146–51. https://doi.org/10.20535/ibb.2019.3.3.172604.

[81]   Sharma P, Kumar A, Dey AD, Behl T, Chadha S. Stem cells and growth factors-based delivery approaches for chronic wound repair and regeneration: A promise to heal from within. Life Sci 2021;268:118932. https://doi.org/10.1016/J.LFS.2020.118932.

[82]   Xiao Y, Peperzak V, Rijn L van, Borst J, Bruijn JD de. Dexamethasone treatment during the expansion phase maintains stemness of bone marrow mesenchymal stem cells. J Tissue Eng Regen Med 2010;4:374–86. https://doi.org/10.1002/TERM.250.

[83]   Sridharan G, Shankar AA. Toluidine blue: A review of its chemistry and clinical utility. J Oral Maxillofac Pathol 2012;16:251. https://doi.org/10.4103/0973-029X.99081.

[84]   Bergholt NL, Lysdahl H, Lind M, Foldager CB. A Standardized Method of Applying Toluidine Blue Metachromatic Staining for Assessment of Chondrogenesis. Cartilage 2019;10:370. https://doi.org/10.1177/1947603518764262.

[85]   Sun C, Lan W, Li B, Zuo R, Xing H, Liu M, et al. Glucose regulates tissue-specific chondro-osteogenic differentiation of human cartilage endplate stem cells via O-GlcNAcylation of Sox9 and Runx2. Stem Cell Res Ther 2019;10. https://doi.org/10.1186/S13287-019-1440-5.

[86]   Underhill TM, Dranse HJ, Hoffman LM. Analysis of chondrogenesis using micromass cultures of limb mesenchyme. Methods Mol Biol 2014;1130:251–65. https://doi.org/10.1007/978-1-62703-989-5_19.

[87]   Phornphutkul C, Wu KY, Gruppuso PA. The role of insulin in chondrogenesis. Mol

Cell Endocrinol 2006;249:107–15. https://doi.org/10.1016/J.MCE.2006.02.002.

[88] Schmitz N, Laverty S, Kraus VB, Aigner T. Basic methods in histopathology of joint tissues. Osteoarthr Cartil 2010;18:S113–6. https://doi.org/10.1016/J.JOCA.2010.05.026.

[89] Safranin Staining – Conduct Science n.d. https://conductscience.com/safranin-staining/ (accessed November 3, 2021).

[90] Safranin O Stain 1%, Aqueous, Special Stains in Histopathology Laboratory n.d. https://www.newcomersupply.com/product/safranin-o-stain-solution-1-aqueous/ (accessed November 3, 2021).

[91] fast green | Encyclopedia.com n.d. https://www.encyclopedia.com/science/dictionaries-thesauruses-pictures-and-press-releases/fast-green (accessed November 3, 2021).

[92] Alcian-Blue Staining Solution | Sigma-Aldrich n.d. https://www.sigmaaldrich.com/PT/en/product/mm/tms010 (accessed January 13, 2022).

[93] Nuclear Fast Red n.d. https://www.bosterbio.com/nuclear-fast-red-ar0008-boster.html (accessed February 24, 2022).

[94] Nuclear Fast Red Stain Solution - Cepham Life Sciences Research Products n.d. https://www.cephamls.com/nuclear-fast-red-stain-solution/ (accessed February 24, 2022).

[95] Richardson SM, Kalamegam G, Pushparaj PN, Matta C, Memic A, Khademhosseini A, et al. Mesenchymal stem cells in regenerative medicine: Focus on articular cartilage and intervertebral disc regeneration. Methods 2016;99:69–80. https://doi.org/10.1016/J.YMETH.2015.09.015.

[96] Diederichs S, Klampfleuthner FAM, Moradi B, Richter W. Chondral Differentiation of Induced Pluripotent Stem Cells Without Progression Into the Endochondral

Pathway. Front Cell Dev Biol 2019;7:270. https://doi.org/10.3389/FCELL.2019.00270/BIBTEX.

[97] Kuk M, Kim Y, Lee SH, Kim WH, Kweon OK. Osteogenic ability of canine adipose-derived mesenchymal stromal cell sheets in relation to culture time. Cell Transplant 2016;25:1415–22. https://doi.org/10.3727/096368915X689532.

[98] Omelyanenko NP, Karalkin PA, Bulanova EA, Koudan E V., Parfenov VA, Rodionov SA, et al. Extracellular Matrix Determines Biomechanical Properties of Chondrospheres during Their Maturation In Vitro. Cartilage 2020;11:521–31. https://doi.org/10.1177/1947603518798890.

[99] Wu Z, Korntner S, Mullen A, Zeugolis D. Collagen type II: From biosynthesis to advanced biomaterials for cartilage engineering. Biomater Biosyst 2021;4:100030. https://doi.org/10.1016/J.BBIOSY.2021.100030.

[100] Crippa S, Bernardo ME. Mesenchymal Stromal Cells: Role in the BM Niche and in the Support of Hematopoietic Stem Cell Transplantation. HemaSphere 2018;2. https://doi.org/10.1097/HS9.0000000000000151.

UNIVERSIDADE da MADEIRA

CQM
CENTRO DE QUÍMICA · DA MADEIRA

Molecular Materials
R E S E A R C H   G R O U P
M A D E I R A   I S L A N D   -   P O R T U G A L

European
Science
Foundation

fct
Fundação
para a Ciência
e a Tecnologia

arditi
agência regional para o
desenvolvimento da investigação
tecnologia e inovação

Interreg
Fundo Europeu de Desenvolvimento Regional

EUROPEAN UNION

MADEIRA 14-20
Programa Operacional da Região Autónoma da Madeira